

Permeability Prediction Using Mercury Injection Capillary

Pressure Data

BY

Hasan Abdul-Elah Nooruddin

A Thesis Presented to the
DEANSHIP OF GRADUATE STUDIES

KING FAHD UNIVERSITY OF PETROLEUM & MINERALS

DHAHRAN, SAUDI ARABIA

In Partial Fulfillment of the
Requirements for the Degree of

MASTER OF SCIENCE

In

PETROLEUM ENGINEERING

January 2013

KING FAHD UNIVERSITY OF PETROLEUM & MINERALS

DHAHRAN- 31261, SAUDI ARABIA

DEANSHIP OF GRADUATE STUDIES

This thesis, written by Hasan Abdul-Elah Nooruddin under the direction of his thesis advisor and approved by his thesis committee, has been presented and accepted by the Dean of Graduate Studies, in partial fulfillment of the requirements for the degree of **MASTER OF SCIENCE IN PETROLEUM ENGINEERING.**



Dr. M. Enamul Hossain
(Advisor)



Dr. Abdullah Sultan
Department Chairman



Dr. Hasan Al-Yousef
(Member)



Dr. Salam A. Zummo
Dean of Graduate Studies



Dr. Taha Okasha
(Member)



Date

© Hasan Abdul-Elah Nooruddin

2012

This work is dedicated to my parents and to my wife

ACKNOWLEDGMENTS

I would like to thank my thesis advisor, Dr. M. Enamul Hossain for his support and encouragement to achieve and complete all thesis requirements. I am also grateful to thesis committee members, Dr. Hasan Al-Yousef and Dr. Taha Okasha for their continuous support and excellent feedback before, during and even after completing my thesis.

I don't want to forget thanking Saudi Aramco management for their support and permission to use some of their data. I also thank the petroleum engineering department at King Fahd University of Petroleum & Minerals for the continuous support and the provided knowledge

I would like to express gratitude toward my wife for her passion and patience.

TABLE OF CONTENTS

ACKNOWLEDGMENTS	V
TABLE OF CONTENTS.....	VI
LIST OF TABLES.....	VIII
LIST OF FIGURES.....	IX
LIST OF ABBREVIATIONS.....	XI
ABSTRACT	XIV
1 CHAPTER 1 INTRODUCTION	1
1.1 Statement of the Problem.....	3
1.2 Objectives	4
1.3 Proposed Approach	4
2 CHAPTER 2 STATE-OF-THE-ART AND PROPOSED MODIFICATION TO PERMEABILITY PREDICTION MODELS.....	5
2.1 Capillary Pressure Description Models	6
2.2 State-of-the-art Permeability Prediction Models Using MICP.....	7
2.3 Proposed Modification to Permeability Prediction Models.....	14
3 CHAPTER 3 LABORATORY DATA DESCRIPTION AND VALIDATION	17
4 CHAPTER 4 RESULTS AND DISCUSSIONS.....	26
4.1 Extraction of Permeability Model Parameters	26
4.2 Comparison of Permeability Models Using Published Constants.....	39
4.3 Comparison of Generalized Permeability Models	50

5	CHAPTER 5 CONCLUSION	66
	REFERENCES.....	69
	APPENDIX A.....	72
	APPENDIX B.....	73
	VITAE	99

LIST OF TABLES

Table 3.1 Statistical description of core data used in the analysis	19
Table 4.1 Statistical description of permeability model parameters	27
Table 4.2 Correlation matrix of model parameters in normal domain	28
Table 4.3 Correlation matrix of model parameters in logarithmic domain	29
Table 4.4 Statistical analysis of model results using published constants	40
Table 4.5 Results of all permeability models with all fitting methods	52
Table 4.6 Coefficients of all permeability models using all methods	53

LIST OF FIGURES

Figure 3.1	Porosity histogram of core data	20
Figure 3.2	Histogram of natural log of permeability of core data.....	21
Figure 3.3	Bulk volume histogram.....	22
Figure 3.4	Pore volume histogram	23
Figure 3.5	Porosity cross-plot between air porosity and MICP porosity	24
Figure 3.6	Numerical derivatives of capillary pressure against mercury saturation	25
Figure 4.1	Entry pressure histogram	30
Figure 4.2	Purcell parameter histogram	31
Figure 4.3	Thomeer geometrical factor histogram	32
Figure 4.4	Winland parameter histogram.....	33
Figure 4.5	Swanson parameter histogram	34
Figure 4.6	Dastidar parameter histogram	35
Figure 4.7	Brooks and Corey index histogram.....	36
Figure 4.8	Pittman parameter histogram	37
Figure 4.9	Buiting and Clerke parameter histogram	38
Figure 4.10	Purcell permeability model results using published constants	41
Figure 4.11	Thomeer permeability model results using published constants	42
Figure 4.12	Winland permeability model results using published constants	43
Figure 4.13	Swanson permeability model results using published constants	44
Figure 4.14	Pittman permeability model results using published constants	45
Figure 4.15	Huet-Blasingame permeability model results using published constants.....	46
Figure 4.16	Dastidar permeability model results using published constants	47

Figure 4.17 Buiting-Clerke permeability model results using Laplace transform	48
Figure 4.18 Buiting-Clerke permeability model results using Thomeer parameters	49
Figure 4.19 Modified Purcell model results using three regression methods	55
Figure 4.20 Modified Thomeer model results using three regression methods	57
Figure 4.21 Modified Winland model results using three regression methods.....	58
Figure 4.22 Modified Swanson model results using three regression methods	60
Figure 4.23 Modified Pittman model results using three regression methods	61
Figure 4.24 Modified Huet-Blasingame model results using three regression methods..	62
Figure 4.25 Modified Dastidar model results using three regression methods	63
Figure 4.26 Modified Buiting-Clerke model results using three regression methods.....	65

LIST OF ABBREVIATIONS

AARE	:	Average Absolute Relative Percent Error
ARE	:	Average Relative Percent Error
a_i	:	Incremental volume of mercury at the i^{th} capillary pressure
a_T	:	Total incremental volume of mercury injected
B_v^∞	:	Fraction of bulk volume occupied by mercury at infinite capillary pressure
B_v^Q	:	Fraction of bulk volume with respect to in logarithmic domain
\hat{B}_v^Q	:	Laplace transformation of fractional bulk volume in logarithmic domain
d	:	Relevant geometric mean
D_λ	:	Fractal dimension
F	:	Purcell lithology factor
F_g	:	Thomeer shape factor
F_p	:	Purcell integral
F_S	:	Swanson parameter
k	:	Absolute permeability
L	:	Sample length
L_d	:	Length of the shortest flow path
L_i	:	Length of the i^{th} portion of the rock
MAE	:	Absolute Relative Percent Error

MICP	:	Mercury Injection Capillary Pressure
P_c	:	Capillary pressure
P_d	:	Entry pressure
R	:	Correlation Coefficient
r	:	Pore throat radius
r_{apex}	:	Pore throat radius at apex of MICP plot
RMS	:	Root Mean Squares
r_{35}	:	Pore throat radius at 35% mercury saturation
Q	:	Natural logarithm of capillary pressure
Q_d	:	Natural logarithm of entry pressure
Q_{max}	:	Maximum rate in two phase displacement model
Q_{min}	:	Minimum rate in two phase displacement model
R_i	:	Pore throat radius at the i^{th} capillary pressure
R_{WGM}	:	Weighted geometric mean of pore throat radii
S	:	Fraction of total pore space occupied by liquid
S_b	:	Percent bulk volume occupied by mercury
$S_{b\infty}$:	Percent bulk volume occupied by mercury at infinite capillary pressure
S_w	:	Wetting phase saturation,
S_{wi}	:	Irreducible wetting phase saturation
w_i	:	Weight function defined at the i^{th} capillary pressure

Greek symbols

λ : Brooks and Corey index

σ : Interfacial tension

σ_{Hg-air} : Interfacial tension for mercury-air system

θ : Contact angle

ϕ : Porosity

ABSTRACT

Full Name : Hasan Abdul-Elah Nooruddin
Thesis Title : Permeability Prediction using Mercury Injection Capillary Pressure Data
Major Field : Petroleum Engineering
Date of Degree : January 2013

In this study, a large dataset containing 225 carbonate rock samples are used to determine capillary pressure profiles using mercury injection capillary pressure technique. A thorough screening and validation process is implemented to remove bad data points. The process involves building porosity cross-plots between mercury porosity and air porosity. A difference of more than one porosity unit is used as a criterion to indicate and remove bad samples. Another validation process proposed in this study involves creating numerical pressure derivatives plots. The degree of dispersion gives an indication of the accuracy of the data. Both processes have caused 19 samples to be decimated from our dataset used to predict permeability. Nine Permeability models that use mercury injection capillary data are compared using a thorough statistical and graphical analysis. The permeability models are: Purcell model, Thomeer model, Winalnd model, Swanson model, Pittman model, Huet-Blasingame model, Dastidar model, Buiting-Clerke model using Laplace transform and Buiting-Clerke model using Thomeer parameters. The adapted methodology used in this comparative study is to compare all models with their published constants first. After that, generalized forms of the permeability models are used and new sets of coefficients are determined that best fit the dataset. Three different fitting methods are applied in this study; i) the ordinary nonlinear least-squares regression, ii) robust

fitting method using weighted nonlinear regression and iii) the multiple regressions of nonlinear models after linearization. The comparison study show that Swanson and Winland permeability models to outperform all other models used in the analysis. The generalized form of Purcell model also show good results.

ملخص الرسالة

الاسم الكامل: حسن عبدالاله نورالدين

عنوان الرسالة: دراسة تحديد قيم نفاذية الصخور باستخدام طريقة حقن الزئبق خلال الاتابيب الدقيقة

التخصص: هندسة نفط

تاريخ الدرجة العلمية: صفر 1434

لقد تم استخدام في هذه الدراسة 225 عينة صخرية منتقاة من بعض مكامن البترول الكربونية وتم قياس الضغط الشعري لكل العينات باستخدام طريقة الحقن الزئبقي. أجرينا عملية تحقيق وتدقيق للبيانات المقاسة بطريقتين مختلفتين. الطريقة الأولى هي طريقة مقارنة قيم المسامية المقاسة عن طريق مقياس المسامية الهوائي والزئبقي. تم استبعاد كل العينات التي يكون ناتج الفرق بين القياسين اكبر من وحدة مسامية واحدة. الطريقة الثانية المستخدمة هي طريقة حساب المشتقة العددية. وهذه الطريقة تتم عن طريق حساب المشتقة الاولى والثانية لقيم الضغط الشعري. لاحظنا ان درجة تشتت القيم يعطي مؤشر عن دقة البيانات المقاسة. باستخدام الطريقتين اتضح ان هناك 19 عينة يجب التخلص منها وازالتها. استخدمت العينات الباقية وهي 206 عينة لحساب قيمة النفاذية باستخدام 9 نماذج مختلفة وقورنت هذه النماذج مع قيم النفاذية الاصلية للعينات مقارنة دقيقة بالاستعانة بالتحليل الاحصائي والرسم البياني. نماذج النفاذية التي تمت مقارنتها هي: بورسيل, ثومير, ونلاندر, سوانسن, بتمان, بلازنقيم-هويت, داستيدار, بوتينج-كليرك. المنهجية المتبعة في هذه الدراسة تمت بمقارنة جميع النماذج كما نشرت في المطبوعات بدون اي تحديث. بعد ذلك تمت مقارنة للنماذج بعد ان تم تحديثها بقاعدة البيانات المتاحة لدينا. عملية التحديث هذه تمت باستخدام ثلاثة طرق مختلفة. اظهرت الدراسة ان نموذج سوانسن و ونلاندر هما افضل النماذج. نموذج بورسيل ايضا اظهر نتائج جيدة بعد التحديث.

CHAPTER 1

INTRODUCTION

Permeability is one of the most important parameters to quantify in any reservoir rock. Its importance arises due to the very critical and essential role this parameter plays during field development plans. Literature shows that permeability can be measured by three major techniques; i) well testing, ii) routine core analysis, and iii) formation testers (Ahmed et al., 1991).

Capillary pressure is defined as the difference in pressure between two immiscible fluids across a curved interface at equilibrium (Taib and Donaldson, 2004). Many authors have attempted to estimate permeability from capillary pressure measurements (Purcell, 1949; Katz and Thompson, 1986; Thompson and Katz, 1987; Comisky et al., 2007; Swanson, 1981; Huet et al., 2005; Pittman, 1992), particularly using mercury injection capillary pressure method (MICP).

Several techniques have been employed to determine capillary pressure profiles for porous media. They mainly fall into three principal categories; i) porous disk measurement, ii) mercury injection, and iii) centrifuge measurement (Taib and Donaldson, 2004).

The porous disk measurement was first introduced by Leverett and by Bruce and Welge (Brown, 1951). It is considered as the most accurate method that meets most oil industry requirements. However, a serious limitation of this method is imposed by the fact that saturation equilibrium may require several days or weeks to be achieved at each pressure step. Other limitation includes the unsuitability of handling relatively small, irregular shaped pieces of rock (Purcell, 1949).

Mercury injection can be used to determine capillary pressure curves very rapidly. It can be used on irregular shaped samples. Other advantages of mercury injection method include the wide and large range of pressure stabilization points that can be reached. MICP has been used extensively in the study of pore size distribution and pore type classification. This is mainly due to the fact that MICP reflects the complexity of the pore geometry and pore throat radius profile of the analyzed samples (Libny, 2001). However, cores cannot be reused for additional testing due to the presence of mercury inside that core. In addition, mercury vapor is very toxic and special procedure must be followed when dealing with mercury (Taib and Donaldson, 2004).

The centrifuge method offers the advantage of reaching saturation equilibrium at relatively short time compared to porous plate technique; however, the calculation of capillary pressure with this technique is somehow tedious (Purcell, 1949).

Although the porous plate technique is considered to be the most reliable and accurate method to estimate capillary pressure curves at reservoir conditions, the mercury injection technique is more practical due to the speed at which results can be obtained. However, the results of mercury injection method have to be converted by a conversion

factor to yield to those capillary pressures obtained at reservoir conditions and fluids (Brown, 1951).

Since the early stage of the oil industry, many authors have recognized the importance of capillary pressure measurements using mercury injection method (MICP) in quantifying pore throats and predicting permeability values. For that reason, numerous permeability models have been developed and proposed in literature (Brown, 1951; Shafer and Nwasham, 2000; Libny, 2001; Wardlaw and Taylor, 1976; Pickell, 1966; Katz and Thompson, 1986).

1.1 Statement of the Problem

MICP data are being used extensively in the oil industry as a direct way to identify and characterize pore geometrical distributions and pore-throat properties. Since pore-throats control the permeability of reservoir rocks, accurate permeability values should be obtained. Literature has reported many permeability models that use different parameters. Some models are purely empirical, and some models have various theoretical backgrounds by considering a porous media as a bundle of capillary tubes. The Inherent oversimplified assumptions of the latter approach may not represent the real phenomena adequately. Therefore, finding the best model to be used in order to obtain accurate permeability prediction is a challenging task.

1.2 Objectives

In this study, a thorough comparison between major permeability models available in literature is demonstrated and evaluated against large data set of MICP experimental tests done on carbonate samples. A method to check and screen MICP data received from laboratory is also presented. Finally, a new approach to estimate permeability is developed.

1.3 Proposed Approach

A large MICP data set will be utilized to test various permeability models. First of all, a description of the tool that is used to measure and determine capillary pressure data is presented followed by a section on possible source of errors in experimental measurement. After that, an explanation of a method to check the experimental data is demonstrated. Next, a program is written to read all MICP data and extract all parameters (e.g., Swanson parameter, area under the curve, threshold entry pressure, capillary pressure at different mercury saturations, Thomeer parameters, Brooks and Cory parameters, ...etc) used in all permeability models. A new approach is also presented to estimate permeability.

CHAPTER 2

STATE-OF-THE-ART AND PROPOSED MODIFICATION TO PERMEABILITY PREDICTION MODELS

MICP data can be used as a direct way to identify and characterize pore geometrical distributions and pore-throat properties. For that reason, MICP data offers a direct indication of permeability which is controlled by those properties (Haro, 2004). Comisky et al. (2007) and others (Gueguen and Palciauskas, 1994) reported that Permeability estimation from MICP data can be categorized into two main categories:

Models derived using Percolation theory:

Percolation is a simple probabilistic model which exhibits a phase transition (Kesten, 2006). It can be applied to model the fluid flow behavior through random porous media (Fleming III, 1983).

Models derived using Poiseuille model:

Poiseuille's equation describes the fluid flow through a bundle of capillary tubes. Most permeability models derived using this approach consider the porous media as a bundle

of capillary tubes. The resultant models are considered as analytical. Capillary tube radii (r) can be estimated in a porous rock using Washburn equation (Washburn, 1921):

$$r = \frac{2\sigma \cos\theta}{P_c} \quad (2.1)$$

where, (σ) is the interfacial tension, (θ) is contact angle and (P_c) is the capillary pressure. It should be mentioned that literature showed large number of permeability models that include some parameters other than those obtained by MICP data (Wyllie and Spangler, 1952; Katz and Thompson, 1987; Hagiwara, 1986; Glover and Zadjali, 2006; Nooruddin and Hossain, 2011). This study focuses only on permeability models derived using MICP data. Following are major and most popular permeability models available in literature. Before that, capillary pressure description models are presented since their parameters are used explicitly in most permeability models.

2.1 Capillary Pressure Description Models

Researchers have noticed that each capillary pressure curve can be uniquely defined using certain parameters. Few models have been reported in literature to describe capillary pressure curves (Thomeer, 1960; Brooks and Corey, 1966). Major models used to describe capillary pressure curves are reported here in their shorter version.

In 1960, Thomeer (1960) showed that each capillary pressure curve using mercury injection method can be described using three pore-network parameters. Thomeer proposed the following model:

$$\frac{S_b}{S_{b\infty}} = e^{-F_g/\log(\frac{P_c}{P_d})} \quad (2.2)$$

where, (S_b) is percent bulk volume occupied by mercury, $(S_{b\infty})$ is percent bulk volume occupied by mercury at infinite capillary pressure or total interconnected pore volume, (F_g) is a parameter defines capillary pressure curve and (P_d) is the mercury/air extrapolated pressure which indicates the entry pressure to the largest pores. Thomeer hypothesized that (F_g) is a shape factor that reflects the pore throat distribution and their associated pore volumes.

Brooks and Corey (1966) proposed a power-law model to characterize capillary pressure curves. The model formula is given by:

$$P_c = P_d \left(\frac{S_w - S_{wi}}{1 - S_{wi}} \right)^{-1/\lambda} \quad (2.3)$$

where, (S_w) is the wetting phase saturation, (S_{wi}) is the irreducible wetting phase saturation and (λ) is an index reflecting pore size distribution according to Brooks and Corey.

2.2 State-of-the-art Permeability Prediction Models Using MICP

Purcell Permeability Model:

In 1949, Purcell introduced for the first time a method to determine capillary pressure curves for porous media by forcing mercury into a core sample that is being held under vacuum pressure. He also proposed a method to calculate permeability by considering the

porous media as a bundle of capillary tubes having similar lengths but different radii. To account for heterogeneity found in natural rock systems, Purcell introduced a lithology factor. The model has the following form:

$$k = \frac{(\sigma_{Hg-air} \cos \theta)^2 F \phi}{2} \int_{S=0}^{S=1} \frac{dS}{P_c^2} \quad (2.4)$$

where, (k) is the permeability in D, (σ_{Hg-air}) is the interfacial tension for mercury-air system in dynes/cm, (θ) is the contact angle in degrees, (F) is the lithology factor in dimensionless quantity, (ϕ) is the porosity in fraction, (S) is fraction of total pore space occupied by liquid and (P_c) is the capillary pressure expressed in atmospheres.

Since (σ_{Hg-air}) and (θ) for mercury-air system can be considered constant at 480 dynes/cm and 140° , respectively. Equation 2.4 can be written as:

$$k = 0.66 \times 10^4 F \phi \int_{S=0}^{S=1} \frac{dS}{P_c^2} \quad (2.5)$$

Expressing (P_c) in psi and (k) in mD will lead to the following expression:

$$k = 1,441,278 F \phi \int_{S=0}^{S=1} \frac{dS}{P_c^2} \quad (2.6)$$

Purcell used a total of 27 rock samples from sandstone formations to test his model. The air permeability in his data set ranged from less than 0.1 mD to 1459 mD. Purcell used a lithology factor (F) of 0.216 to estimate permeability values.

Thomeer Permeability Model:

Thomeer proposed two permeability models (Thomeer, 1969; 1983). The latter model is basically an update of the first one with an additional parameter (F_g) and new constants.

Thomeer permeability model is given by:

$$k = 3.8068 F_g^{-1.3334} \left(\frac{S_{b\infty}}{P_d} \right)^2 \quad (2.7)$$

where, (F_g) and $(S_{b\infty})$ are Thomeer parameters defined previously in Equation 2.2.

Thomeer used 279 rock samples in which 165 are sandstones and 114 are carbonates. He used uncorrected air permeability measurements ranging from less than 0.1 mD to more than 2000 mD.

Winland Permeability Model:

Winland developed a correlation to estimate absolute permeability using pore throat radius that corresponds to 35% mercury saturation using mixed dataset of 82 samples (56 sandstones and 26 carbonates) that have corrected low permeability measurements and 240 uncorrected permeability samples (Pittman, 1992). The equation has the following form (Kolodize, 1980):

$$\log r_{35} = -1.002 + 0.588 \log k - 0.867 \log \phi \quad (2.8)$$

Winland found that the (r_{35}) gives the best correlation with permeability and porosity.

Rewriting Equation 2.8 in terms of permeability (k) :

$$k = 49.45 r_{35}^{1.7} \phi^{1.47} \quad (2.9)$$

Swanson Permeability Model:

In 1981, Swanson proposed a correlation that relates air permeability to MICP data using 319 rock samples; 203 sandstones and 116 carbonate samples. The relationship is given by:

$$k = 399 \left(\frac{S_b}{P_c} \right)_A^{1.691} \quad (2.10)$$

where, $\left(\frac{S_b}{P_c} \right)_A$ is taken at point (A) that represents the apex of a hyperbolic log-log plot of capillary pressure against mercury saturation. Swanson argued that this point defines the effective pore throats that contribute to the fluid flow.

Pittman Permeability Model:

Pittman (1992) developed multiple correlations to determine pore aperture radii at different mercury saturation percentile. He showed that uncorrected air permeability is best estimated at the apex shown on the plot of the ratio of mercury saturation over capillary pressure against mercury saturation. The following expression was developed:

$$\log r_{apex} = -0.315 + 0.475 \log k - 0.099 \log \phi \quad (2.11)$$

Pittman found that (r_{apex}) at average is closer to 36% mercury saturation. Pittman's data set contained 202 rock samples from sandstone reservoirs only. Uncorrected air permeability values were measured and ranged from 0.05 mD to 998 mD.

Rewriting Equation 2.11 in terms of permeability(k):

$$k = 4.6 r_{apex}^{2.105} \phi^{0.208} \quad (2.12)$$

Huet-Blasingame Permeability Model:

In 2005, Huet et al. proposed a semi-analytical model based on modified Purcell/Burdine model . The mathematical formula is given by the following expression:

$$k = 10.66 \alpha (\sigma_{Hg-air} \cos \theta)^2 (1 - S_{wi})^4 \phi^2 \frac{1}{P_d^2} \left[\frac{\lambda}{\lambda + 2} \right] \quad (2.13)$$

where, (α) is a fit parameter, and (λ) is the Brooks and Corey index . A dataset of 89 sandstone samples have been used to test this model. The following constants have been adjusted to their dataset:

$$k = 1017003 (1 - S_{wi})^{0.5475} \phi^{1.6498} \frac{1}{P_d^{1.7846}} \left[\frac{\lambda}{\lambda + 2} \right]^{1.6575} \quad (2.14)$$

Since for MICP data, S_{wi} is very small and can be ignored and hence, Equation 2.14 is reduced to:

$$k = 1017003 \phi^{1.6498} \frac{1}{P_d^{1.7846}} \left[\frac{\lambda}{\lambda + 2} \right]^{1.6575} \quad (2.15)$$

Dastidar Permeability Model:

Dastidar et al. (2007) proposed an empirical correlation to estimate permeability using a weighted geometric mean of pore throat radii. Dastidar and his co-authors argued that weighted geometric mean of pore throat radii accounts for contribution of small radii especially in tighter rocks. A data set of 150 samples was used to develop their permeability model. The following correlation was developed:

$$\log k = 3.61 + 3.06 \log \phi + 1.64 \log R_{WGM} \quad (2.16)$$

where (R_{WGM}), weighted geometric mean of pore throat radii , is calculated by:

$$R_{WGM} = [\prod_{i=1}^n R_i^{w_i}]^{1/\sum_{i=1}^n w_i} \quad (2.17)$$

where (w_i) is a weight function having the following expression:

$$w_i = \frac{a_i}{a_T} \quad (2.18)$$

where (a_i) is the incremental volume of mercury at the i^{th} capillary pressure and (a_T) is the total incremental volume of mercury introduced into the sample in volume units. 150 samples with klinkenberg-corrected permeability measurements have been used to test and validate the proposed model.

Buiting and Clerke Permeability Model:

Recently, Buiting and Clerke¹ developed a fundamental expression of permeability by considering the porous media as a bundle of tortuous and fractal capillary tubes. The developed model has a very special feature; that is, no fitting constants are required to obtain the solution. They showed that permeability of well-connected porous media can be expressed in terms of the Laplace transformation; the model has the following form:

$$k = \frac{1}{4} D_\lambda e^{-2(1-D_\lambda)Q_d} \left(\frac{L}{L_d}\right)^2 \hat{B}_v^Q(2D_\lambda) \quad (2.19)$$

where (D_λ) is the fractal dimension and should be between 1.5 and 1.8 for tortuous fluid flow path in porous media according to Buiting and Clerke, (Q_d) is equal to $\ln(P_d)$, $\left(\frac{L}{L_d}\right)$

¹ Personnel communication with the authors. This model will be published soon in JPSE.

is the ratio of sample length to the length of the shortest flow path, and the term $\hat{B}_v^Q(2D_\lambda)$ is the complete Laplace transform of the fractional bulk volume (B_v) in (Q) domain, where $Q = \ln(P_c)$, and have the following expression:

$$\hat{B}_v^Q(2D_\lambda) = \int_{Q=0}^{\infty} B_v^Q(Q) e^{-2D_\lambda Q} dQ \quad (2.20)$$

Buiting and Clerke stated that the parameters $\left(\frac{L}{L_d}\right)$ and (D_λ) are global parameters and can be determined by the fractal pore geometry's topology. They also showed that $\left(\frac{L}{L_d}\right)$ and (D_λ) can be approximated as 0.5 and 1.56, respectively. The global parameters have been adjusted numerically using a dataset containing more than 500 data points.

Another model has been formulated using Thomeer parameters with some approximation to Equation 2.19. The mathematical expression is given by:

$$k = 506000 \frac{B_v^\infty}{P_d^2} e^{-4.43\sqrt{F_g}} \quad (2.21)$$

where (B_v^∞) is similar to $(S_{b\infty})$ defined in Thomeer model.

Comisky et al. (2007) made an extensive comparison of permeability models using MICP measurements using 63 tight gas sand samples. The permeability of the dataset ranged from 0.0001 mD to 0.2 mD. The authors compared in their study eight different models: Purcell, Swanson, Walls-Amaefule, Katz-Thompson, Pittman, Kamath, Huet-Blasingame and Dastidar models. The study showed that Katz-Thompson model provided the best permeability estimation. They also demonstrated that Purcell's correlation can provide good results by modifying the lithology factor (F) from published value of 0.216 to an optimized value of 0.15.

2.3 Proposed Modification to Permeability Prediction Models

Permeability models published in literature have been calibrated using authors datasets. In comparison studies, it is recommended to pinch mark all models to a reference dataset. All permeability models' coefficients should also be calibrated to the same dataset used to make the comparison.

Although the original form of Purcell permeability model given in Equation 2.6 has only one parameter, Purcell parameter (F), to be calibrated, it is found that this parameter depends on permeability resulting in a nonlinear relation between permeability and Purcell integral (F_p). Therefore, a power law model between Purcell integral and permeability is recommended. Similarly, porosity has a nonlinear relation to permeability and hence, a power law model is suggested. Combining these two observations leads to the modified Purcell permeability model proposed in this study. The mathematical expression of the model is given by:

$$k = a_{p1} \phi^{a_{p2}} \left(\int_0^1 \frac{dS}{p_c^2} \right)^{a_{p3}} \quad (2.22)$$

For Thomeer permeability model, the original model (Equation 2.7) contains three coefficients. The modified Thomeer model, however, has four coefficients to be optimized. The additional coefficient to be determined is introduced to give better fit to the data. The modified form is given by the following equation:

$$k = a_{t1} F_g^{a_{t2}} S_{bo}^{a_{t3}} \left(\frac{1}{p_d} \right)^{a_{t4}} \quad (2.23)$$

The Modified Winland permeability model will not have any additional coefficients other than those that appear in the original form given is Equation 2.9. The modified model is given by:

$$k = a_{w1} r_{35}^{a_{w2}} \phi^{a_{w3}} \quad (2.24)$$

Similar to Winalnd model, the modified Swanson permeability model will have the same number of coefficients as the original form given by Equation 2.10. It can be noticed that Swanson model has the least number of constants between all permeability models used in this study. The modified Swanson model is given by the following expression:

$$k = a_{s1} \left(\frac{S_b}{P_c} \right)_A^{a_{s2}} \quad (2.25)$$

The original form of Pittman permeability model (Equation 2.12) contains three coefficients that are similar to the modified model given by:

$$k = a_{i1} r_{apex}^{a_{i2}} \phi^{a_{i3}} \quad (2.26)$$

The modified Huet-Blasingame permeability model contains four coefficients which is similar to the original model (Equation 2.15). The mathematical expression of the modified Huet-Blasingame permeability model is given by:

$$k = a_{h1} \phi^{a_{h2}} \frac{1}{P_d^{a_{h3}}} \left[\frac{\lambda}{\lambda+2} \right]^{a_{h4}} \quad (2.27)$$

The modified Dastidar permeability model shows three parameters to be adjusted, which is similar to the original form given in Equation 2.16. The modified form is given by the following equation:

$$k = a_{d1} \phi^{a_{d2}} R_{WGM}^{a_{d3}} \quad (2.28)$$

From previous section, Buiting and Clerke showed two permeability models. The first one uses Laplace transform of the fractional bulk volume (B_v) in (Q) domain (Equation 2.19). The other model is a practical approximation of the original model using Thomeer parameters and is given by Equation 2.21. Since the first model contains global parameters that should not change regardless of the dataset used, the second model is only used to be modified. The modified form is given by:

$$k = a_{b1} \frac{B_v^{\infty a_{b2}}}{P_d^{a_{b3}}} e^{-a_{b4} \sqrt{Fg}} \quad (2.29)$$

The modified permeability models will be used to calibrate all coefficients using the dataset that is obtained for this comparison study.

CHAPTER 3

LABORATORY DATA DESCRIPTION AND VALIDATION

In this study, a total of 225 samples from carbonate reservoirs have been used to generate capillary pressure profiles using MICP test. Air porosity and uncorrected-air permeability were determined beforehand. The permeability and porosity of the dataset range from less than 0.05 mD to 3570 mD and from 5 to 30 percent porosity unit, respectively. **Table 3.1** contains more statistical description of the MICP dataset used in this study. **Figures 3.1** through **Figure 3.4** also show graphical description and histograms of the data.

Air porosity measurements have been used to cross validate porosity measured using MICP experiment. All samples that show more than one porosity unit difference were excluded from the comparison study. The validation process of the data indicated 19 out of 225 samples as invalid. **Figure 3.5** displays the cross plot of MICP porosity versus air porosity. The plot shows that air porosity measurements are very close to porosity obtained from MICP.

A numerical derivative approach is also proposed in order to have an indication of the accuracy of the MICP data. **Figure 3.6** shows 1st and 2nd numerical derivatives of the capillary pressure curve. The figure indicates that as the order of derivatives increases, the data spreading increases as well. The degree of dispersion of the data gives an

indication of the accuracy of the lab measurements. Our dataset showed good responses and within acceptable limits.

Closure correction is another area of great uncertainty and has considerable impact on predicted permeability values. Closure correction is the process of adjusting the maximum entry pressure of a certain sample due to the fact that part of the mercury intruded into the sample must fill first the empty space between the plug outer surface and the pore body. Many authors have attempted to explain and resolve this issue. Clerke et al. (2008) gave a comprehensive explanation of this phenomenon. They also showed the process of correcting closure correction.

MICP data, in this study, has not been corrected for closure correction since the raw data appears not very much affected by this phenomenon. In addition, the correction process is very subjective and affects the permeability prediction significantly.

Table 3.1 Statistical description of core data used in the analysis

Sample Property	Min	Max	Average	St. Dev	Skewness	Kurtosis
Porosity (ϕ) , fraction	0.05	0.30	0.18	0.06	0.02	2.17
Permeability (k), mD	0.04	3570	115	354	6.54	55.0
Ln(k), mD	-3.35	8.18	2.13	2.73	-0.15	2.20
Pore Volume (V_p), cc	0.34	3.26	1.55	0.56	0.27	2.33
Bulk Volume (V_b), cc	3.76	12.73	8.69	1.44	-1.39	6.70

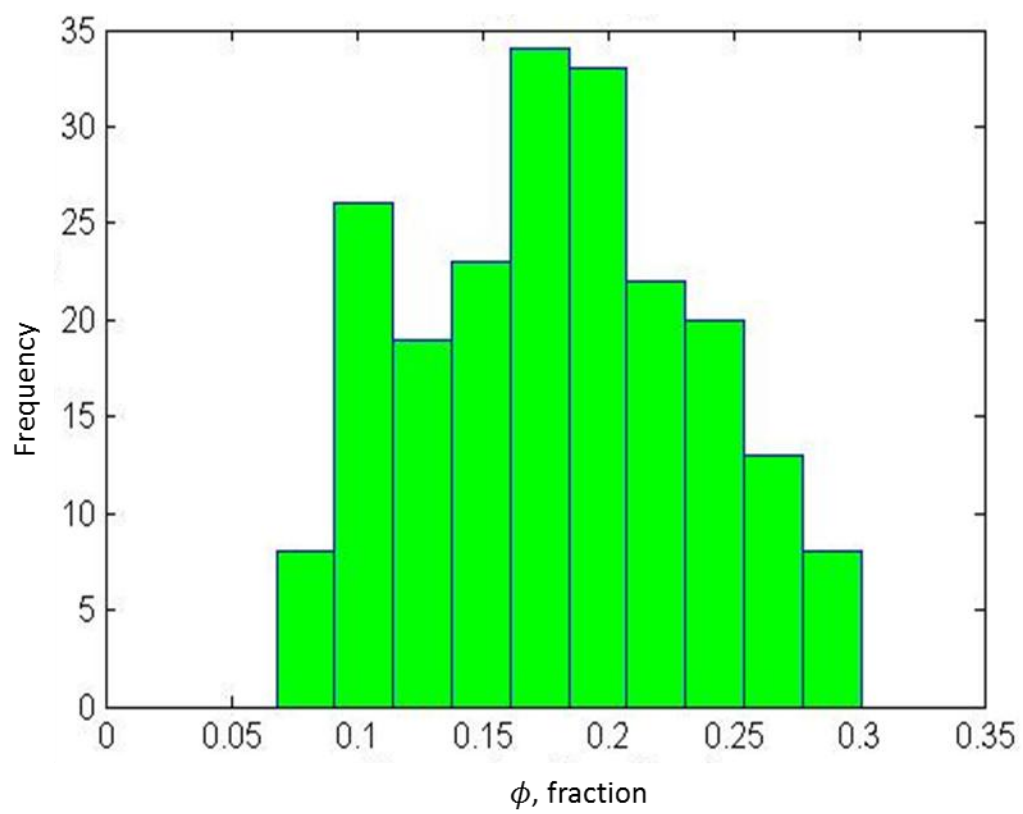


Figure 3.1 Porosity histogram of core data

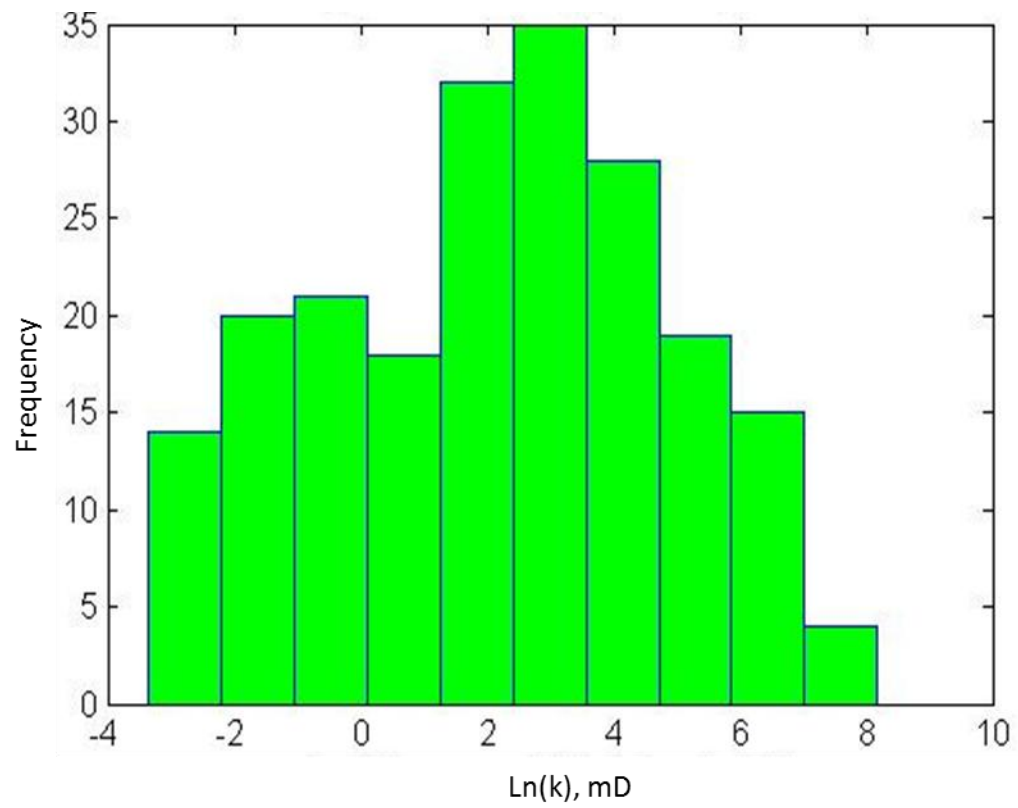


Figure 3.2 Histogram of natural log of permeability of core data

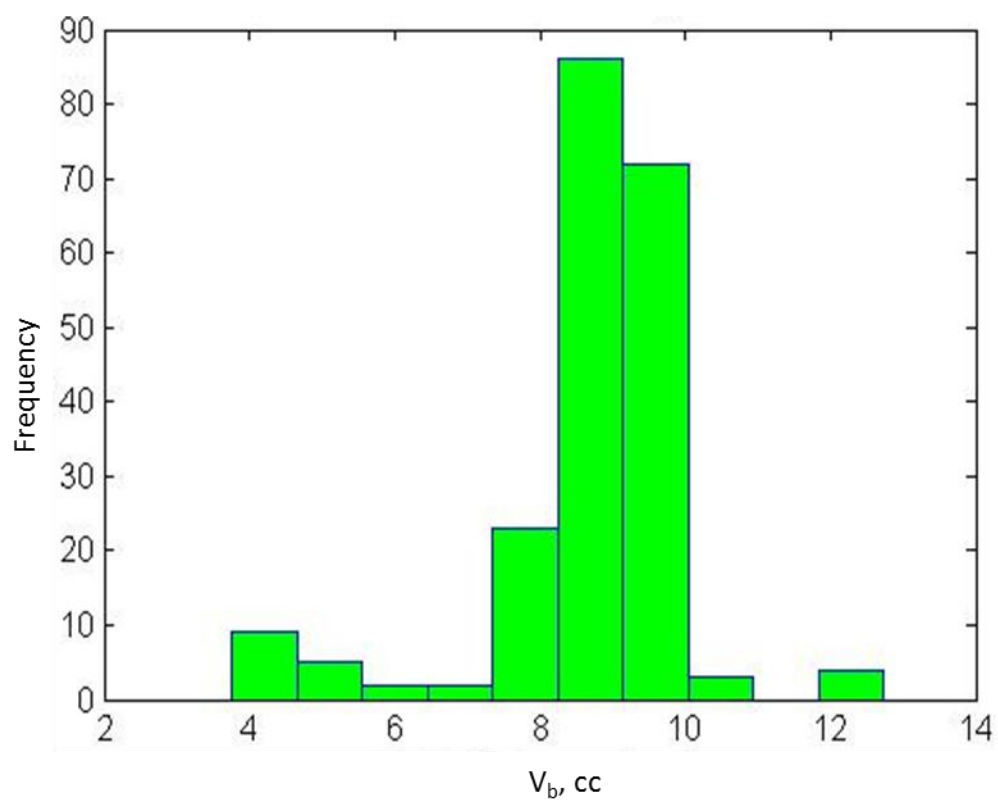


Figure 3.3 Bulk volume histogram

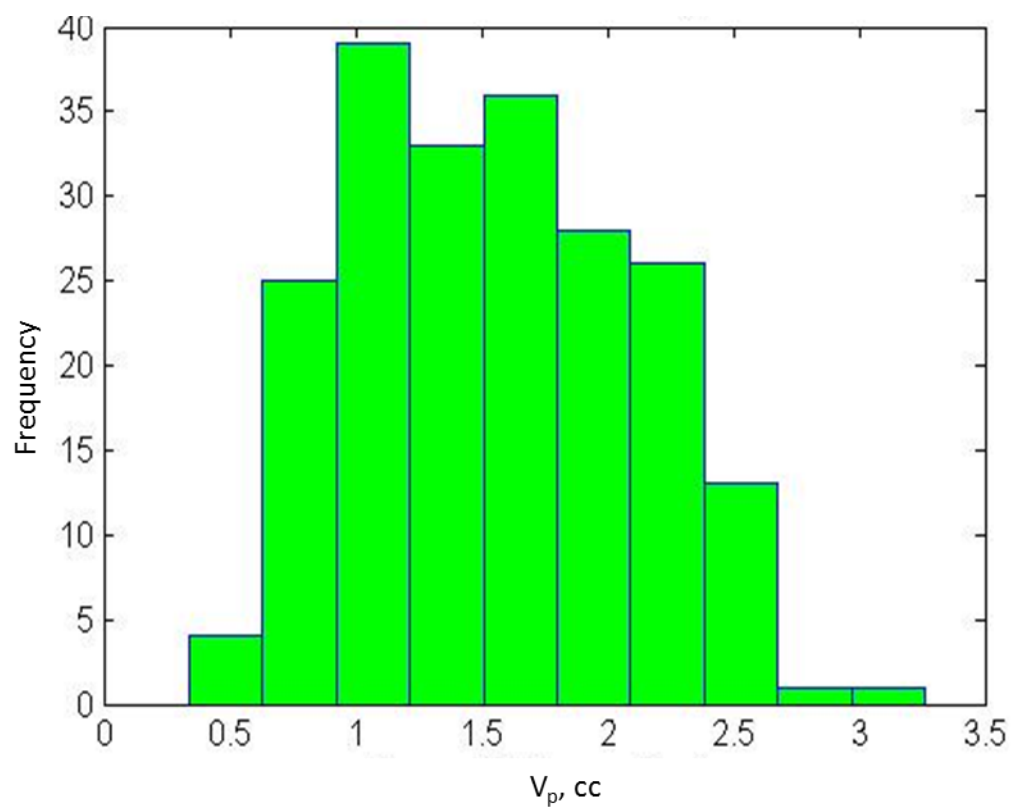


Figure 3.4 Pore volume histogram

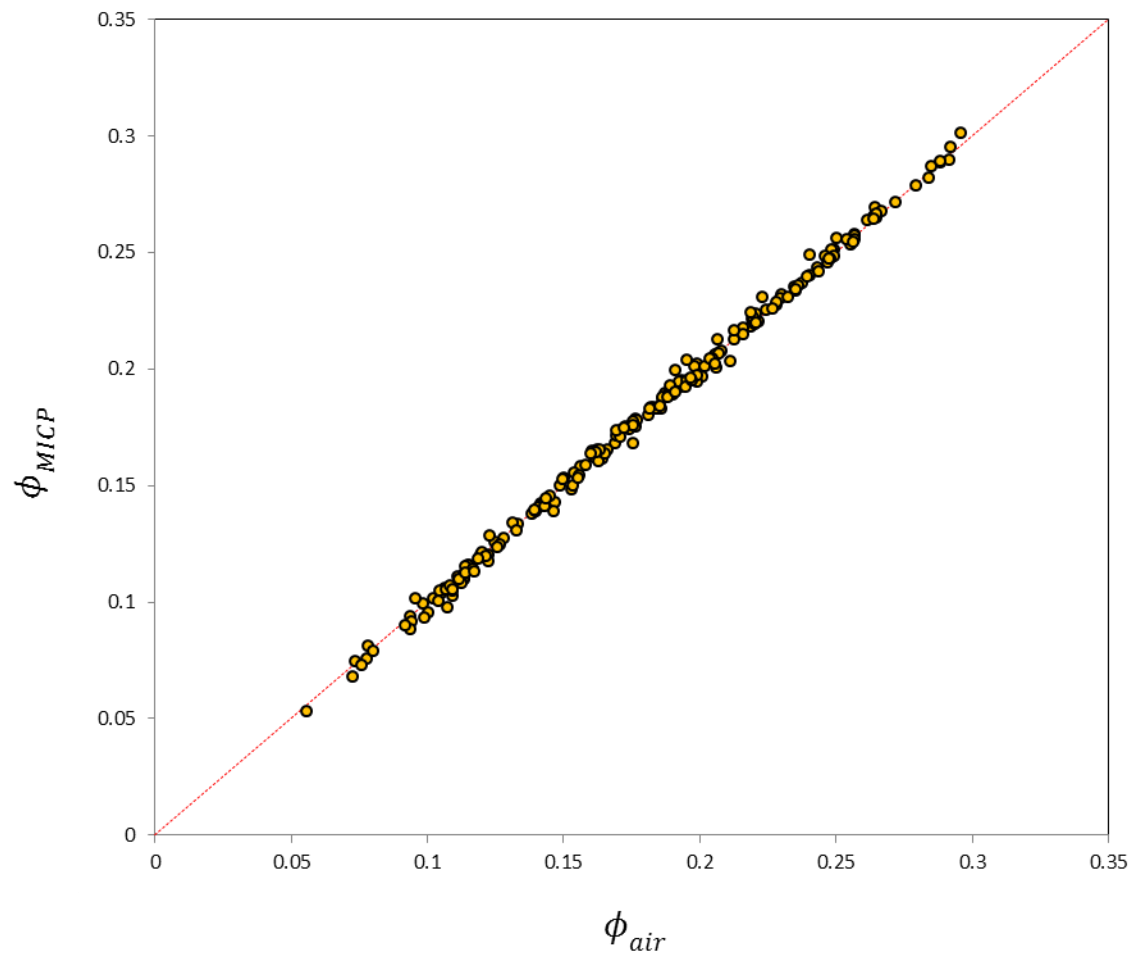


Figure 3.5 Porosity cross-plot between air porosity and MICP porosity

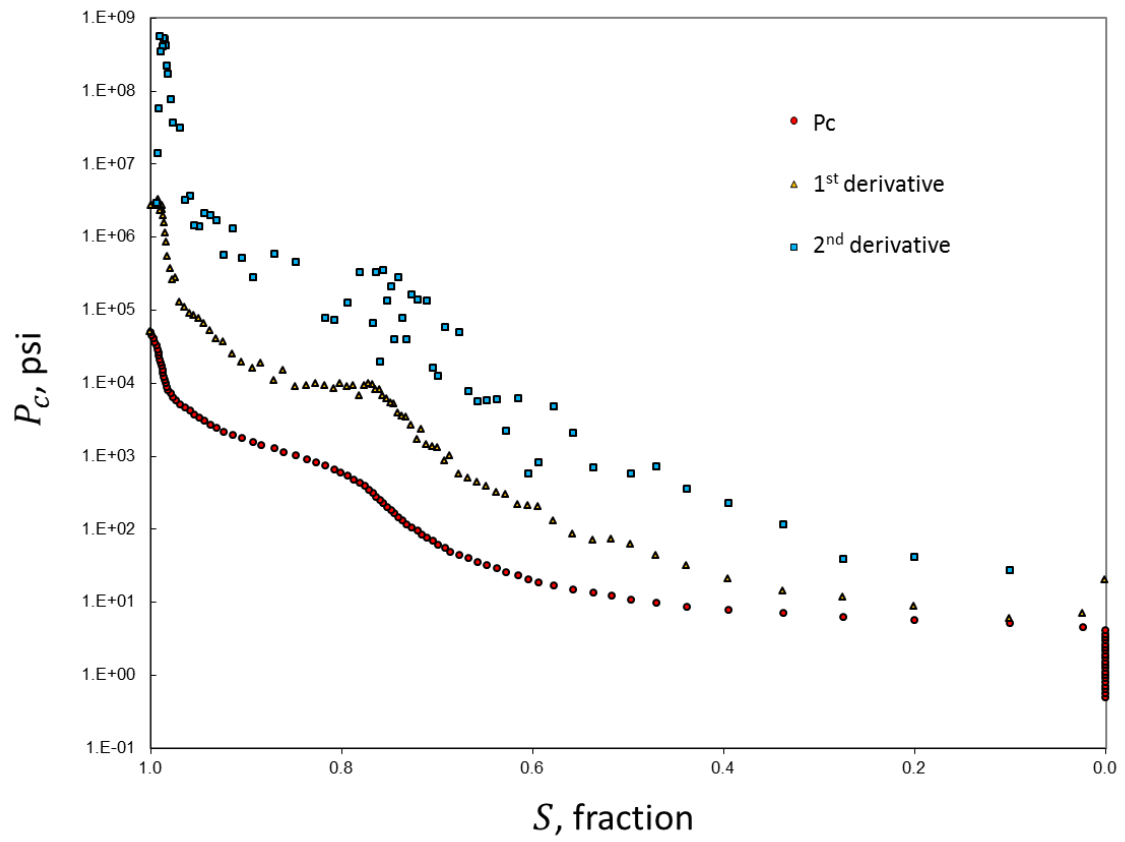


Figure 3.6 1st and 2nd numerical derivatives of the capillary pressure curve against mercury saturation

CHAPTER 4

RESULTS AND DISCUSSIONS

4.1 Extraction of Permeability Model Parameters

206 out of 225 samples have been used to extract all parameters used in permeability models described previously. Statistical description is presented in **Table 4.1**. Correlation matrix between all extracted parameters and core permeability values are presented in normal domain and in logarithmic domain as well in **Table 4.2** and **Table 4.3**, respectively. Correlation matrix indicates strong relation between core permeability and the following parameters, in order, $\hat{B}_v^Q(2D_\lambda)$, $\int_0^1 \frac{dS}{P_c^2}$ and $\left(\frac{S_b}{P_c}\right)_A$. While in logarithmic domain, all parameters show strong relation to air permeability except for F_g and λ . Swanson parameter $\left(\frac{S_b}{P_c}\right)_A$ has the highest value at 0.97.

Histograms are also presented in **Figures 4.1** to **Figure 4.9**. It is clearly observed that all parameters show log normal distribution except for Thomeer geometrical factor (F_g) (**Figure 4.3**). Brooks and Cory Index (λ) also exhibits close behavior to normal distributions (**Figure 4.7**).

Table 4.1 Statistical description of permeability model parameters

Model Parameters	Min	Max	Average	St. Dev	Skewness	Kurtosis
P_d, psi	1.6	2089.8	127.7	287.3	3.6	18.8
$\int_0^1 \frac{dS}{P_c^2}, psi^{-2}$	9.63E-08	0.0610	0.0039	0.0085	3.954	22.414
F_g, dim	0.089	0.878	0.416	0.158	0.486	2.871
$r_{35}, \mu m$	0.035	29.099	3.801	5.130	2.164	8.133
$r_{apex}, \mu m$	0.02361	29.842	4.3797	5.1984	1.8609	6.9279
$\left(\frac{S_b}{P_c}\right)_A, psi^{-1}$	1.29E-05	0.0237	0.0028	0.0040	2.435	9.892
$R_{WGM}, \mu m$	0.008	0.175	0.054	0.035	0.794	3.161
λ, dim	0.578	2.185	1.026	0.276	1.477	5.049
$\hat{B}_v^Q(2D_\lambda)$	4.23E-13	0.00173	5.40E-05	0.000191	6.3038	47.9

Table 4.2 Correlation matrix of air permeability and all extracted parameters in normal domain

	k, mD	$\int_0^1 \frac{dS}{P_c^2}, psi^{-2}$	P_d, psi	F_g, dim	$r_{35}, \mu m$	$\left(\frac{S_b}{P_c}\right)_A, psi^{-1}$	$R_{WGM}, \mu m$	λ, dim	$r_{apex}, \mu m$	$\hat{B}_v^Q(2D_\lambda)$
k, mD	1	0.8896	-0.1412	0.0028	0.8091	0.8478	0.6117	-0.2953	0.7405	0.8981
$\int_0^1 \frac{dS}{P_c^2}, psi^{-2}$	0.8896	1	-0.1983	0.0807	0.9247	0.9270	0.7568	-0.3997	0.9114	0.9365
P_d, psi	-0.1412	-0.1983	1	-0.4655	-0.3079	-0.2923	-0.5002	0.8725	-0.3517	-0.1233
F_g, dim	0.0028	0.0807	-0.4655	1	0.0032	0.0375	0.0846	-0.4850	0.2480	0.0873
$r_{35}, \mu m$	0.8091	0.9247	-0.3079	0.0032	1	0.9775	0.9200	-0.5497	0.9419	0.7713
$\left(\frac{S_b}{P_c}\right)_A, psi^{-1}$	0.8478	0.9270	-0.2923	0.0375	0.9775	1	0.8849	-0.5222	0.9367	0.8112
$R_{WGM}, \mu m$	0.6117	0.7568	-0.5002	0.0846	0.9200	0.8849	1	-0.7484	0.8829	0.5560
λ, dim	-0.2953	-0.3997	0.8725	-0.4850	-0.5497	-0.5222	-0.7484	1	-0.6039	-0.2624
$r_{apex}, \mu m$	0.7405	0.9114	-0.3517	0.2480	0.9419	0.9367	0.8829	-0.6039	1	0.7684
$\hat{B}_v^Q(2D_\lambda)$	0.8981	0.9365	-0.1233	0.0873	0.7713	0.8112	0.5560	-0.2624	0.7684	1

Table 4.3 Correlation matrix of air permeability and all extracted parameters in logarithmic domain

	k, mD	$\int_0^1 \frac{dS}{P_c^2}, psi^{-2}$	P_d, psi	F_g, dim	$r_{35}, \mu m$	$\left(\frac{S_b}{P_c}\right)_A, psi^{-1}$	$R_{WGM}, \mu m$	λ, dim	$r_{apex}, \mu m$	$\hat{B}_v^Q(2D_\lambda)$
k, mD	1	0.9422	-0.9199	0.2924	0.9529	0.9691	0.9526	-0.8416	0.9223	0.9433
$\int_0^1 \frac{dS}{P_c^2}, psi^{-2}$	0.9422	1	-0.9938	0.4611	0.9771	0.9792	0.9849	-0.9395	0.9934	0.9987
P_d, psi	-0.9199	-0.9938	1	-0.5484	-0.9521	-0.9571	-0.9636	0.9435	-0.9912	-0.9958
F_g, dim	0.2924	0.4611	-0.5484	1	0.2979	0.3105	0.3131	-0.5289	0.5082	0.4807
$r_{35}, \mu m$	0.9529	0.9771	-0.9521	0.2979	1	0.9858	0.9949	-0.9020	0.9565	0.9708
$\left(\frac{S_b}{P_c}\right)_A, psi^{-1}$	0.9691	0.9792	-0.9571	0.3105	0.9858	1	0.9883	-0.8873	0.9630	0.9789
$R_{WGM}, \mu m$	0.9526	0.9849	-0.9636	0.3131	0.9949	0.9883	1	-0.9156	0.9662	0.9796
λ, dim	-0.8416	-0.9395	0.9435	-0.5289	-0.9020	-0.8873	-0.9156	1	-0.9385	-0.9353
$r_{apex}, \mu m$	0.9223	0.9934	-0.9912	0.5082	0.9565	0.9630	0.9662	-0.9385	1	0.9932
$\hat{B}_v^Q(2D_\lambda)$	0.9433	0.9987	-0.9958	0.4807	0.9708	0.9789	0.9796	-0.9353	0.9932	1

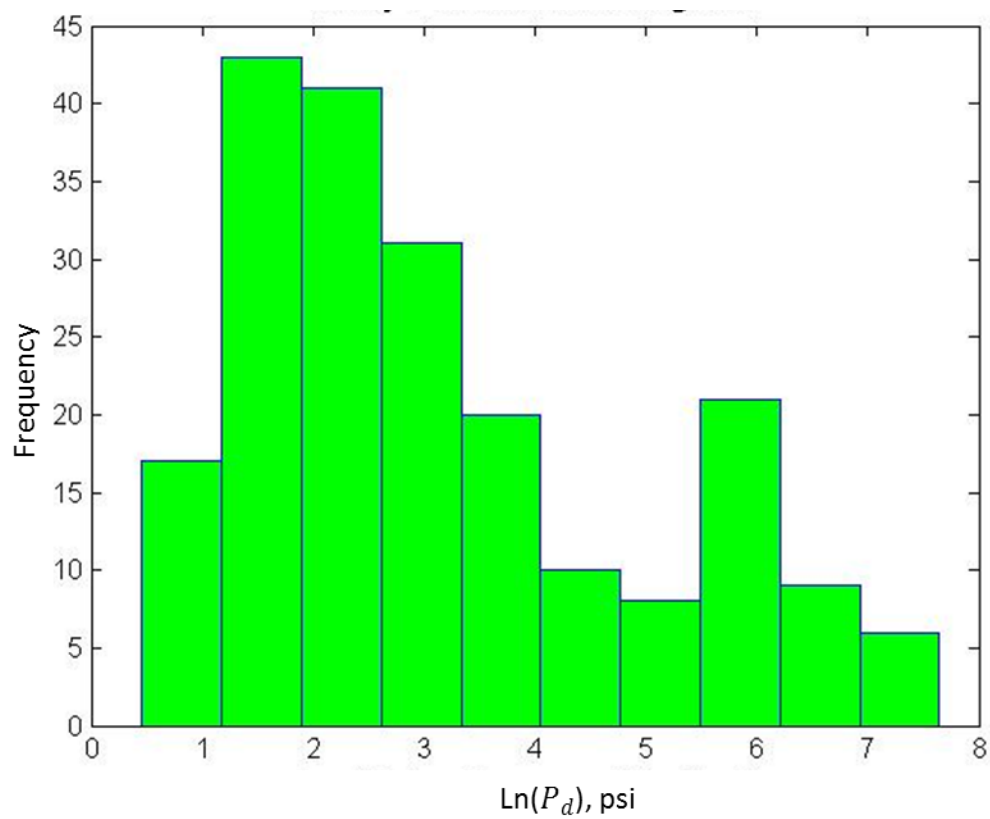


Figure 4.1 Entry pressure (P_d) histogram

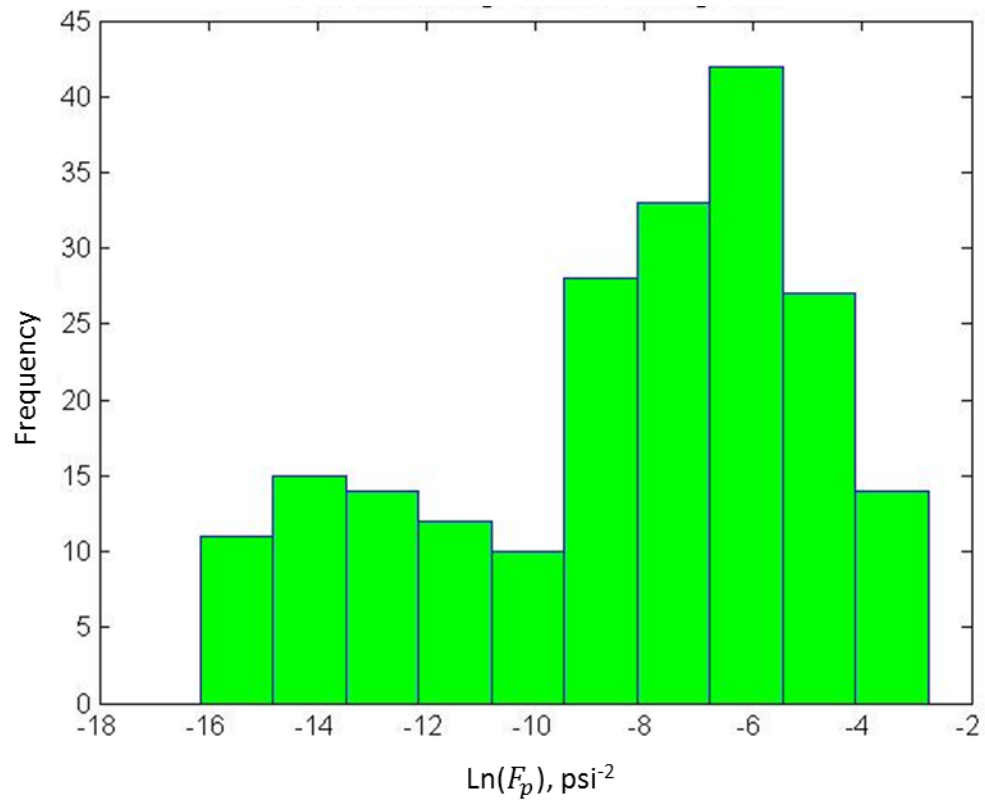


Figure 4.2 Purcell integration $\left(\int_0^1 \frac{dS}{p_c^2}\right)$ histogram

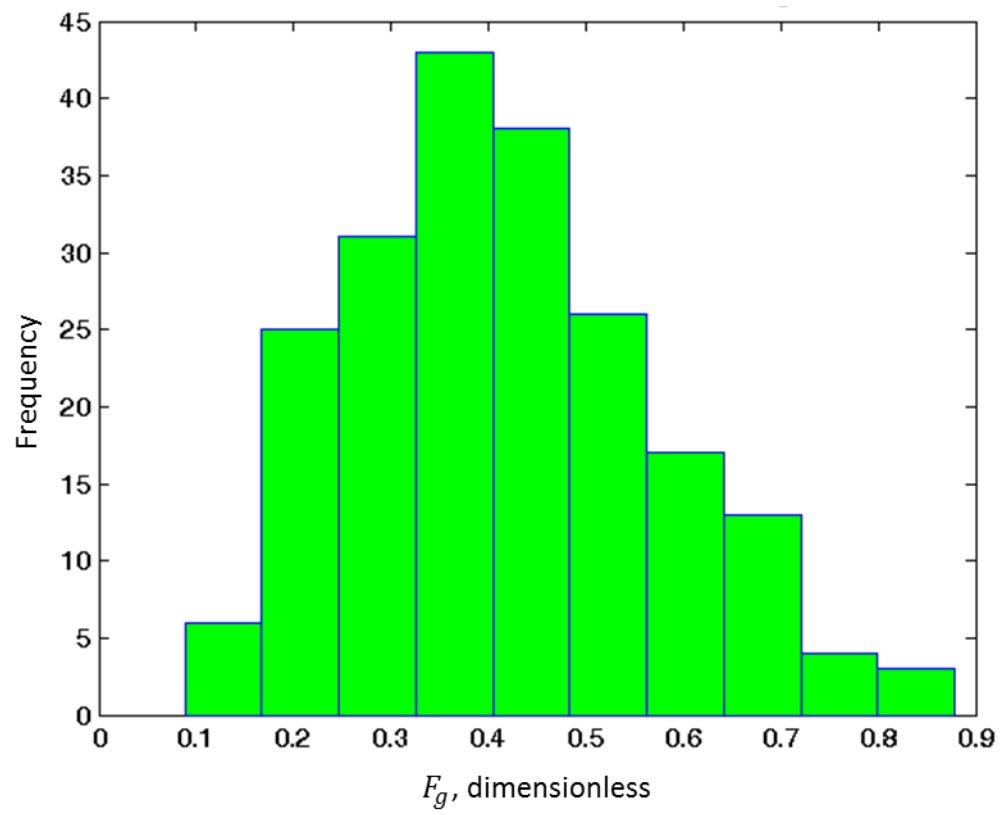


Figure 4.3 Thomeer geometrical factor (F_g) histogram

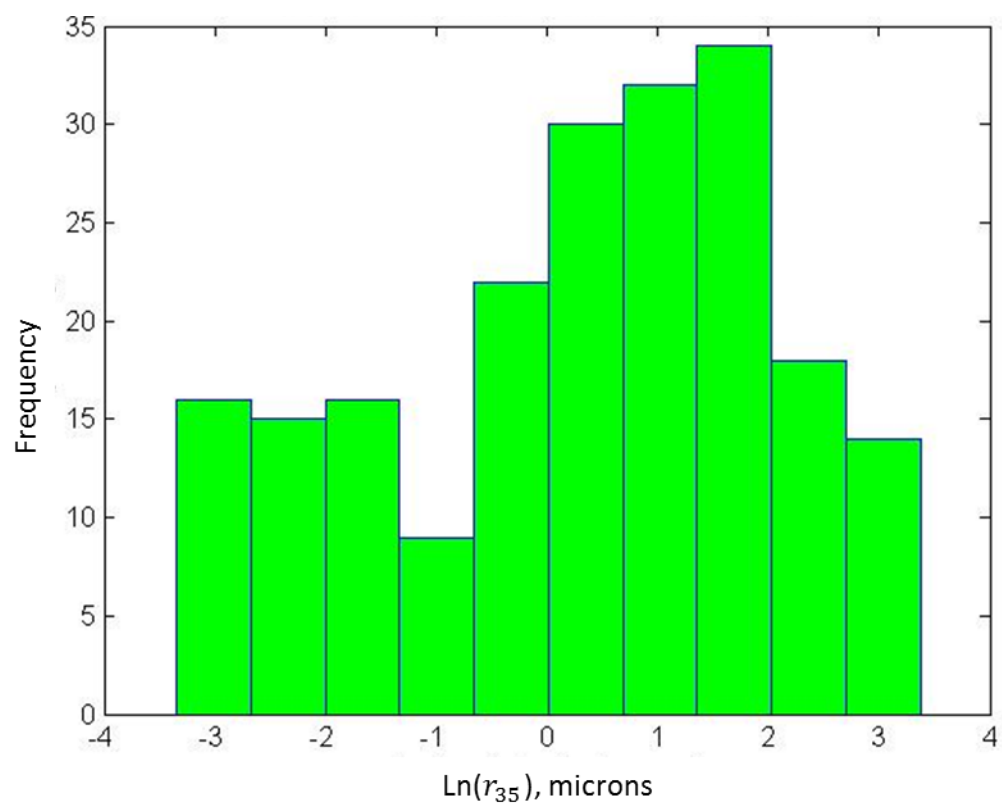


Figure 4.4 Winland parameter (r_{35}) histogram

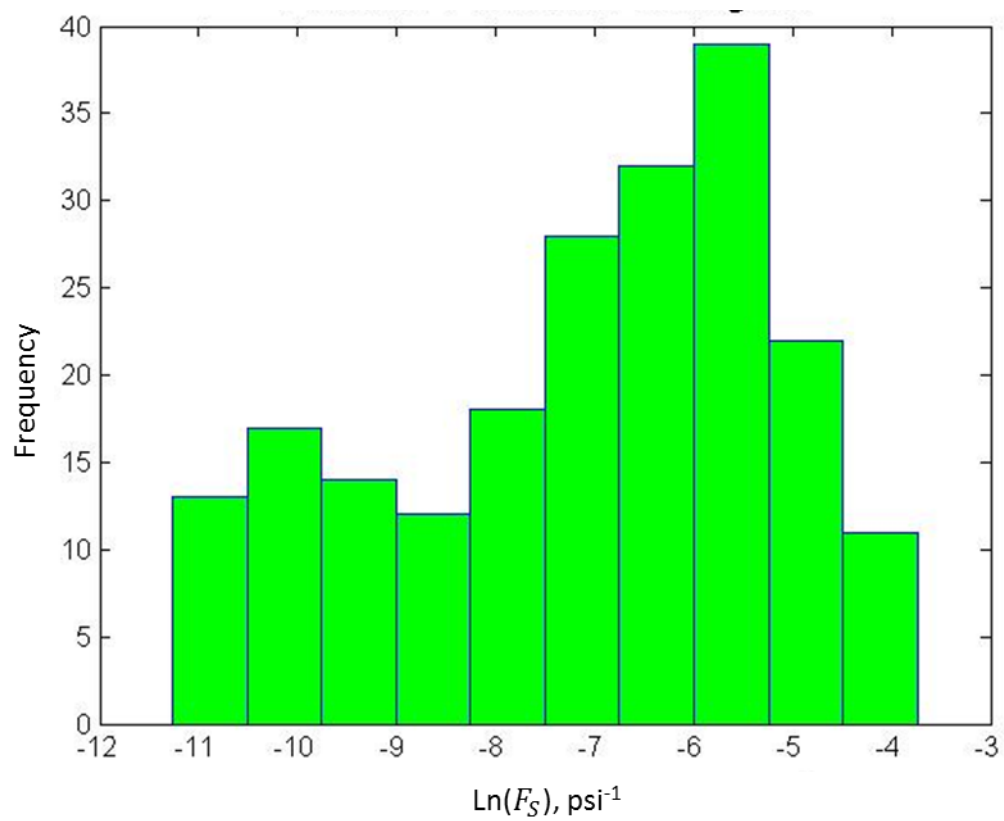


Figure 4.5 Swanson parameter $\left(\frac{S_b}{p_c}\right)_A$ histogram

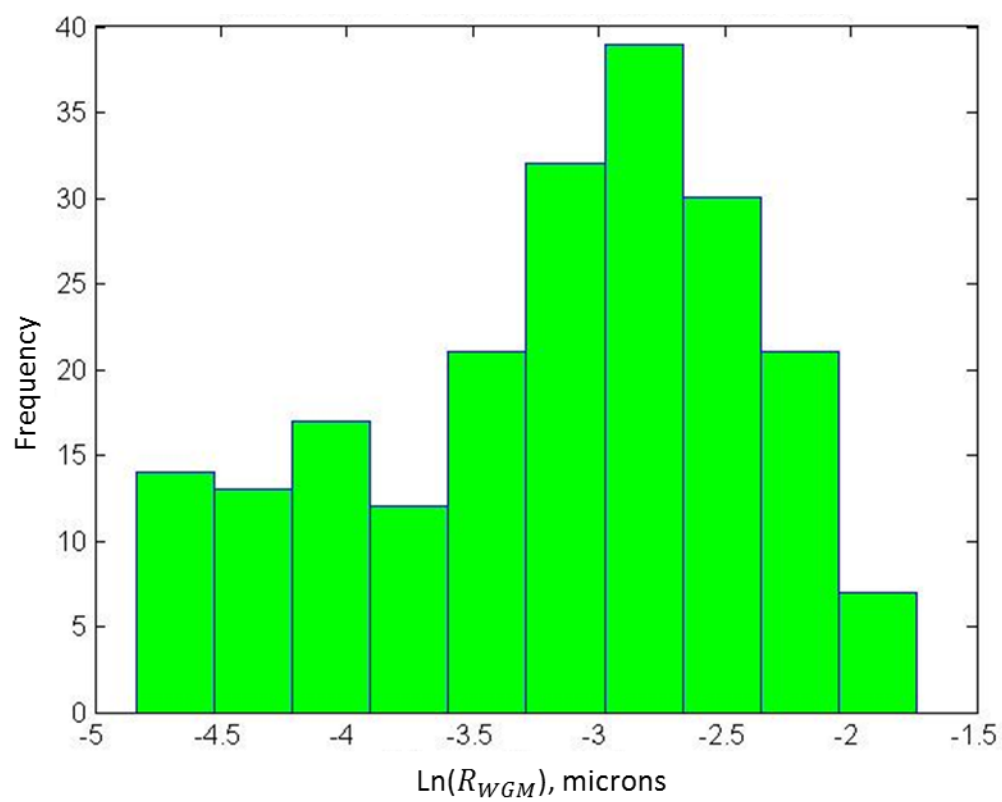


Figure 4.6 Dastidar parameter (R_{WGM}) histogram

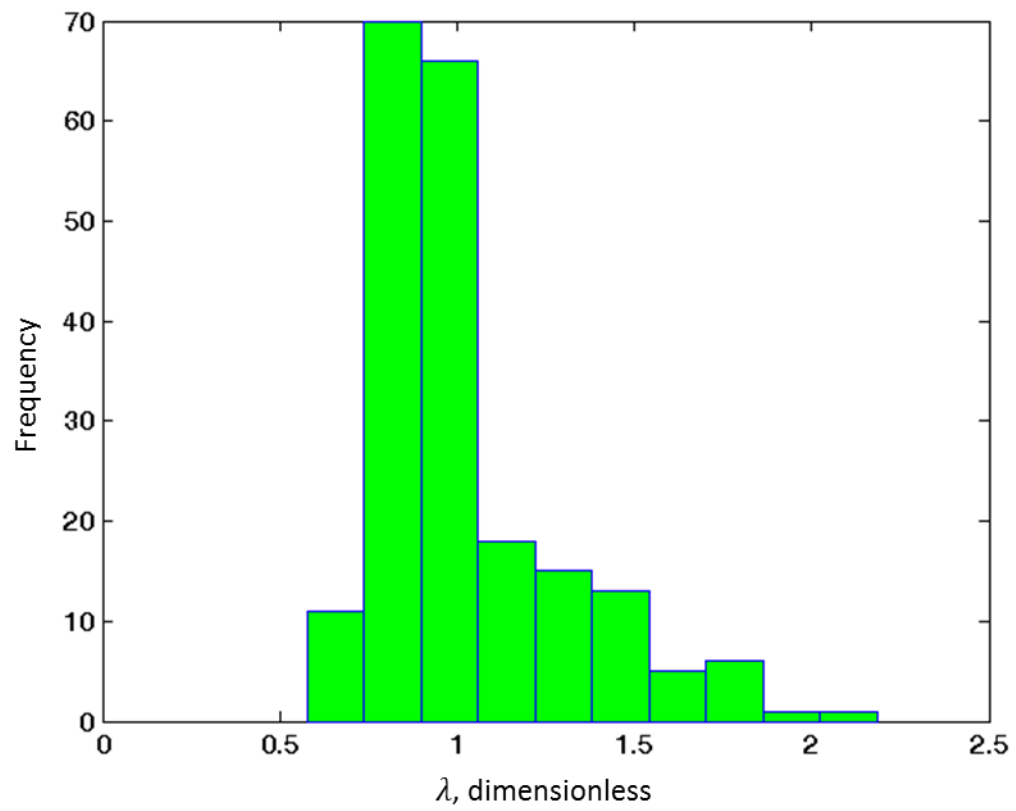


Figure 4.7 Brooks and Corey index (λ) histogram

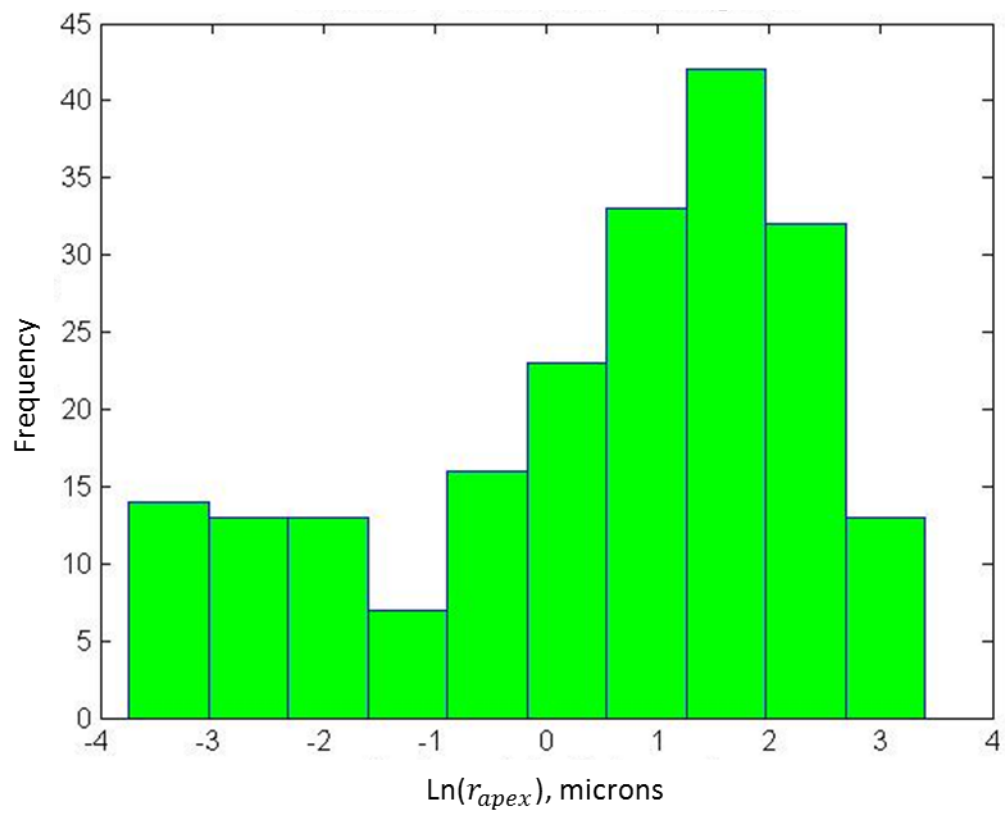


Figure 4.8 Pittman parameter (r_{apex}) histogram

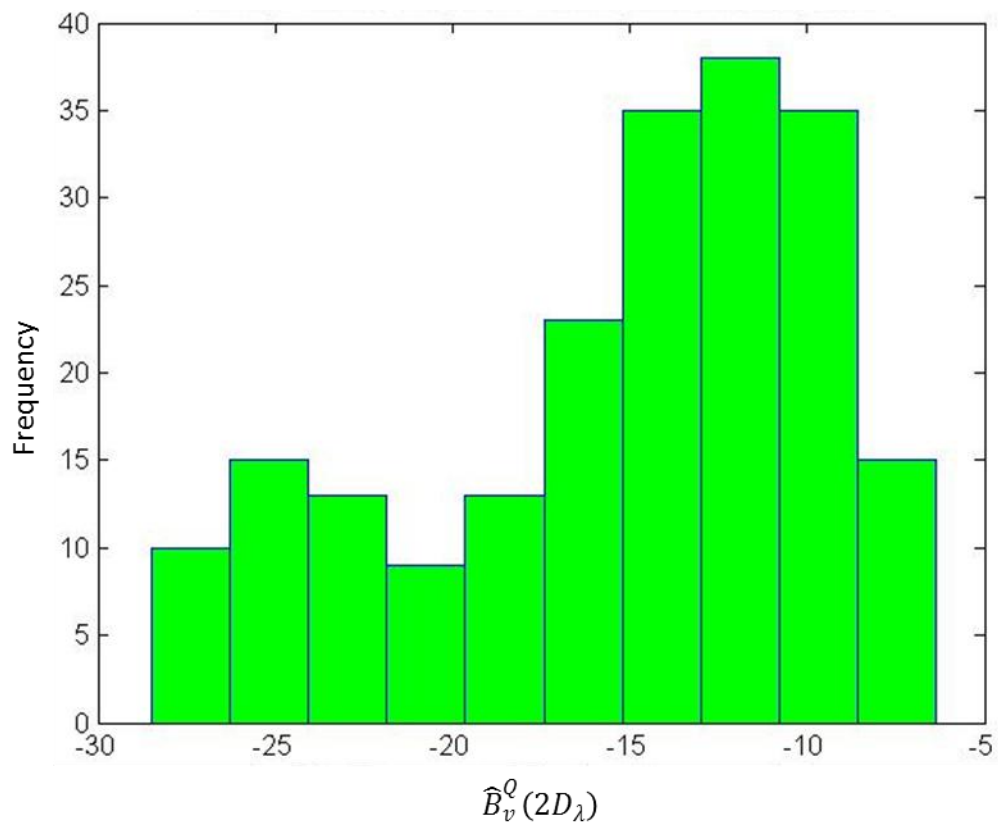


Figure 4.9 Laplace of bulk volume $\left(\hat{B}_v^Q(2D_\lambda)\right)$ histogram

4.2 Comparison of Permeability Models Using Published Constants

Permeability values have been estimated using published constants and then compared to actual data. **Table 4.4** summarizes the error measures used in this study including Maximum Absolute Percent Error (MAE), Average Relative Percent Error (ARE), Average Absolute Relative Percent Error (AARE), Correlation Coefficient (R), Standard Deviation (s) and Root Mean Squares (RMS). Mathematical expressions of all error measures used in this study are presented in Appendix A.

It is shown that Dastidar model has the lowest AARE at 63% followed by Swanson at 67.0%, followed by Winland at 71.5%. Huet-Blasingame model gives the highest AARE at 671%. In terms of correlation Coefficient (R), Swanson model is ranked first at 0.947 followed by Winland at 0.942 followed by Buiting and Clerk model (Equation 2.19) at 0.921, however, Dastidar model shows the lowest (R) of 0.733. For RMS, Winland shows the lowest value at 145, followed by Swanson at 160 followed by Buiting and Clerk model (Equation 2.19) at 183.

Figures 4.10 through **Figure 4.18** display permeability cross-plot of actual data measurements versus predicted values. Permeability cross-plots indicate that some models performed relatively good in predicting permeability values greater than 1.0 mD while not as good for low permeability values. Winland (**Figure 4.12**), Swanson (**Figure 4.13**), Buiting-Clerke (**Figure 4.18**), Thomeer (**Figure 4.11**) and Pittman (**Figure 4.14**) fall under this category. Permeability values lower than 1.0 mD were not predicted properly except by two models; Dastidar (**Figure 4.16**) and Huet-Blasingame (**Figure 4.15**).

Table 4.4 Statistical analysis of permeability model results using published constants

Model Name	MAE	ARE	AARE	R	s	RMS
Purcell	5037	-207	244.6	0.911	342	374
Thomeer	2810	-90	142.1	0.870	205	214
Winland	1353	-8	71.5	0.942	145	145
Swanson	1459	-5	67.0	0.947	159	160
Pittman	4357	-177	229.1	0.858	263	277
Huet-Blasingame	11173	-659	671.4	0.748	625	695
Dastidar	445	52	63.0	0.733	344	359
Buiting-Clerke (Eq. 2.19)	3064	-104	151.6	0.921	171	183
Buiting-Clerke (Eq. 2.21)	4484	-126	168.2	0.869	195	205

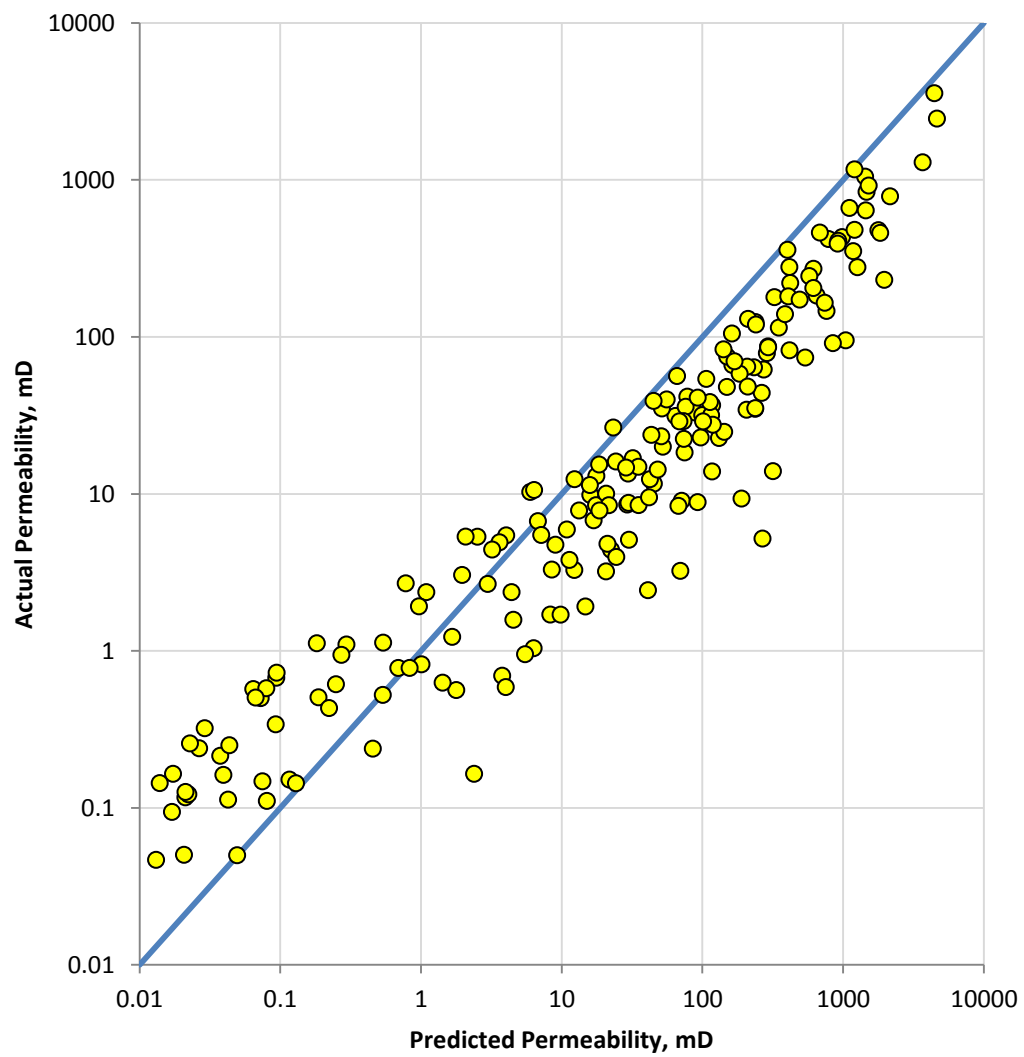


Figure 4.10 Purcell permeability model results using published constants

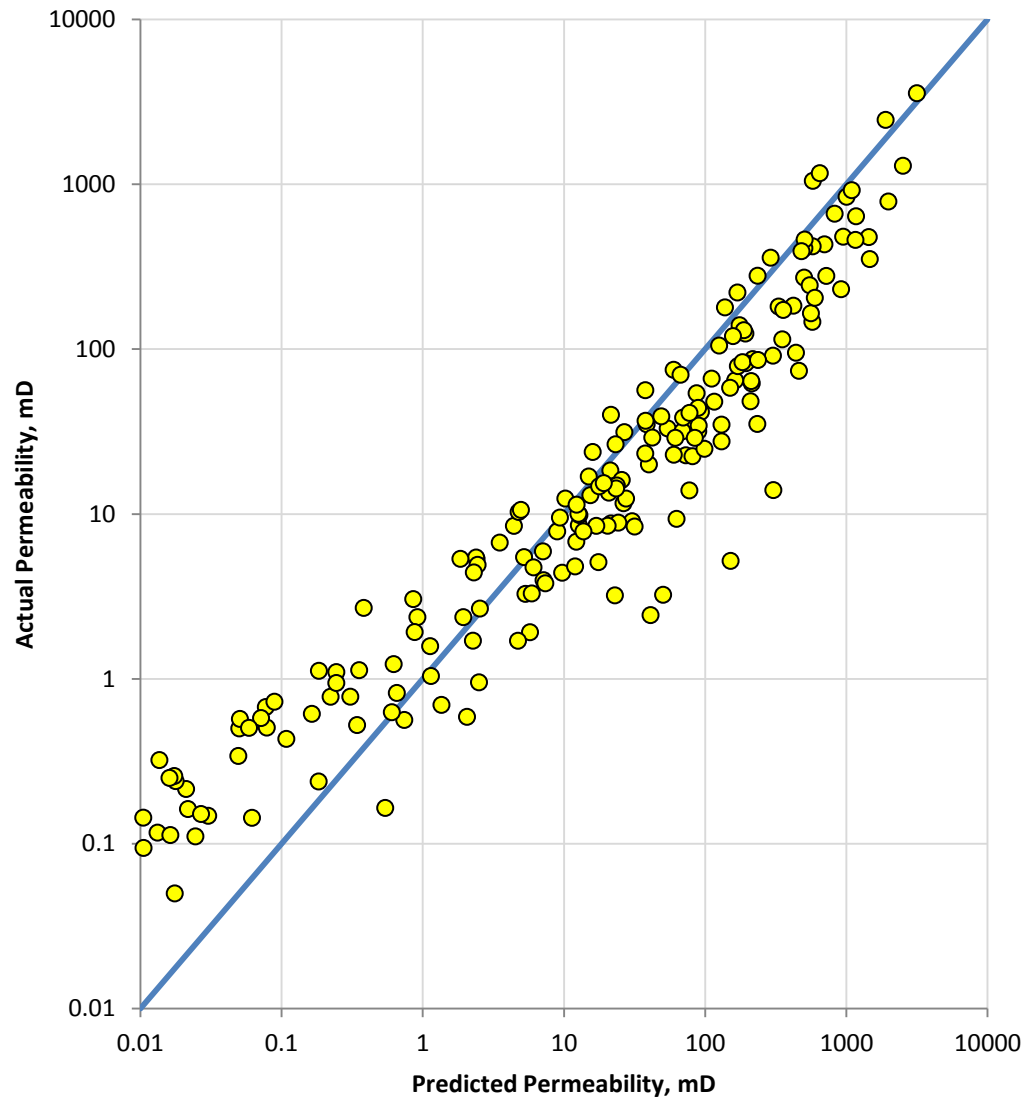


Figure 4.11 Thomeer permeability model results using published constants

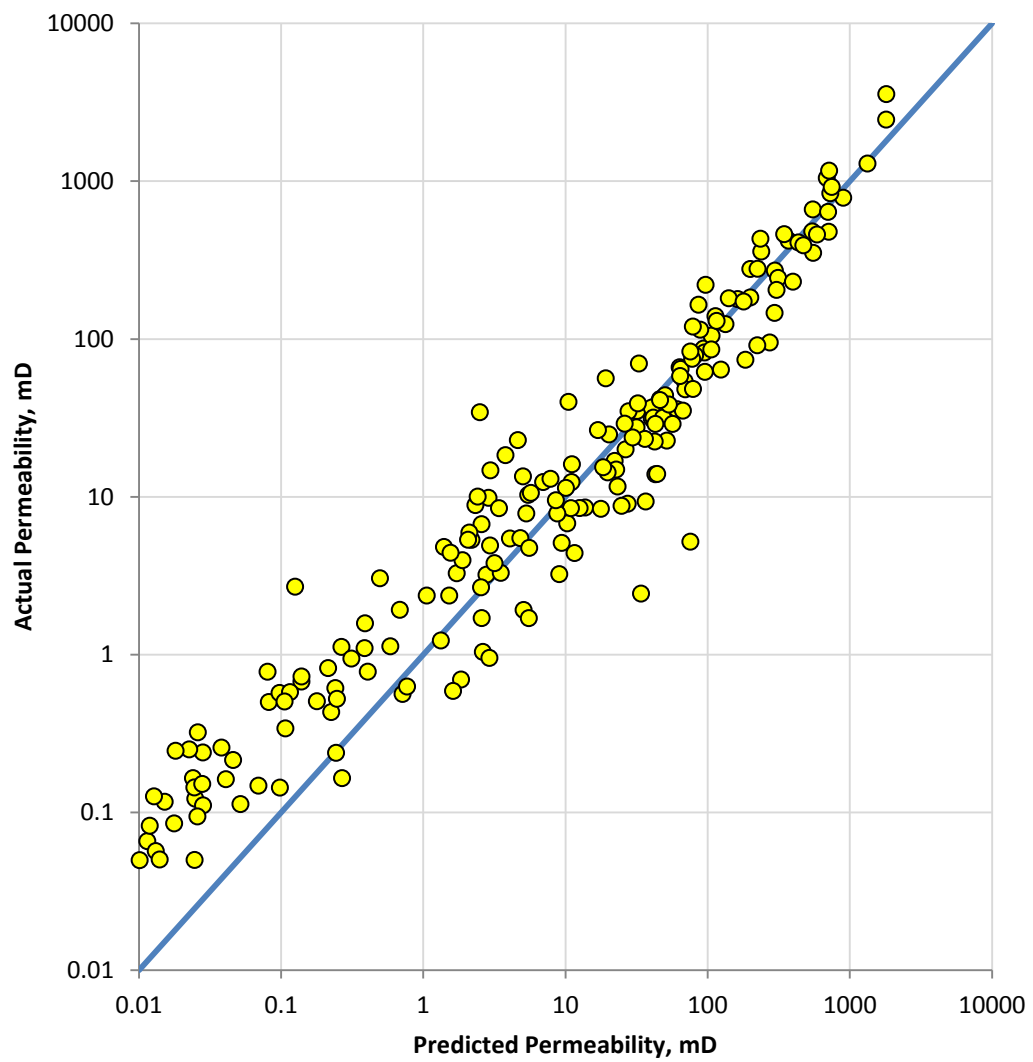


Figure 4.12 Winland permeability model results using published constants

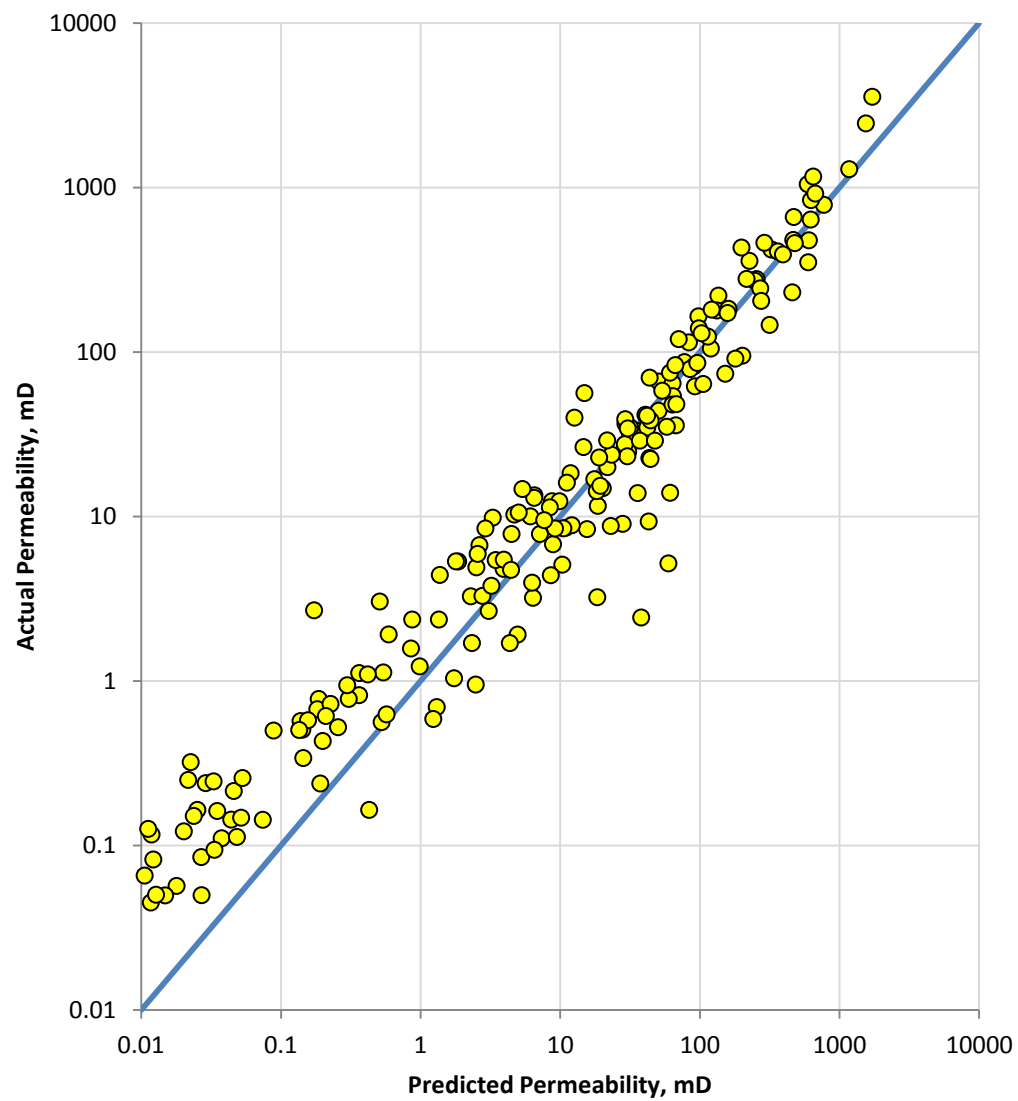


Figure 4.13 Swanson permeability model results using published constants

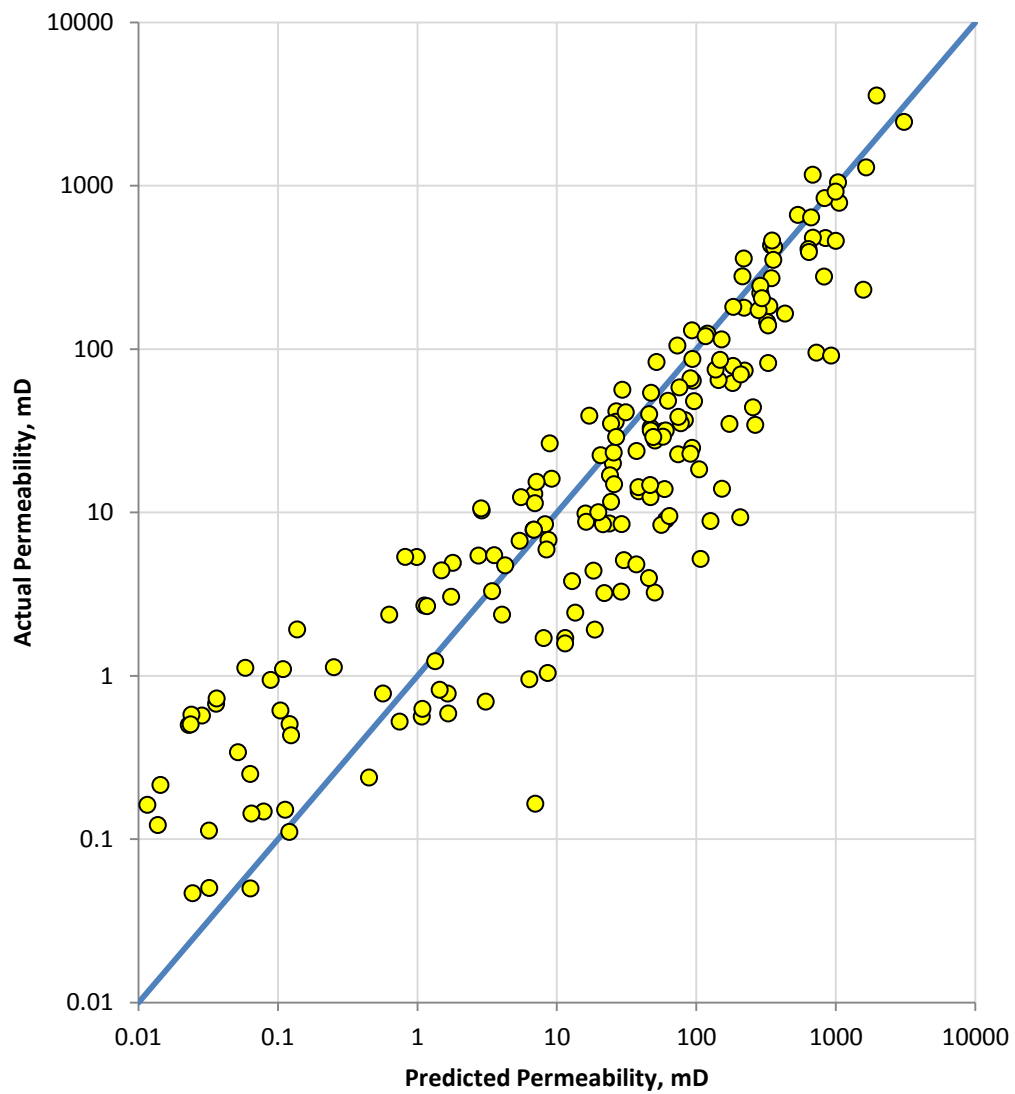


Figure 4.14 Pittman permeability model results using published constants

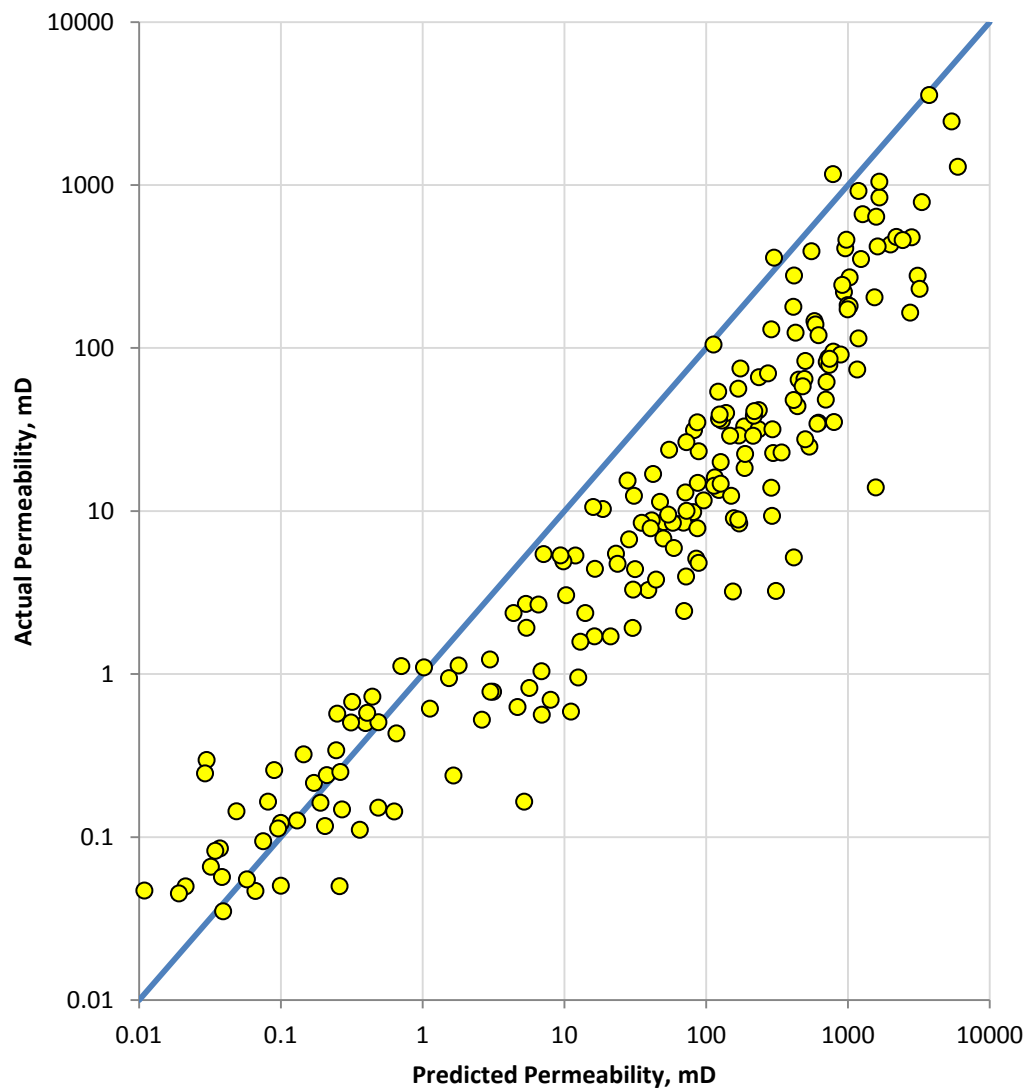


Figure 4.10 Huet-Blasingame permeability model results using published constants

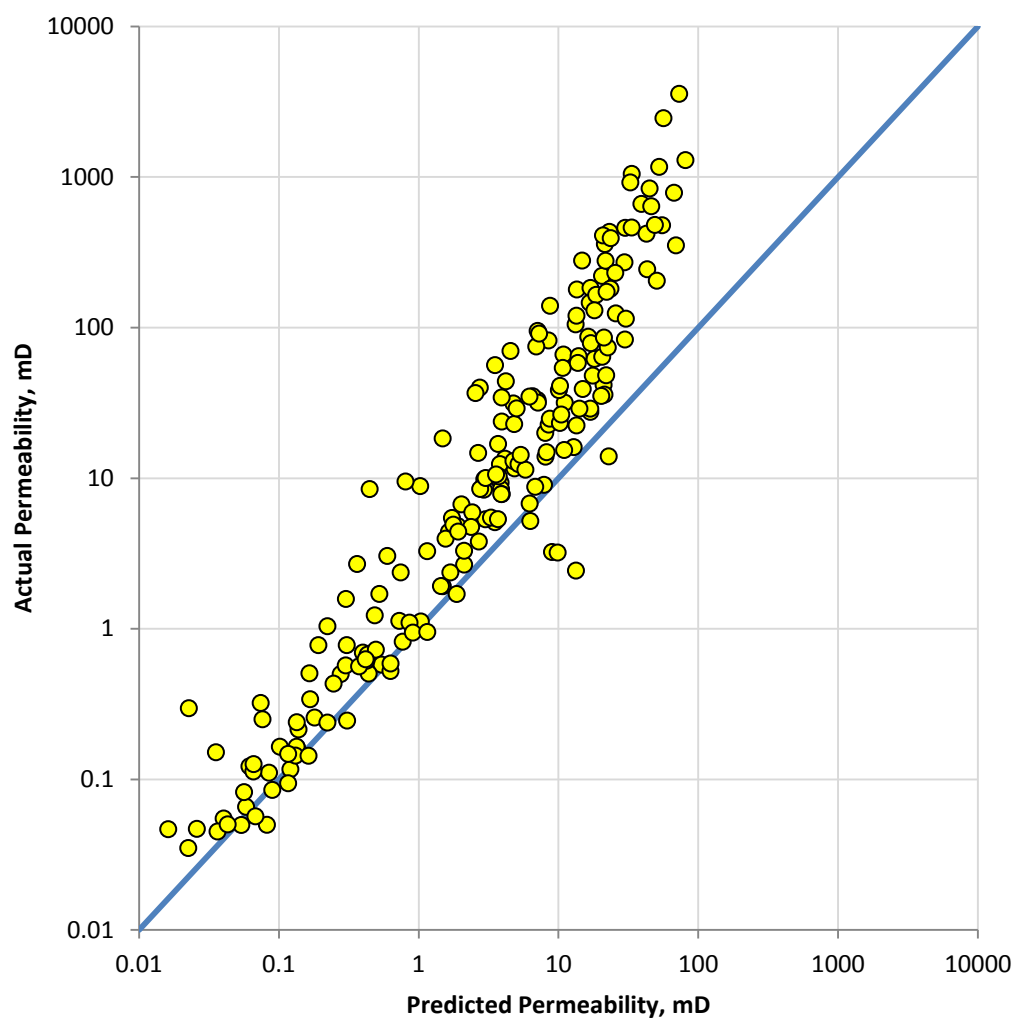


Figure 4.11 Dastidar permeability model results using published constants

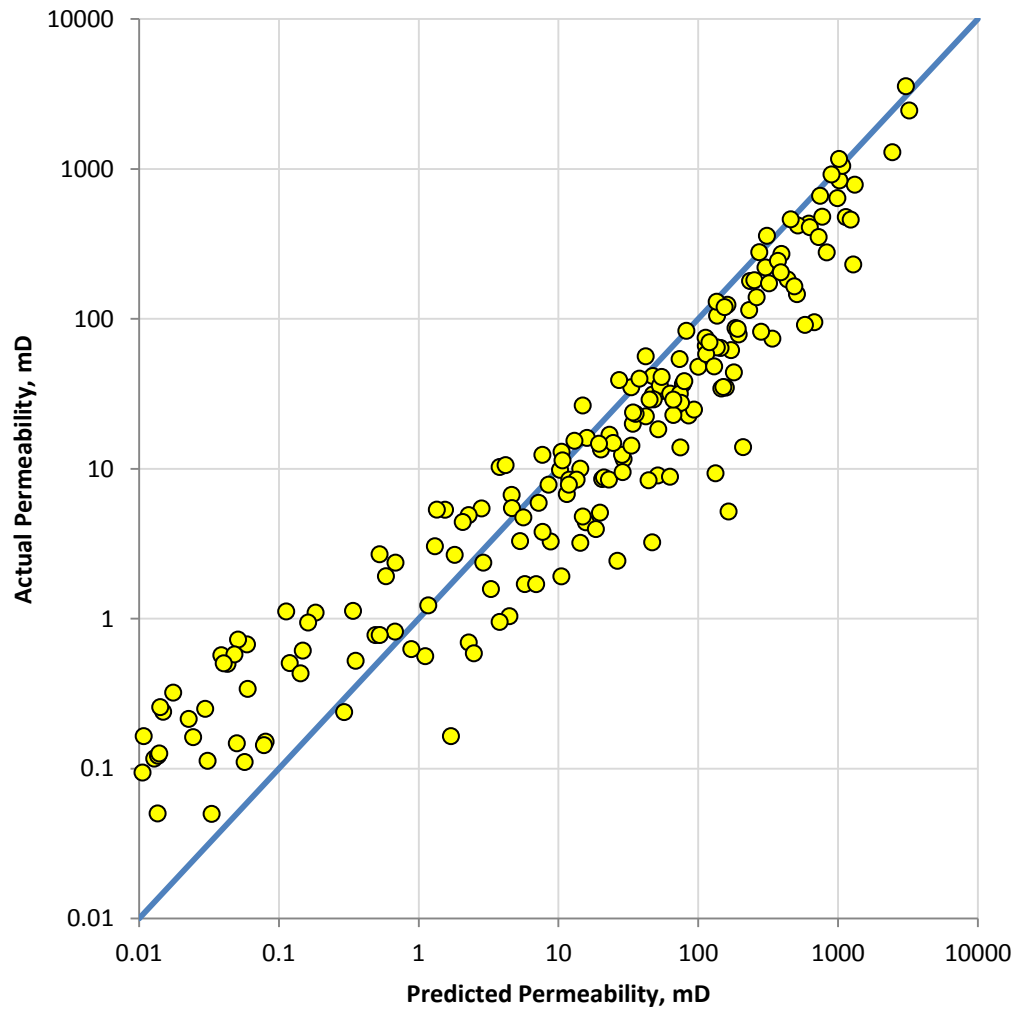


Figure 4.12 Buiting-Clerke permeability model results using Laplace transform – no fitting constants

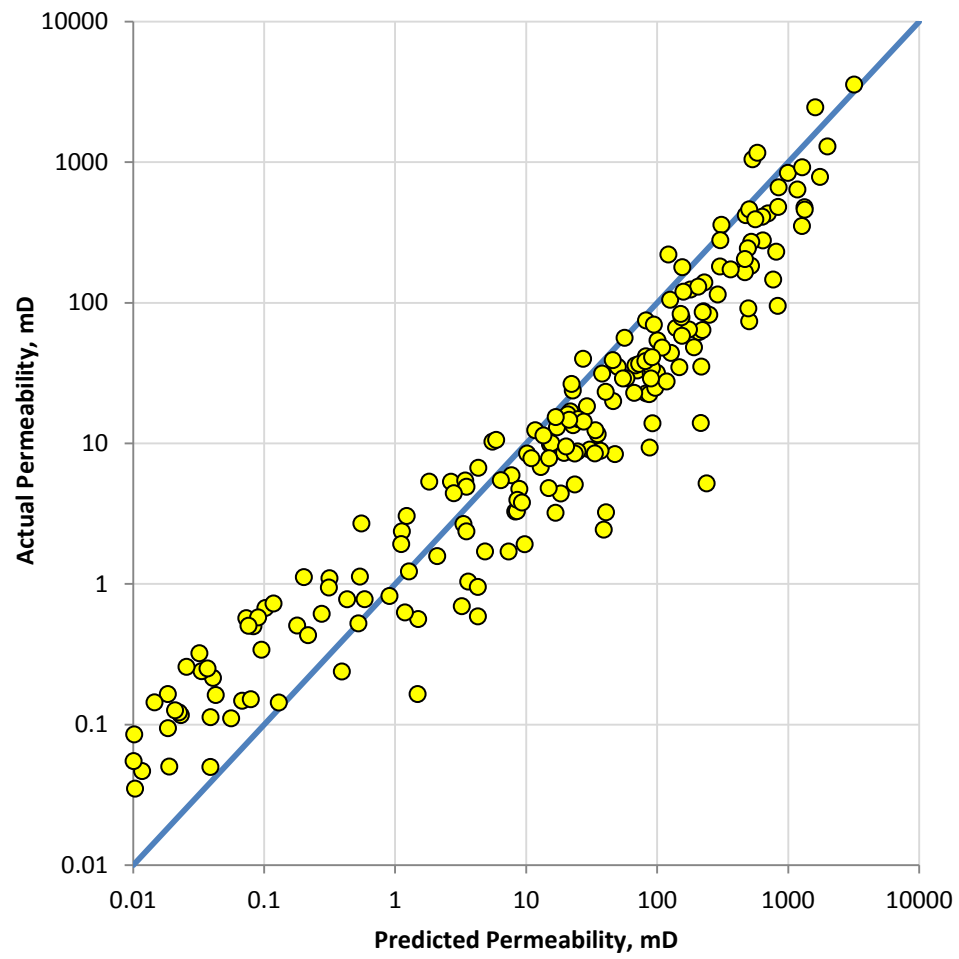


Figure 4.13 Buiting-Clerke permeability model results using Thomeer parameters

It is clearly shown that weighted geometric mean of pore throat radii (R_{WGM}) confirmed to account for contribution of small radii especially in tighter rocks as proposed by Dastidar. On the other hand, Buiting-Clerke model using Laplace transform (Equation 2.19) achieved good results even without fitting constants. The practical approximation (Equation 2.21) also showed very close results to the original model confirming the validity of the proposed approximation.

4.3 Comparison of Generalized Permeability Models

Another comparison has been made but using generalized forms of permeability models this time. A generalized form for each model has been used and new fitting constants have been calculated. All error measures described in previous section has been applied and results have been tabulated. Three different methods have been used to determine the coefficients that best fit dataset for the modified models. The first one is the nonlinear regression option in MATLAB R2010b[®] (see Statistics Toolbox User's Guide) that employs ordinary nonlinear least-squares data fitting by utilizing Gauss-Newton method. The other method uses MATLAB R2010b[®] robust fitting that reduces the effect of outliers by using weighted nonlinear regression that utilizes certain weight function. The third method determines constants by utilizing multiple regressions after linearization. (see Appendix B for more detail)

Table 4.5 summarizes results for all modified permeability models used in this study. This includes, as was stated earlier, results of permeability models with published

constants and other methods used to determine the constants. All fitted constants to our dataset are listed in **Table 4.6** as well.

Results of modified Purcell permeability model has improved significantly as a comparison to the results of the original model by using the nonlinear regression, robust fitting approaches and multiple regressions after linearization. AARE has dropped from 245% down to ranges between 75-85% for the three methods. Nonlinear regression scored the highest correlation coefficient of 0.93 among other techniques used. Standard deviation (s) and RMS also dropped by more than 50% for the nonlinear regression and robust fitting methods. Permeability cross-plot of modified Purcell model (**Figure 4.19**) indicates

Table 4.5 Results of all permeability models used in the comparison study with all methods

	MAE	ARE	AARE	R	s	RMS
Purcell Model-Published Constants	5037	-207.0	244.6	0.911	342	374
Nonlinear Regression	1251	44.1	83.2	0.931	129	130
Robust Fitting	1495	16.5	78.5	0.924	137	137
Fitting after Linearization	1219	-38.5	76.9	0.828	284	290
Thomeer Model- Published Constants	2810	-90.0	142.1	0.870	205	214
Nonlinear Regression	1124	56.6	87.5	0.908	149	150
Robust Fitting	1217	17.6	73.9	0.876	192	193
Fitting after Linearization	1601	-35.0	70.4	0.814	278	283
Winland Model- Published Constants	1353	-8.0	71.5	0.942	145	145
Nonlinear Regression	797	57.5	77.6	0.972	84	85
Robust Fitting	1067	32.3	67.8	0.963	99	99
Fitting after Linearization	1532	-31.5	67.1	0.890	252	257
Swanson Model- Published Constants	1459	-4.7	67.0	0.947	159	160
Nonlinear Regression	513	56.1	74.2	0.971	85	85
Robust Fitting	1016	27.3	67.9	0.966	92	92
Fitting after Linearization	1484	-31.8	67.7	0.914	247	252
Pittman Model- Published Constants	4141	-140.0	193.0	0.855	192	195
Nonlinear Regression	1029	-23.1	103.1	0.867	177	177
Robust Fitting	992	-6.0	91.1	0.866	182	182
Fitting after Linearization	1683	-51.2	93.0	0.788	294	300
Huet-Blasingame Model- Published Constants	11173	-659.0	671.4	0.748	625	695
Nonlinear Regression	1992	6.6	100.1	0.808	209	209
Robust Fitting	1426	-5.0	91.9	0.793	228	229
Fitting after Linearization	1870	-52.0	94.6	0.731	302	309
Dastidar Model- Published Constants	445	52.0	63.0	0.733	344	359
Nonlinear Regression	1203	26.7	72.9	0.898	156	156
Robust Fitting	1336	22.6	72.5	0.897	158	158
Fitting after Linearization	1801	-33.9	69.9	0.858	262	267
Buiting-Clerck Model - Published Constants	4484	-126.0	168.2	0.869	195	205
Nonlinear Regression	1218	55.9	87.4	0.905	151	152
Robust Fitting	1327	19.7	73.3	0.876	192	193
Fitting after Linearization	1532	-35.3	71.4	0.812	279	284

Table 4.6 Coefficients of all modified permeability models used in this study using all methods

	a_{p1}	a_{p2}	a_{p3}	
Purcell Model-Published Constants	311316	1	1	
Nonlinear Regression	417940	0.7188	1.4193	
Robust Fitting	3.72E+05	1.2309	1.1759	
Fitting after Linearization	55270.8	2.1059	0.60576	
	a_{t1}	a_{t2}	a_{t3}	a_{t4}
Thomeer Model- Published Constants	3.8068	-1.3334	2	2
Nonlinear Regression	46.851	-1.8142	1.2778	3.2841
Robust Fitting	1.0495	-1.7755	2.1052	2.11
Fitting after Linearization	1.42805	-1.5623	1.6482	1.4006
	a_{w1}	a_{w2}	a_{w3}	
Winland Model- Published Constants	49.45	1.7	1.47	
Nonlinear Regression	2.7603	2.5287	1.0301	
Robust Fitting	17.822	2.0888	1.4353	
Fitting after Linearization	156.2098	1.2467	1.8324	
	a_{s1}	a_{s2}		
Swanson Model- Published Constants	399	1.691		
Nonlinear Regression	402.13	2.3686		
Robust Fitting	473.62	2.0548		
Fitting after Linearization	259.5891	1.3703		
	a_{i1}	a_{i2}	a_{i3}	
Pittman Model- Published Constants	4.6	2.105	0.208	
Nonlinear Regression	9.2359	2.1168	1.0676	
Robust Fitting	16.495	2.0529	1.4374	
Fitting after Linearization	420.4813	1.0648	2.4678	
	a_{h1}	a_{h2}	a_{h3}	a_{h4}
Huet-Blasingame Model- Published Constants	1017003	1.6498	1.7846	1.6575
Nonlinear Regression	633.09	1.4967	2.2537	-3.3191
Robust Fitting	222.14	2.3923	1.5891	-4.4749
Fitting after Linearization	1538.71	2.6088	0.91696	-2.0602
	a_{d1}	a_{d2}	a_{d3}	
Dastidar Model- Published Constants	107132.4	3.06	1.64	
Nonlinear Regression	2.63E+08	2.4025	4.4745	
Robust Fitting	2.13E+08	2.5325	4.2953	
Fitting after Linearization	1792282	1.8183	2.8497	
	a_{b1}	a_{b2}	a_{b3}	a_{b4}
Buiting-Clerck Model - Published Constants	506000	1	2	-4.43

Nonlinear Regression	2.78E+06	1.2328	3.2649	-5.5107
Robust Fitting	2.31E+06	1.9747	2.1357	-5.4026
Fitting after Linearization	281531.6	1.6923	1.3766	-4.9101

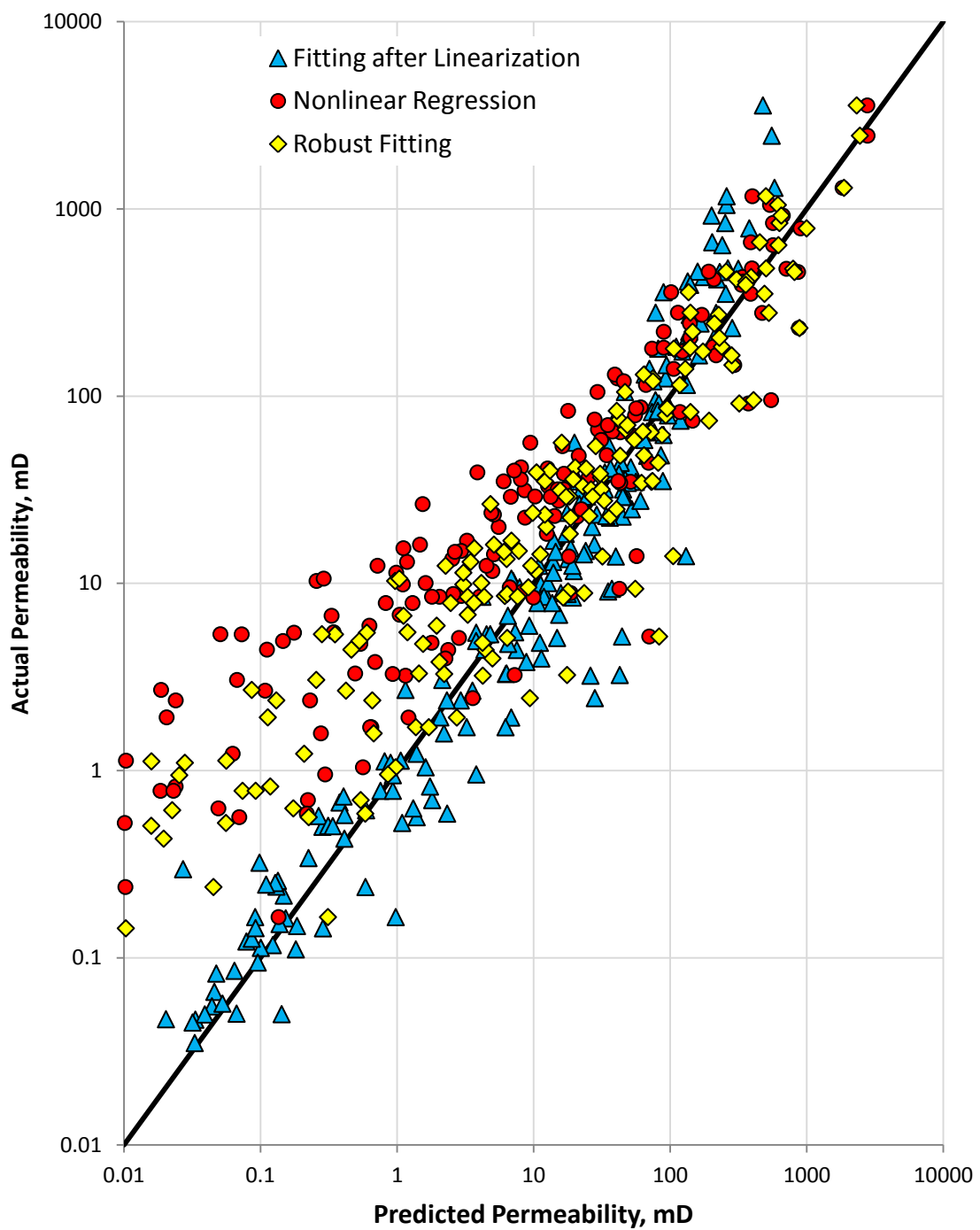


Figure 4.19 Modified Purcell permeability model results using three regression methods

clearly that nonlinear regression and robust fitting perform better in predicting high permeability values while are quite off for the low measurements. On the other hand, multiple regressions after linearization performs much better in predicting low permeability values but fail in predicting the high values. This observation indicates that Purcell model cannot be used to predict permeability values for wide ranges of permeability.

Modified Thomeer permeability model shows a substantial improvement in results when using the generalized form (Equation 4.2). Similar to Modified Purcell model results, AARE dropped from 142% to 70-80% for all three methods and nonlinear regression scored the highest correlation coefficient (R) of 0.91 among other techniques used. Standard deviations (s) and RMS showed a noticeable drop of about 25% by using nonlinear regression method only. Graphical analysis represented by permeability cross-plot of predicted and measured permeability values using the three proposed methods (**Figure 4.20**) show similar observations to Modified Purcell model behaviors.

Modified Winland permeability model shows a reduction in RMS and Standard deviations (s) by about 43% as a comparison to published constant model's results when using nonlinear regression and robust fitting. AARE showed a slight improvement when using robust fitting and multiple regressions after linearization by going from 71.5% down to 67.8% and 67.1%, respectively. Nonlinear regression shows the best R at 0.97. **Figure 4.21** shows the permeability cross-plot using the three fitting techniques. It is obvious that the same issues with previous modified models are also encountered in this model as well. Multiple regressions after linearization produces better results when used

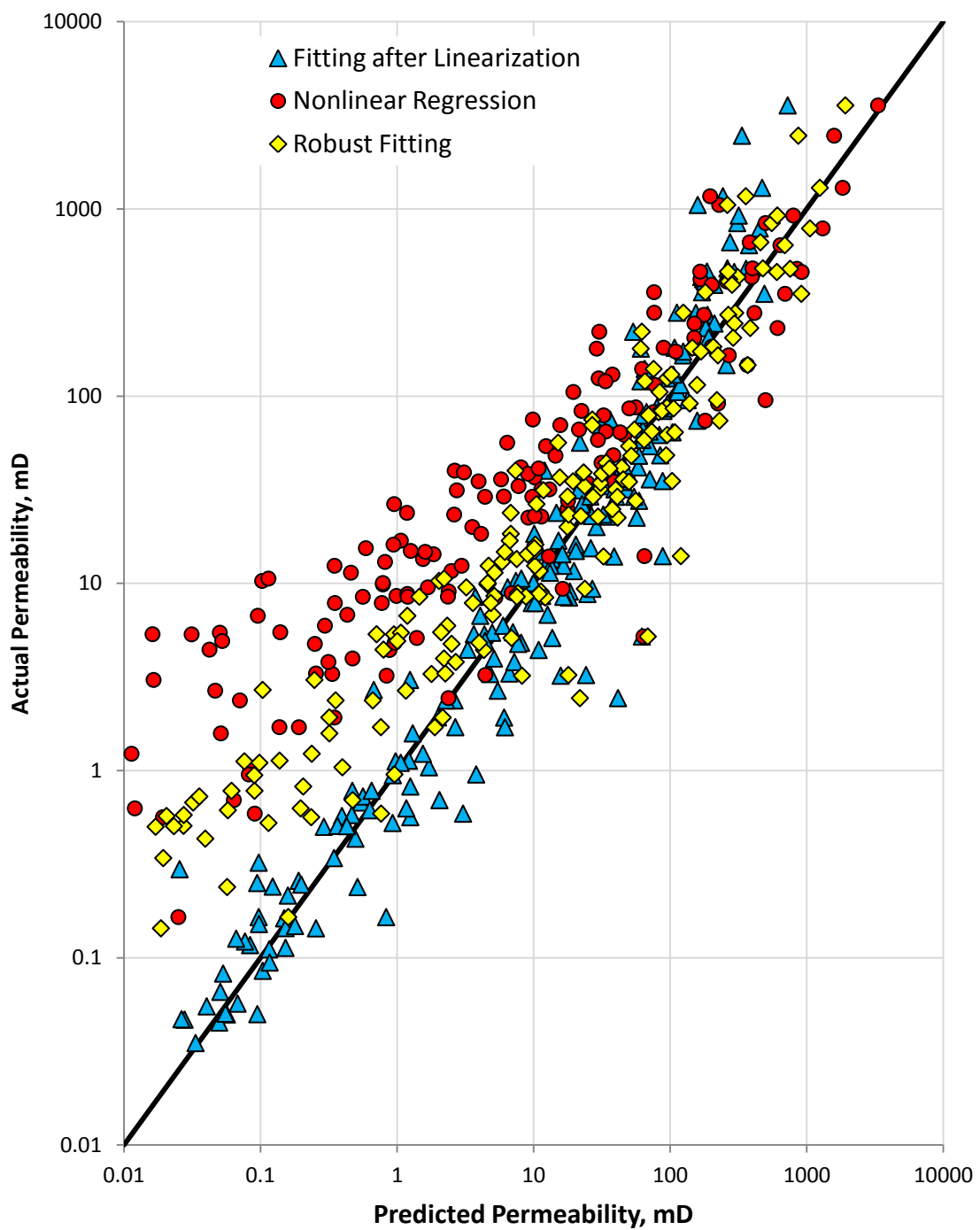


Figure 4.20 Modified Thomeer model results using three regression results

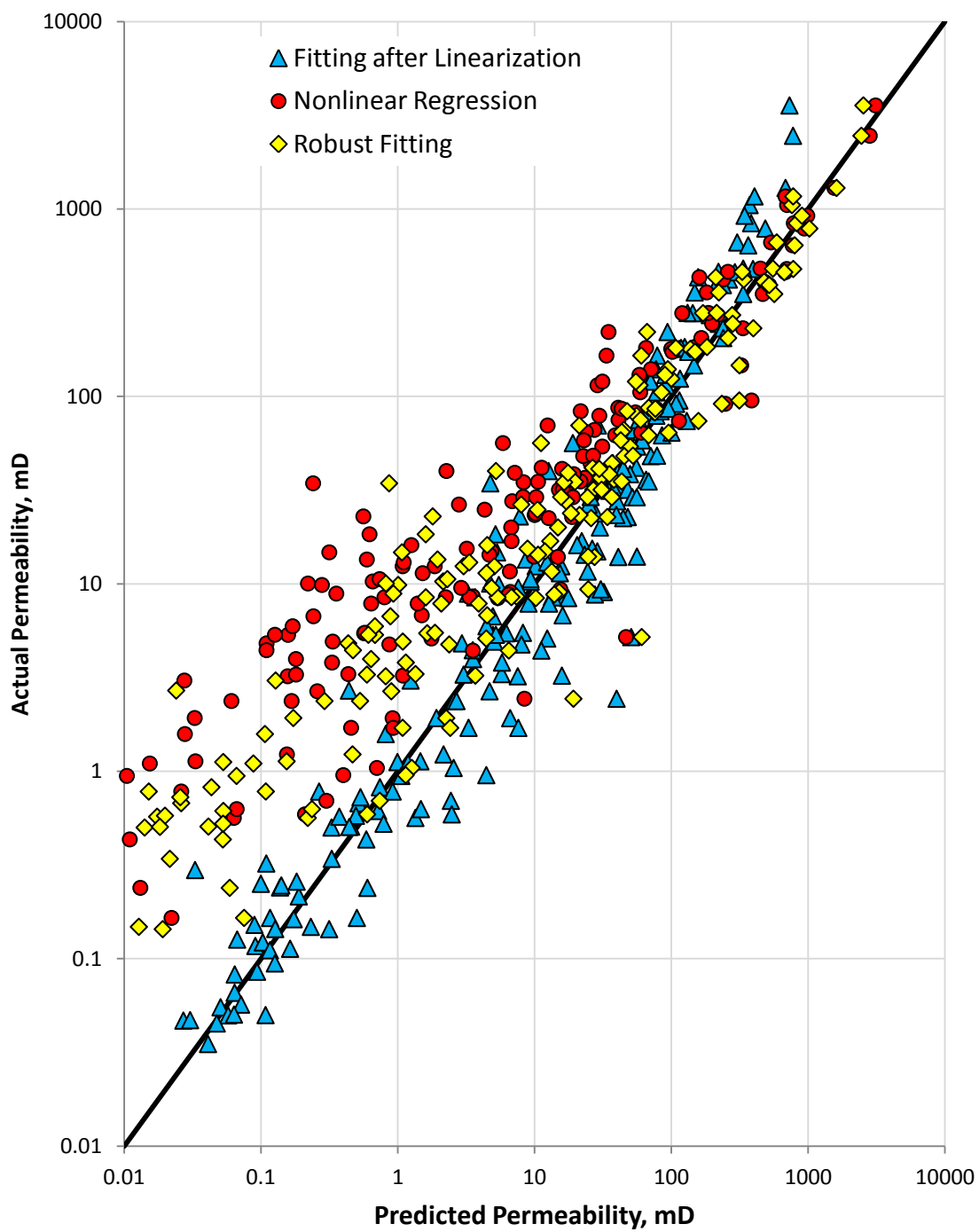


Figure 4.21 Modified Winland permeability model results using three regression methods

to predict low permeability values while nonlinear regression and robust fitting perform better in predicting high permeability values. One set of coefficients cannot be used for the whole dataset since permeability variations are huge. Modified Swanson model shows very close results to Modified Winland model. Although AARE has not improved by any of the three methods, Standard deviations (s) and RMS have improved greatly by about 50%. Nonlinear regression and robust fitting also indicate slight modification in correlation coefficient (R) by going from 0.95 to 0.97. Swanson model is considered one of the best models used in this study. **Figure 4.22** shows the permeability cross-plot and the same issue with previous models appears here as well but at a lesser degree.

Modified Pittman model shows slight improvements in AARE, R, s and RMS when compared to the model with published constants; however, the model produces high errors in the overall. The permeability cross-plot can be seen in **Figure 4.23**. Huet-Blasingame model also shows similar results to Pittman. In terms of performance, the two models give the worse prediction among all permeability models used in this study. **Figure 4.24** shows the permeability cross-plot of the Modified Huet-Blasingame model using the three fitting techniques.

In Modified Dastidar permeability model, an increase in AARE has been seen by almost 10% when using the three regression methods, however, the correlation coefficient (R), standard deviations (s) and RMS showed a noticeable improvement. **Figure 4.25** shows the permeability cross-plot of this model.

The modified Buiting-Clerke model shows a substantial decrease in AARE from 168% to 70-80%. Correlation coefficient (R), standard deviations and RMS also shows an increase

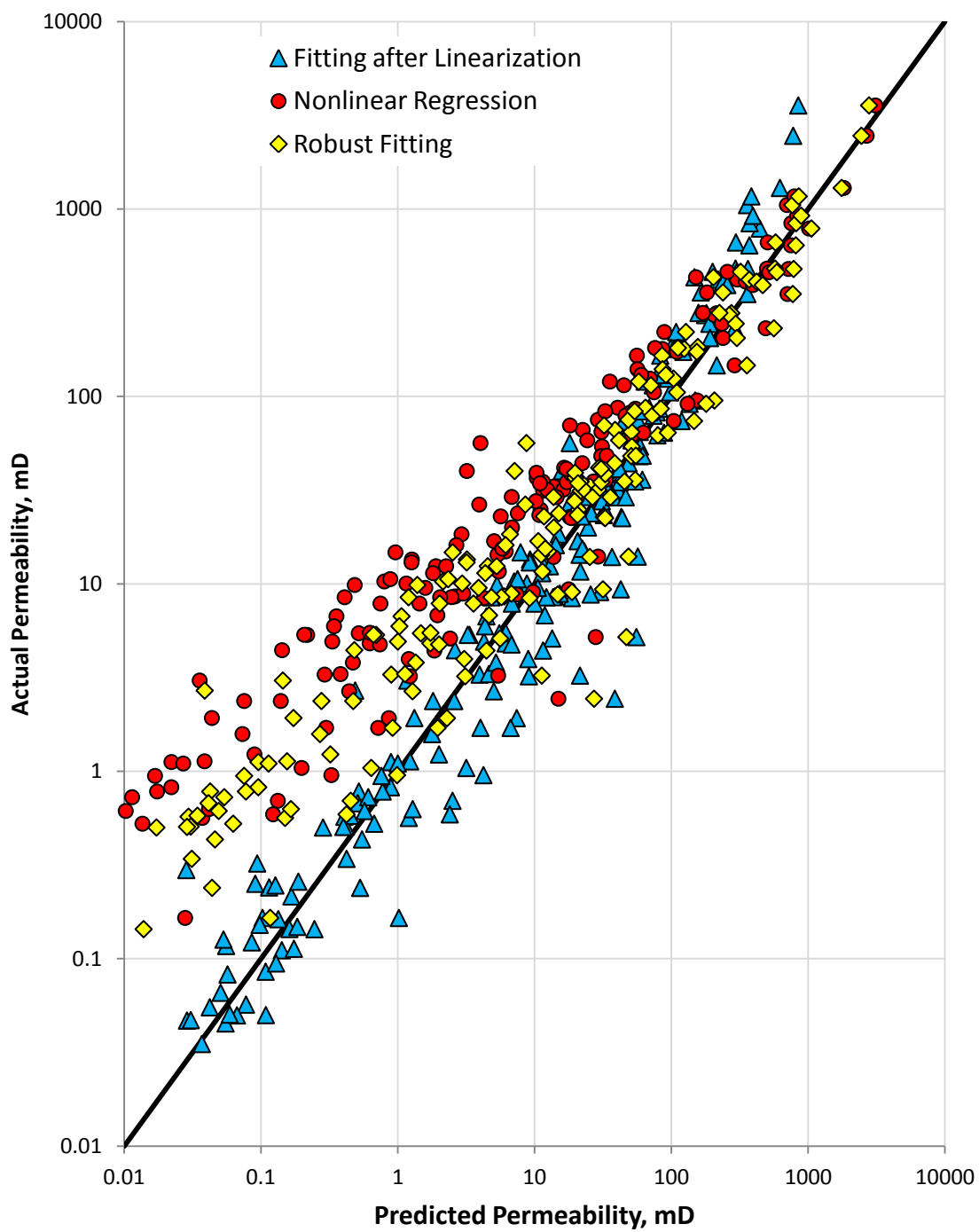


Figure 4.14 Modified Swanson permeability model results using three regression methods

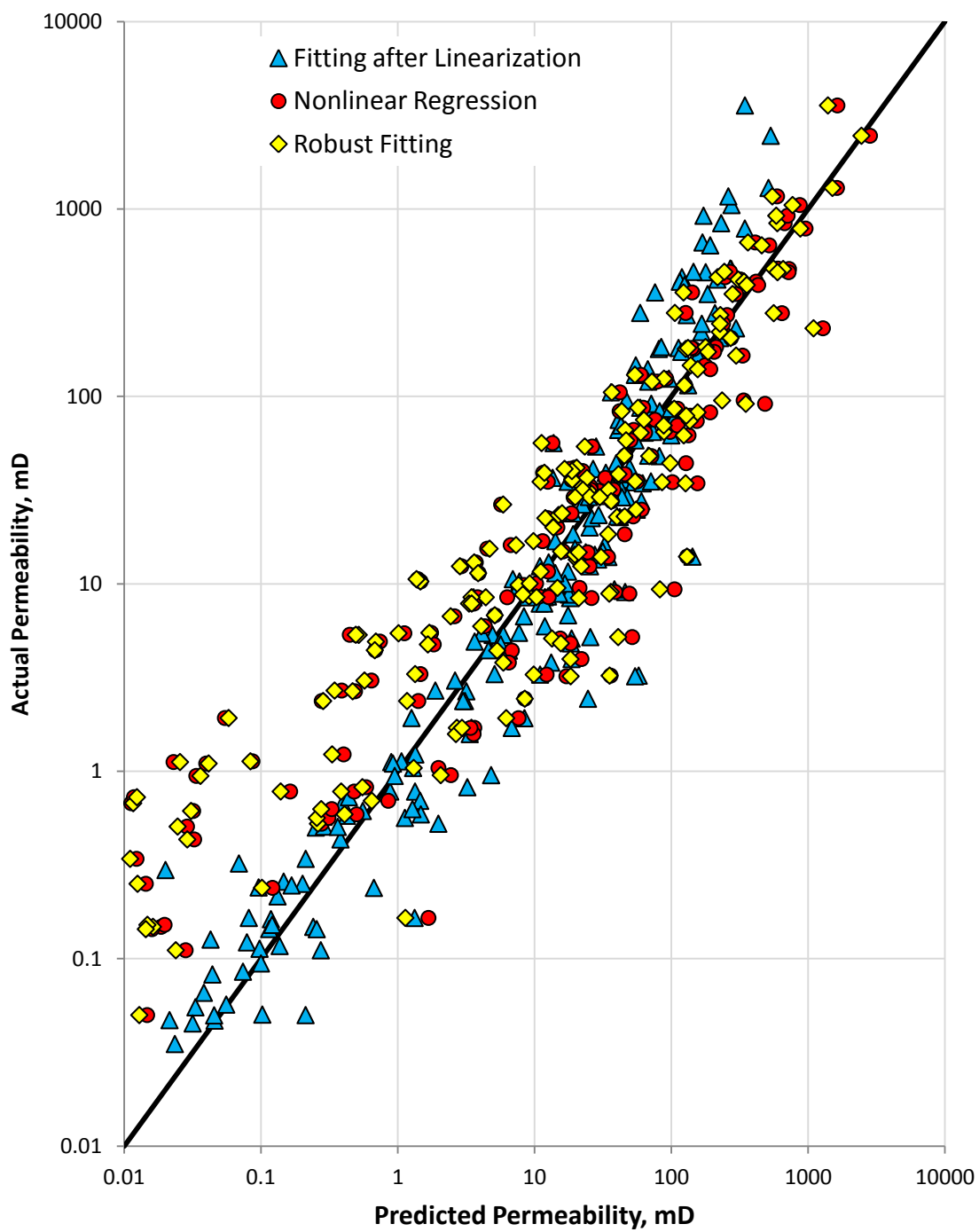


Figure 4.15 Modified Pittman permeability model results using three regression methods

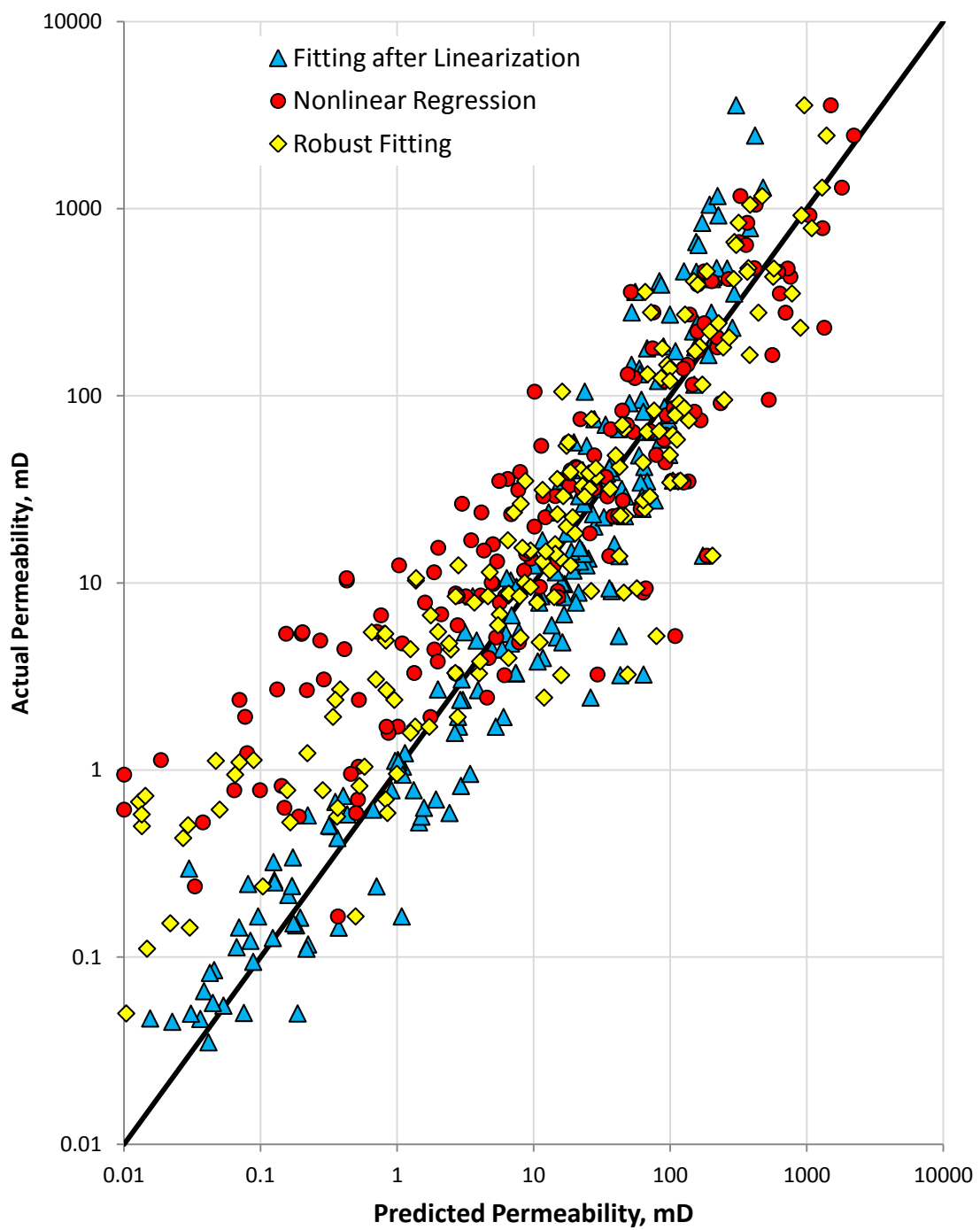


Figure 4.16 Modified Huet-Blasingame permeability model results using three regression methods

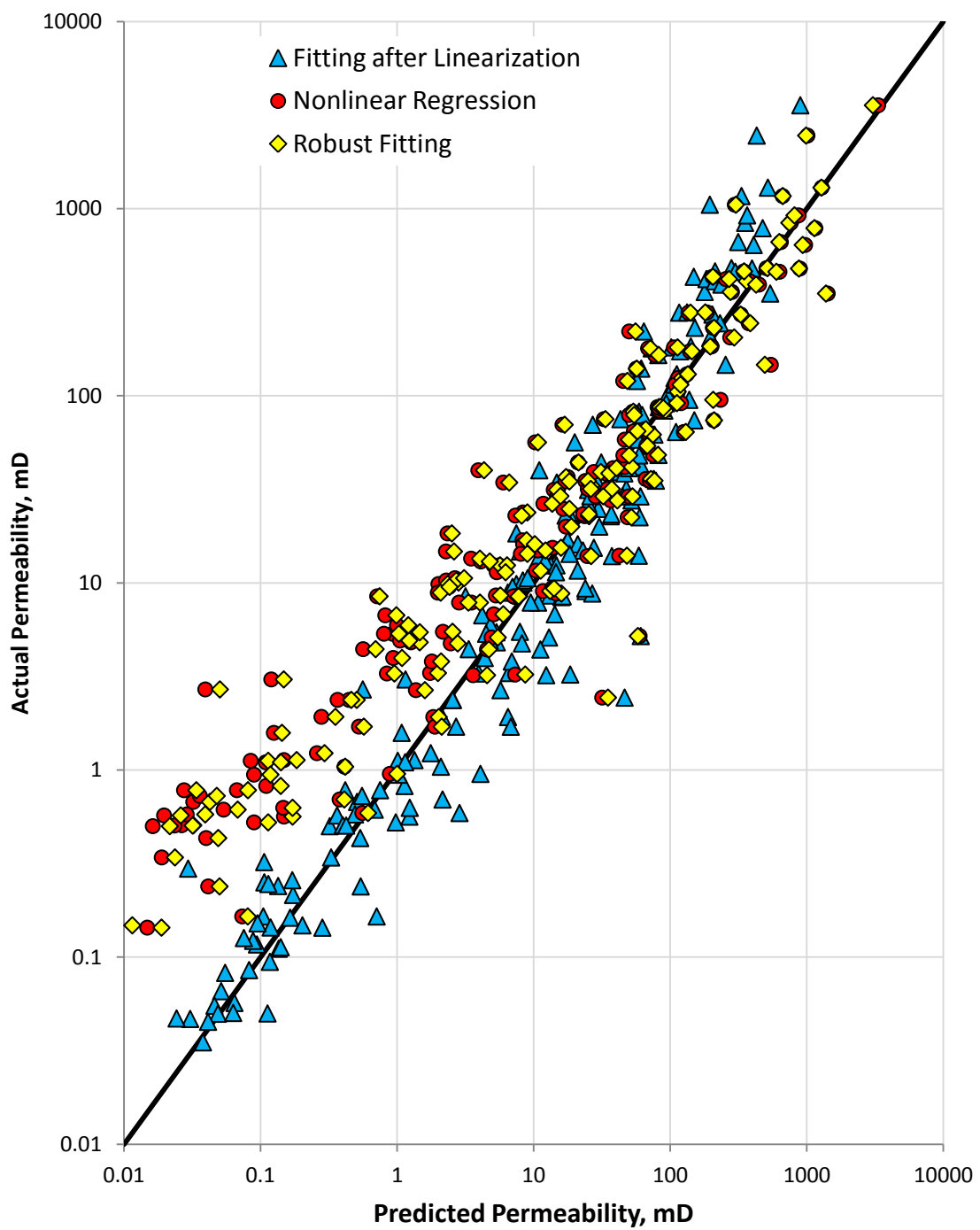


Figure 4.17 Modified Dasidar permeability model results using three regression methods

except for multiple regressions after linearization method. Permeability cross-plot of modified Buiting-Clerke model can be seen in **Figure 4.26**.

From all model results, it can be observed that multiple regressions after linearization produces better results when used for low permeability values while nonlinear regression and robust fitting perform better in predicting high permeability values. The best explanation of this observation is that in nonlinear regression and robust fitting methods, the objective function is to minimize the sum of squares of errors. Therefore, the error in predicting high permeability values dominates and the algorithm focuses in minimizing those errors over the errors produced by the low permeability values. This usually has a tendency to produce low standard deviations (s) and RMS in comparison to the other methods. The multiple regressions after linearization method, however, tends to reduce AARE that appears to be dominated by errors of low permeability values.

Since uncorrected air permeability is being used, measurements in low permeability rocks tend to be higher than actual permeability values. This is mainly due to the slippage effect that takes place when using gas phase to measure permeability. This can be avoided by using Klinkenberg permeability that takes care of slippage effect. Unfortunately, the permeability measurements used in this study have not been corrected.

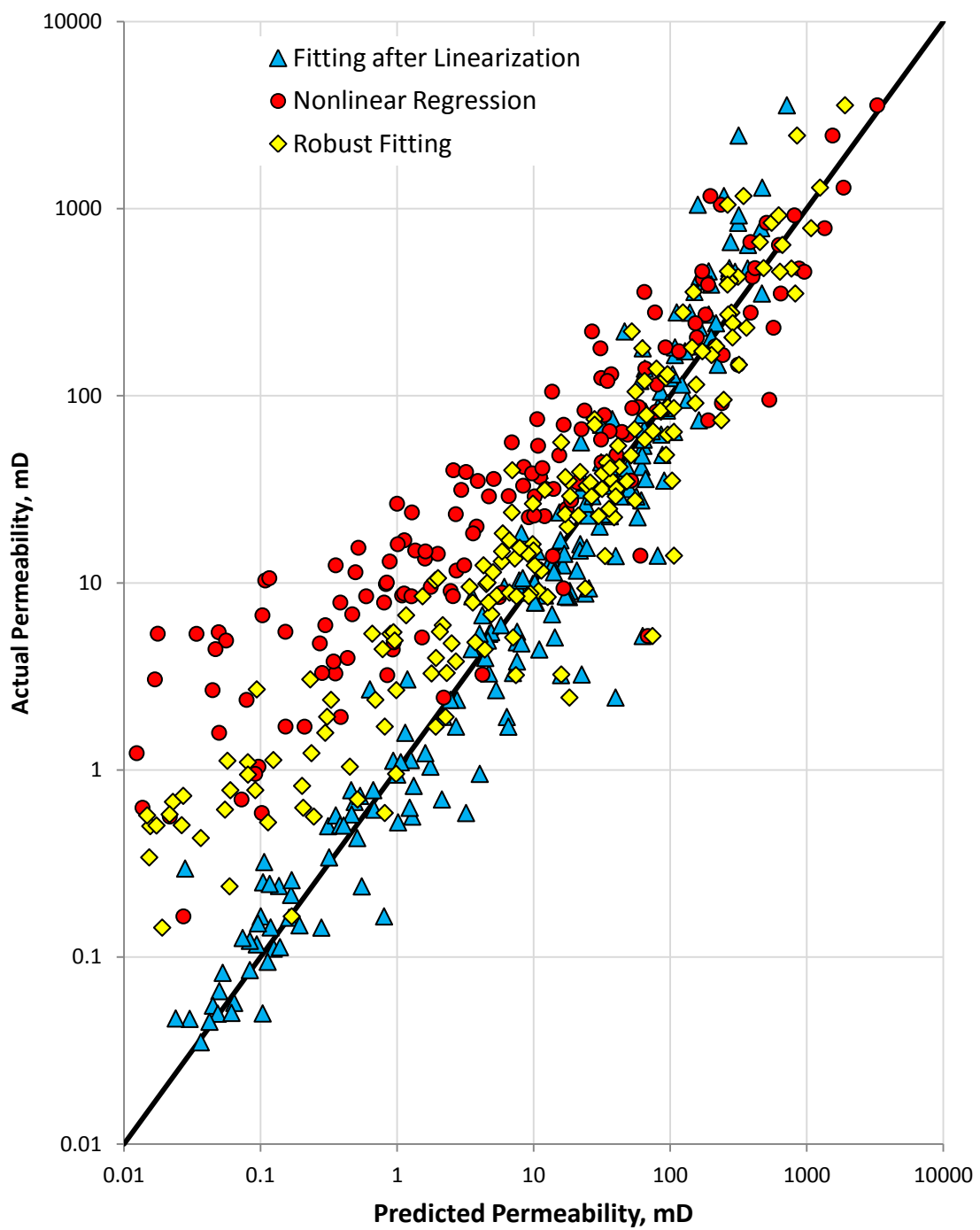


Figure 4.18 Modified Buiting-Clerke permeability model results using three regression methods

CHAPTER 5

CONCLUSION

In this study, a total of 225 carbonate rock samples are used to generate capillary pressure curves using mercury porosimetry. A validation process is conducted using porosity cross plots and pressure derivative plots and resulted in decimating 19 samples from the dataset. The validated samples; 206 samples, are then used to predict permeability from MICP data.

Nine permeability models are compared in this study: Purcell model, Thomeer model, Winalnd model, Swanson model, Pittman model, Huet-Blasingame model, Dastidar model, Buiting-Clerke model using Laplace transform, in addition to Buiting-Clerke model using Thomeer parameters.

The adapted methodology used in this comparative study is to compare all models with their published constants first. After that, new sets of coefficients are determined that best fit the dataset. Three different fitting methods are applied in this study. The first technique is the ordinary nonlinear least-squares regression that utilizes Gauss-Newton method. The second technique is the robust fitting method that reduces the effect of outliers by using weighted nonlinear regression by applying certain weight function. The third method uses the multiple regressions of nonlinear models after linearization.

Using the extracted parameters and permeability predictive models, permeability values are estimated using published constants and the other sets of constants determined using

the three regression techniques. Results are then compared to actual data. Maximum Absolute Percent Error (MAE), Average Relative Percent Error (ARE), Average Absolute Relative Percent Error (AARE), Correlation Coefficient (R), Standard Deviation (s) and Root Mean Squares (RMS) are used as basis for interpreting the results.

Comparison study using published constants indicates that, in general, most permeability models produce high errors when compared to actual data measurements. The Swanson permeability model is ranked first with R of 0.947 and AARE of 67.0%. Winland and Buiting-Clerke permeability models come next with R of 0.942 and 0.921 and AARE of 71.5% and 151.6%, respectively. For RMS, Winland shows the lowest value at 145, followed by Swanson at 160 followed by Buiting and Clerk model at 183. It is observed that some permeability models perform better in predicting high permeability values where permeability generally is higher than one mD but fail in predicting low permeability measurements accurately. Winland, Swanson, Buiting-Clerke, Thomeer and Pittman permeability models fall under this category. In contrast, Dastidar model perform much better in estimating low permeability values where rock permeability is less than one mD.

Major improvements in results, however, have been accomplished when using the generalized permeability models with calibrated coefficients to the dataset. Modified Winland and Swanson models show the best results and surpass all other models with close performance to each other. Modified Purcell model also shows significant improvement with the updated constants.

From most permeability model results, it can be observed that multiple regressions after linearization produces better results when used to predict low permeability values while nonlinear regression and robust fitting perform better in predicting high permeability values. The best explanation of this issue is that in nonlinear regression and robust fitting methods, the objective function is to minimize the sum of squares of errors. Therefore, the errors in predicting high permeability values dominate and the algorithm focuses in minimizing those errors over the errors produced by the low permeability values. This usually has a tendency to produce low standard deviations (s) and RMS in comparison to the other methods. The multiple regressions after linearization method, however, tends to reduce AARE that appears to be dominated by errors of low permeability values.

Due to the log-normal distribution nature of permeability and the wide ranges that they can exist at in a certain reservoirs, especially in carbonates, permeability modeling is and will be always a very challenging task. Errors encountered when calibrating permeability models' coefficients could be reduced by using corrected air permeability measurements to decrease slippage effect especially in low permeability rocks. Careful lab experimental procedures are also very critical and need more attention. It is also recommended for future studies to incorporate time information taken at each pressure step as one of the main parameters. Such information would help greatly in building more robust permeability models from MICP data.

REFERENCES

- Ahmed, U., Crary, S.F., and Coates, G.R. (1991): "Permeability Estimation: The Various Sources and Their Interrelationships," JPT (May) 578; Trans., AIME, 291.
- Buiting, J.J.M, Clerke, E.A, (2012): "Permeability from Porosimetry Measurements, Derivation for a Tortuous and Fractal Tubular Bundle " *J. Petrol.Science and Engineering* (in press).
- Brooks, R.H., and Corey, A.T.(1966): "Properties of Porous Media Affecting Fluid Flow," J. Irrig. And Drain. Div., ASCE (1966) ,92: 61-88.
- Brown, H. W. (1951):"Capillary pressure investigations" Trans., AIME, Vol. 192, 67-74.
- Clerke, E.A., Mueller III, H.W., Phillips, E.C., Eyvazzadeh, R.Y., Jones, D.H., Raghu Ramamoorthy, R. and Srivastava, A.(2008):" Application of Thomeer Hyperbolas to decode the pore systems, facies and reservoir properties of the Upper Jurassic Arab D Limestone, Ghawar field, Saudi Arabia: A "Rosetta Stone" approach." *GeoArabia*, vol. 13, no. 4, 2008, p.113-160
- Comisky, J.T., Newsham, K.E., Rushing, J.A., and Blasingame, T.A.(2007):" A Comparative Study of Capillary-Pressure-Based Empirical Models for Estimating Absolute Permeability in Tight Gas Sands." Paper SPE 110050, SPE Annual Technical Conference and Exhibition held in Anaheim, California, U.S.A., 11–14, November 2007.
- Dastidar, R., Sondergeld, C.H., and Rai, C.S.(2007): "An Improved Empirical Permeability Estimator from Mercury Injection for Tight Clastic Rocks," *Petrophysics*, Vol. 48, No. 3, (June, 2007) 186-187.
- Fleming III, P.D.(1983): "An Interpretation of the Petrophysical Properties of Reservoir Rocks Based in Percolation Theory,"paper SPE 12515 available from SPE, Richardson, Texas.
- Glover, P.W.J., Zadjali, I.I., and Frew, K.A.(2006):"Permeability prediction from MICP and NMR data using an electrokinetic approach." *Geophysics*,Vol. 71, No. 4 ,(July-August 2006), P. F49–F60.
- Gueguen, Y., and Palciauskas, V.(1994): *Introduction to the Physics of Rocks*, Princeton University Press, Princeton, NJ.
- Hagiwara, T.(1986): "Archie's "M" for Permeability," *The Log Analyst* (January 1986), Vol.27, No. 1, 39-42.

- Haro, C. F.(2004): “The Perfect Permeability Transform Using Logs and Cores,” paper SPE 89516, Ann. Tech. Conf. and Exhib., Houston, Texas, USA, 26-29 September 2004
- Huet, C.C., Rushing, J.A., Newsham, K.E., and Blasingame, T.A.(2005): "A Modified Purcell/Burdine Model for Estimating Absolute Permeability from Mercury Injection Capillary Pressure Data," paper IPTC 10994 presented at the 2005 International Technology Conference, Doha, Qatar, Nov.21-23.
- Katz, A.J. and Thompson, A.H.(1986): "Quantitative Prediction of Permeability in Porous Rock," Physical Review B, Vol. 34, No. 11, 8179-8181
- Kesten, H.(2006):”What is Percolation?” NOTICES OF THE AMS, Vol. 53, No. 5, May 2006, 572-573.
- Kolodize, S., Jr.(1980):”Analysis of Pore Throat Size and Use of the Waxman-Smiths Equation to Determine OOIP in Spindle Field, Colorado,” paper SPE 9382 presented at the 1980 Annual Fall Technical Conference of Society of Petroleum Engineers, Sep. 21-24 1980.
- Libny L., Roberto B., Alfonso Q., Juan, C. P., Hugo L.(2001):”Bimodal Behavior of Mercury-Injection Capillary Pressure Curve and its Relationship to Pore Geometry, Rock-Quality and Production Performance in a laminated and Heterogeneous Reservoir” SPE 69457.
- MATLAB[®] *Statistics Toolbox User’s Guide*, © COPYRIGHT 1993 - 2003 by The MathWorks, Inc.
- Nooruddin, H.A., and Hossain, M.E.(2011), “Modified Kozeny–Carmen correlation for enhanced hydraulic flow unit characterization”, J. Pet. Sci. Eng., doi:10.1016/j.petrol.2011.11.003. Volume 80, Issue 1, Dec. 2011, Pages 107–115
- Pittman, E.D.(1992): "Relationship of Porosity and Permeability to Various Parameters Derived from Mercury Injection-Capillary Pressure Curves for Sandstone," AAPG Bull., vol.76, No. 2 (February 1992) 191-198.
- Pickell, J. J., Swanson, B. F. and Hickman, W. B., (1966), Application of air-mercury and oil-air capillary pressure data in the study of pore structure and fluid distribution: SPE-1227, Mar. issue, P. 55-61.
- Purcell, W. R. (1949): “Capillary Pressures – Their Measurements Using Mercury and the Calculation of Permeability Therefrom”, Trans., AIME Vol. 186, 39-48.
- Shafer, J., Neasham, J.(2000): “Mercury Porosimetry Protocol for Rapid Determination of Petrophysical and Reservoir Quality Properties” SCA 2000-21.

- Swanson, B.F.(1981): "A Simple Correlation between Permeability and Mercury Capillary Pressures," JPT, (Dec. 1981), 2488-2504.
- Taib, D., and Donaldson, E.C.,(2004). Petrophysics: theory and practice of measuring reservoir rock and fluid transport properties. Gulf Prof., p.313-359.
- Thomeer, J.H.M.(1960): "Introduction of a Pore Geometrical Factor Defined by the capillary Pressure Curve," Trans., AIME (1960) 219, 354-58.
- Thomeer, J.H.M.(1983): "Air Permeability as a Function of Three Pore-Network Parameters," J. Pet. Tech. (Jan. 1983)
- Thompson, A.H., Katz, A.J., and Raschke, R.A.(1987): "Estimation of Absolute Permeability from Capillary Pressure Measurements," paper SPE 16794 presented at the 1987 SPE Annual Technical Conference and Exhibition, Dallas, TX, Sept. 27-30.
- Wardlaw, N. C., and Taylor, R. P.(1976): "Mercury Capillary Pressure Curves and the Interpretation of Pore Structure and Capillary Behavior in Reservoir Rock". Bulletin of Canadian Petroleum Geology, NO. 2, P. 225-262.
- Washburn, E. W.(1921), Note on a method of determining the distribution of pore sizes in a porous material, Proceedings: National Academy of Science, vol. 7, p. 115–116. 1921.
- Wyllie M.R.J., and Spangler, M.B.(1952): "Application of Electrical Resistivity Measurements to Problem of Fluid Flow in Porous Media," Bull. Am. Assoc. Petro. Geologists (February 1952), 359.

APPENDIX A

All mathematical formulas of error measures used in this study are given below including Maximum Absolute Relative Percent Error (MAE), Average Relative Percent Error (ARE), Average Absolute Relative Percent Error (AARE), Correlation Coefficient (R), Standard Deviation (s) and Root Mean Squares (RMS).

$$MAE = \max \left(\left| \frac{k_a - k_m}{k_a} \times 100 \right| \right) \quad (\text{Eq.A-1})$$

where (k_a) is actual permeability and (k_b) is predicted permeability

$$ARE = \frac{1}{n} \sum_{i=1}^n \frac{(k_a)_i - (k_m)_i}{(k_a)_i} \times 100 \quad (\text{Eq.A-2})$$

$$AARE = \frac{1}{n} \sum_{i=1}^n \left| \frac{(k_a)_i - (k_m)_i}{(k_a)_i} \times 100 \right| \quad (\text{Eq.A-3})$$

$$R = \frac{\sum_{i=1}^n ((k_a)_i - \bar{k}_a)((k_m)_i - \bar{k}_m)}{\sqrt{\sum_{i=1}^n ((k_a)_i - \bar{k}_a)^2 \sum_{i=1}^n ((k_m)_i - \bar{k}_m)^2}} \quad (\text{Eq.A-4})$$

where $\bar{k}_m = \frac{1}{n} \sum_{i=1}^n (k_m)_i$ and $\bar{k}_a = \frac{1}{n} \sum_{i=1}^n (k_a)_i$

$$s = \left(\frac{1}{n-1} \sum_{i=1}^n (e_i - \bar{e})^2 \right)^{\frac{1}{2}} \quad (\text{Eq.A-5})$$

where $e_i = (k_a)_i - (k_m)_i$ and $\bar{e} = \frac{1}{n} \sum_{i=1}^n e_i$

$$RMS = \sqrt{\frac{1}{n-2} \sum_{i=1}^n e_i^2} \quad (\text{Eq.A-6})$$

APPENDIX B

In this study, three regression methods are used to come up with permeability model coefficients. All these techniques are built-in functions within MATLAB R2010b[®]. Those methods are:

- **Ordinary least-squares nonlinear regression**

Ordinary least-squares nonlinear regression uses the Levenberg-Marquardt algorithm for nonlinear least squares to compute non-robust fits. The main disadvantage of this method is that it can be significantly influenced by outliers.

- **Robust fitting**

Robust fitting method reduces the effect of outliers by using weighted nonlinear regression. This can be achieved by applying certain weight function. MATLAB2012R[®] provides a wide variety of weight functions.

For robust fits, an algorithm is used that iteratively refits a weighted nonlinear regression, where the weights at each iteration are based on each observation's residual from the previous iteration. These weights serve to downweight points that are outliers so that their influence on the fit is decreased. Iterations continue until the weights converge. (1984-2010 The MathWorks, Inc.)

The weight function that has been used this study is:

$$w = \frac{1}{1+abs(r)} \quad (\text{Eq.B-1})$$

where r is:

$$r = \frac{resid}{tune*s*\sqrt{1-h}} \quad (\text{Eq.B-2})$$

where $resid$ is the vector of residuals from previous iteration, h is the vector of leverage values from least-squares fit, $tune$ is a tuning constant that is divided into the residual vector before computing weights, and s is an estimate of standard deviation of the error term. The parameter s can be estimated by:

$$s = \frac{MAD}{0.6745} \quad (\text{Eq.B-3})$$

where MAD is the median absolute deviation from their median and the constant 0.6745 is used to make to estimate unbiased for the normal distribution.

- **Multiple regressions of nonlinear models after linearization**

All permeability models used in this study have been linearized and then coefficients have been determined. With this approach, a unique solution is guaranteed. the following MATLAB codes have been used to determine all coefficients.

Matlab code used for permeability models with multiple regressions of nonlinear models after linearization

```

%% Purcell Permeability Model
% Correlation calculation
int          = ones(size(k));
A            = [int log(phi_inj) log(purcell)];
b            = regress(log(k),A);
k_mod_pur    = exp(A*b);
Er_pur       = Error(k,k_mod_pur);
% .....
% .....
% plots - Purcell Permeability Model
figure(1)    % Crossplot
subplot(2,2,[1 3]) ; loglog(k_mod_pur,k,'ko','MarkerFaceColor','y');
title ('Purcell Permeability Model');
xlabel('Measured Permeability');ylabel('Estimated Permeability');grid
on;refline(1,0);
axis([0.01 10000 0.01 10000]);
%-----
%-----
subplot(2,2,2); plot(k-k_mod_pur,'ro','MarkerFaceColor','r')
xlabel('Number of data sample');ylabel('Errors');grid on;refline(0,0);
axis([0 207 -100 100]);
%-----
%-----
subplot(2,2,4);histfit(k-k_mod_pur)
hr = findobj(gca,'Type','patch');set(hr,'FaceColor','g','EdgeColor','b');
title ('Histogram of Errors');xlabel('Residuals or Percent Relative
Errors');ylabel('Frequency')
%      %=====

%% Thomeer Permeability Model
% Correlation calculation
int          = ones(size(k));
A1           = [int log(Fg1) log(100.*phi_inj./pd1)];
A2           = [int log(Fg2) log(phi_inj./pd2)];
b1           = regress(log(k),A1);
b2           = regress(log(k),A2);
k_mod_th1    = exp(A1*b1);
k_mod_th2    = exp(A2*b2);
Er_th1       = Error(k,k_mod_th1);
Er_th2       = Error(k,k_mod_th2);
% .....
% .....
% plots - Thomeer Permeability Model
figure(2)    % Crossplot
subplot(2,2,[1 3]) ; loglog(k_mod_th1,k,'ko','MarkerFaceColor','y');
title ('Thomeer Permeability Model');
xlabel('Measured Permeability');ylabel('Estimated Permeability');grid
on;refline(1,0);
axis([0.01 10000 0.01 10000]);
%-----
%-----
subplot(2,2,2); plot(k-k_mod_th1,'ro','MarkerFaceColor','r')
xlabel('Number of data sample');ylabel('Errors');grid on;refline(0,0);
axis([0 207 -100 100]);
%-----
%-----

```

```

subplot(2,2,4);histfit(k-k_mod_th1)
hr = findobj(gca,'Type','patch');set(hr,'FaceColor','g','EdgeColor','b');
title ('Histogram of Errors');xlabel('Residuals or Percent Relative
Errors');ylabel('Frequency')

figure(3) % Crossplot
subplot(2,2,[1 3]) ; loglog(k_mod_th2,k,'ko','MarkerFaceColor','y');
title ('Thomeer Permeability Model');
xlabel('Measured Permeability');ylabel('Estimated Permeability');grid
on;refline(1,0);
axis([0.01 10000 0.01 10000]);
%-----
%-----
subplot(2,2,2); plot(k-k_mod_th2,'ro','MarkerFaceColor','r')
xlabel('Number of data sample');ylabel('Errors');grid on;refline(0,0);
axis([0 207 -100 100]);
%-----
%-----
subplot(2,2,4);histfit(k-k_mod_th2)
hr = findobj(gca,'Type','patch');set(hr,'FaceColor','g','EdgeColor','b');
title ('Histogram of Errors');xlabel('Residuals or Percent Relative
Errors');ylabel('Frequency')
% %=====

%% Huet-Blasingame Permeability Model
%% Correlation calculation
int = ones(size(k));
A1 = [int log(int.*phi_inj) log(pd1) log(Lumda1./(2+Lumda1))];
A2 = [int log(int.*phi_inj) log(pd2) log(Lumda2./(2+Lumda2))];
b1 = regress(log(k),A1);
b2 = regress(log(k),A2);
k_mod_HB1 = exp(A1*b1);
k_mod_HB2 = exp(A2*b2);
Er_HB1 = Error(k,k_mod_HB1);
Er_HB2 = Error(k,k_mod_HB2);
% .....
% .....
% plots - Huet-Blasingame Permeability Model
figure(4) % Crossplot
subplot(2,2,[1 3]) ; loglog(k_mod_HB1,k,'ko','MarkerFaceColor','y');
title ('Huet-Blasingame Permeability Model');
xlabel('Measured Permeability');ylabel('Estimated Permeability');grid
on;refline(1,0);
axis([0.01 10000 0.01 10000]);
%-----
%-----
subplot(2,2,2); plot(k-k_mod_HB1,'ro','MarkerFaceColor','r')
xlabel('Number of data sample');ylabel('Errors');grid on;refline(0,0);
axis([0 207 -100 100]);
%-----
%-----
subplot(2,2,4);histfit(k-k_mod_HB1)
hr = findobj(gca,'Type','patch');set(hr,'FaceColor','g','EdgeColor','b');
title ('Histogram of Errors');xlabel('Residuals or Percent Relative
Errors');ylabel('Frequency')

figure(5) % Crossplot
subplot(2,2,[1 3]) ; loglog(k_mod_HB2,k,'ko','MarkerFaceColor','y');
title ('Huet-Blasingame Permeability Model');
xlabel('Measured Permeability');ylabel('Estimated Permeability');grid
on;refline(1,0);
axis([0.01 10000 0.01 10000]);

```

```

%-----
%-----
subplot(2,2,2); plot(k-k_mod_HB2,'ro','MarkerFaceColor','r')
xlabel('Number of data sample');ylabel('Errors');grid on;refline(0,0);
axis([0 207 -100 100]);
%-----
%-----
subplot(2,2,4);histfit(k-k_mod_HB2)
hr = findobj(gca,'Type','patch');set(hr,'FaceColor','g','EdgeColor','b');
title ('Histogram of Errors');xlabel('Residuals or Percent Relative
Errors');ylabel('Frequency')
%      %=====
%

%% Swanson Permeability Model
% Correlation calculation
A      = [int log(100.*apex_swan)];
b      = regress(log(k),A);
k_mod_swan = exp(A*b);
Er_swan  = Error(k,k_mod_swan);
% .....
% .....
% plots - Swanson Permeability Model
figure(6) % Crossplot
subplot(2,2,[1 3]) ; loglog(k_mod_swan,k,'ko','MarkerFaceColor','y');
title ('Swanson Permeability Model');
xlabel('Measured Permeability');ylabel('Estimated
Permeability');refline(1,0);
axis([0.01 10000 0.01 10000]);
%-----
%-----
subplot(2,2,2); plot(k-k_mod_swan,'ro','MarkerFaceColor','r')
xlabel('Number of data sample');ylabel('Errors');grid on;refline(0,0);
axis([0 207 -100 100]);
%-----
%-----
subplot(2,2,4);histfit(k-k_mod_swan)
hr = findobj(gca,'Type','patch');set(hr,'FaceColor','g','EdgeColor','b');
title ('Histogram of Errors');xlabel('Residuals or Percent Relative
Errors');ylabel('Frequency')
%      %=====
%

%% Winland Permeability Model
% Correlation calculation

% A      = [int log(int.*phi_inj) log(r_apex)] ;
A      = [int log(int.*phi_inj) log(r35)] ;
b      = regress(log(k),A);
k_mod_win = exp(A*b);
Er_win  = Error(k,k_mod_win);
% .....
% .....
% plots - Winland Permeability Model
figure(7) % Crossplot
subplot(2,2,[1 3]) ; loglog(k_mod_win,k,'ko','MarkerFaceColor','y');
title ('Winland Permeability Model');
xlabel('Measured Permeability');ylabel('Estimated
Permeability');refline(1,0);
axis([0.01 10000 0.01 10000]);
%-----
%-----
subplot(2,2,2); plot(k-k_mod_win,'ro','MarkerFaceColor','r')
xlabel('Number of data sample');ylabel('Errors');grid on;refline(0,0);

```

```

axis([0 207 -100 100]);
%-----
%-----
subplot(2,2,4);histfit(k-k_mod_win)
hr = findobj(gca,'Type','patch');set(hr,'FaceColor','g','EdgeColor','b');
title ('Histogram of Errors');xlabel('Residuals or Percent Relative
Errors');ylabel('Frequency')
% =====
%
%% Dastidar Permeability Model
% Correlation calculation
A = [int log(int.*phi_inj) log(rwgm)] ;
b = regress(log(k),A);
k_mod_ou = exp(A*b);
Er_ou = Error(k,k_mod_ou)
% .....
% .....
% plots - Winland Permeability Model
figure(8) % Crossplot
subplot(2,2,[1 3]) ; loglog(k_mod_ou,k,'ko','MarkerFaceColor','y');
title ('OU Permeability Model');
xlabel('Measured Permeability');ylabel('Estimated
Permeability');refline(1,0);
axis([0.01 10000 0.01 10000]);
%-----
%-----
subplot(2,2,2); plot(k-k_mod_ou,'ro','MarkerFaceColor','r')
xlabel('Number of data sample');ylabel('Errors');grid on;refline(0,0);
axis([0 207 -100 100]);
%-----
%-----
subplot(2,2,4);histfit(k-k_mod_ou)
hr = findobj(gca,'Type','patch');set(hr,'FaceColor','g','EdgeColor','b');
title ('Histogram of Errors');xlabel('Residuals or Percent Relative
Errors');ylabel('Frequency')
% =====
%% Buiting and Clerke Permeability Model
% Correlation calculation
int = ones(size(k));
A1 = [int log(int.*phi_inj) log(pd1) Fg1.^0.5];
A2 = [int log(int.*phi_inj) log(pd2) Fg2.^0.5];
% A2 = [int log(phi_inj./pd1.^2) Fg1.^0.5];
b1 = regress(log(k),A1)
b2 = regress(log(k),A2);
k_mod_bc1 = exp(A1*b1);
k_mod_bc2 = exp(A2*b2);
Er_bc1 = Error((k),(k_mod_bc1))
Er_bc2 = Error((k),(k_mod_bc2));
% .....
% .....
% plots - Buiting and Clerke Permeability Model
figure(9) % Crossplot
subplot(2,2,[1 3]) ; loglog(k_mod_bc1,k,'ko','MarkerFaceColor','y');
title ('Buiting and Clerke Permeability Model');
xlabel('Measured Permeability');ylabel('Estimated
Permeability');refline(1,0);
axis([0.01 10000 0.01 10000]);
%-----
%-----
subplot(2,2,2); plot(k-k_mod_bc1,'ro','MarkerFaceColor','r')
xlabel('Number of data sample');ylabel('Errors');grid on;refline(0,0);
axis([0 207 -100 100]);
%-----

```

```

%-----
subplot(2,2,4);histfit(k-k_mod_bc1)
hr = findobj(gca,'Type','patch');set(hr,'FaceColor','g','EdgeColor','b');
title ('Histogram of Errors');xlabel('Residuals or Percent Relative
Errors');ylabel('Frequency')
xlim([-1000 1000]);

figure(10) % Crossplot
subplot(2,2,[1 3]) ; loglog(k_mod_bc2,k,'ko','MarkerFaceColor','y');
title ('Buiting and Clerke Permeability Model');
xlabel('Measured Permeability');ylabel('Estimated
Permeability');refline(1,0);
axis([0.01 10000 0.01 10000]);
%-----
%-----
subplot(2,2,2); plot(k-k_mod_bc2,'ro','MarkerFaceColor','r')
xlabel('Number of data sample');ylabel('Errors');grid on;refline(0,0);
axis([0 207 -100 100]);
%-----
%-----
subplot(2,2,4);histfit(k-k_mod_bc2)
hr = findobj(gca,'Type','patch');set(hr,'FaceColor','g','EdgeColor','b');
title ('Histogram of Errors');xlabel('Residuals or Percent Relative
Errors');ylabel('Frequency')
xlim([-1000 1000]);
%=====

%% Hasan Permeability Model
% Correlation calculation
int = ones(size(k));
A1 = [int (dpp) log(apex_swan)];
% A2 = [int (kDt) log(phi_inj.*s_apex./pc_apex)];
% A2 = [ int (kDt).^0.5 2.*log(phi_inj) log(r35)];
A2 = [int (dpp2) log(apex_swan)];
% A2 = [int (phi_inj.*kDt) log(int.*phi_inj.*s_apex)
log(pc_apex)];
% A2 = [int (phi_inj.*kDt) log(int.*phi_inj.*s_apex)
log(pc_apex)];

% b1 = regress(log(k),A1);
b1 = regress(log(k),A1);
b2 = regress(log(k),A2);
k_mod_ha1 = exp(A1*b1)
k_mod_ha2 = exp(A2*b2);
[k exp(A2*b2) abs(k-exp(A2*b2))];
Er_ha1 = Error((k),(k_mod_ha1))
Er_ha2 = Error((k),(k_mod_ha2));
% .....
% .....
% plots - Hasan Permeability Model
figure(11) % Crossplot
subplot(2,2,[1 3]) ; loglog(k_mod_ha1,k,'ko','MarkerFaceColor','y');
title ('Hasan Permeability Model');
xlabel('Measured Permeability');ylabel('Estimated Permeability');grid
on;refline(1,0);
axis([0.01 10000 0.01 10000]);
%-----
%-----
subplot(2,2,2); plot(k-k_mod_ha1,'ro','MarkerFaceColor','r')
xlabel('Number of data sample');ylabel('Errors');grid on;refline(0,0);
axis([0 207 -100 100]);
%-----

```

```

%-----
subplot(2,2,4);histfit(k-k_mod_ha1)
hr = findobj(gca,'Type','patch');set(hr,'FaceColor','g','EdgeColor','b');
title ('Histogram of Errors');xlabel('Residuals or Percent Relative
Errors');ylabel('Frequency')
xlim([-1000 1000]);

figure(12) % Crossplot
subplot(2,2,[1 3]) ; loglog(k_mod_ha2,k,'ko','MarkerFaceColor','y');
title ('Hasan Permeability Model');
xlabel('Measured Permeability');ylabel('Estimated Permeability');grid
on;refline(1,0);
axis([0.01 10000 0.01 10000]);
%-----
%-----
subplot(2,2,2); plot(k-k_mod_ha2,'ro','MarkerFaceColor','r')
xlabel('Number of data sample');ylabel('Errors');grid on;refline(0,0);
axis([0 207 -100 100]);
%-----
%-----
subplot(2,2,4);histfit(k-k_mod_ha2)
hr = findobj(gca,'Type','patch');set(hr,'FaceColor','g','EdgeColor','b');
title ('Histogram of Errors');xlabel('Residuals or Percent Relative
Errors');ylabel('Frequency')
xlim([-1000 1000]);
%=====

```

```

%% Error Function
function [Error_model] = Error(perm,perm_model)
Er      =((perm-perm_model)./perm)*100;
MaxEr   = max(abs(Er));
MinEr   = min(abs(Er));
ARE     = mean(Er);
AARE    = mean(abs(Er));
Std     = std(perm-perm_model);
R = corrcoef(perm,perm_model);
Mse= mse(perm-perm_model);
Rms = Mse.^0.5;
Error_model= [ MaxEr  ARE AARE  R(2,1) Std Rms];

```


Matlab code used for permeability models with robust fitting and nonlinear

regression

```
function perm_models(varargin)
clear all;           % removes all variables, globals and functions
close all;          % closes all the open figure windows
clc;                % clear command window
format short g;     % Set output format
warning off;
%% Reading Input Data
data = xlsread('Model_Parameter_Output_Final.xls','matlab_output');
%
%

k = data(:,1);
phi_plug = data(:,2);
phi_inj = data(:,3);
Vb = data(:,4);
Vp = data(:,5);
purcell = data(:,6);
pd1 = data(:,7);
pd2 = data(:,8);
Fg1 = data(:,9);
Fg2 = data(:,10);
r35 = data(:,11);
apex_swan = data(:,12);
rwgm = data(:,13);
Lumda1 = data(:,14);
Lumda2 = data(:,15);
r36 = data(:,16);
fzi = data(:,18);
ct = data(:,19);
kDt = data(:,20);
rqi = data(:,21);
s_apex = data(:,23);
pc_apex = data(:,24);
r_apex = data(:,25);

%% apply filter on perm
% filter = 0.00001;
% k = k(find(k>filter));
% phi_plug = phi_plug(find(k>filter));
% phi_inj = phi_inj(find(k>filter));
% Vb = Vb(find(k>filter));
% Vp = Vp(find(k>filter));
% purcell = purcell(find(k>filter));
% pd1 = pd1(find(k>filter));
% pd2 = pd2(find(k>filter));
% Fg1 = Fg1(find(k>filter));
% Fg2 = Fg2(find(k>filter));
% r35 = r35(find(k>filter));
% apex_swan = apex_swan(find(k>filter));
% rwgm = rwgm(find(k>filter));
% Lumda1 = Lumda1(find(k>filter));
% Lumda2 = Lumda2(find(k>filter));
% r36 = r36(find(k>filter));
% fzi = fzi(find(k>filter));
% ct = ct(find(k>filter));
```

```

% kDt      = kDt(find(k>filter));
% rqi      = rqi(find(k>filter));
% s_apex   = s_apex(find(k>filter));
% pc_apex  = pc_apex(find(k>filter));
% r_apex   = r_apex(find(k>filter));

options     = statset('MaxIter',3000,'TolFun',1e-
10,'Robust','on','Tune',1,'WgtFun','fair');
% options   = statset('MaxIter',2000,'TolFun',1e-8);
% .....
%% Purcell Permeability Model
% Correlation calculation
int         = ones(size(k));
A           = [phi_inj purcell];
b           = [55270.79894 2.1 0.6];
% options   = statset('MaxIter',2000,'TolFun',1e-8);
% options = addObjective(options, 'newObj', 'min')
bn          = nlinfit(A,k,@k_function_pur,b,options);
k_mod_pur   = k_function_pur(bn,A);
Er_pur      = Error(k,k_mod_pur);
% .....
% .....
% plots - Purcell Permeability Model
figure(1)   % Crossplot
subplot(2,2,[1 3]) ; loglog(k_mod_pur,k,'ko','MarkerFaceColor','y');
title('Purcell Permeability Model');
xlabel('Measured Permeability');ylabel('Estimated Permeability');grid
on;refline(1,0);
%axis([0.0001 9000 0.01 9000]);
%-----
%-----
subplot(2,2,2); plot(k-k_mod_pur,'ro','MarkerFaceColor','r')
xlabel('Number of data sample');ylabel('Errors');grid on;refline(0,0);
axis([0 207 -100 100]);
%-----
%-----
subplot(2,2,4);histfit(k-k_mod_pur)
hr = findobj(gca,'Type','patch');set(hr,'FaceColor','g','EdgeColor','b');
title('Histogram of Errors');xlabel('Residuals or Percent Relative
Errors');ylabel('Frequency')
%=====

%% Thomeer Permeability Model
% Correlation calculation
int         = ones(size(k));
A1          = [int.*phi_inj pd1 Fg1];
A2          = [int.*phi_inj pd2 Fg2];
b           = [3.8068 -1.3334 2 -2];
% options   = statset('MaxIter',2000,'TolFun',1e-8);
bn1         = nlinfit(A1,k,@k_function_th,b,options);
bn2         = nlinfit(A2,k,@k_function_th,b,options);
k_mod_th1   = k_function_th(bn1,A1);
k_mod_th2   = k_function_th(bn2,A2);
Er_th1      = Error(k,k_mod_th1);
Er_th2      = Error(k,k_mod_th2);
% .....
% .....
% plots - Thomeer Permeability Model
figure(2)   % Crossplot
subplot(2,2,[1 3]) ; loglog(k_mod_th1,k,'ko','MarkerFaceColor','y');

```

```

    title ('Thomeer Permeability Model');
    xlabel('Measured Permeability');ylabel('Estimated Permeability');grid
on;refline(1,0);
    %axis([0.0001 9000 0.01 9000]);
    %-----
    %-----
    subplot(2,2,2); plot(k-k_mod_th1,'ro','MarkerFaceColor','r')
    xlabel('Number of data sample');ylabel('Errors');grid on;refline(0,0);
    axis([0 207 -100 100]);
    %-----
    %-----
    subplot(2,2,4);histfit(k-k_mod_th1)
    hr = findobj(gca,'Type','patch');set(hr,'FaceColor','g','EdgeColor','b');
    title ('Histogram of Errors');xlabel('Residuals or Percent Relative
Errors');ylabel('Frequency')

    figure(3) % Crossplot
    subplot(2,2,[1 3]) ; loglog(k_mod_th2,k,'ko','MarkerFaceColor','y');
    title ('Thomeer Permeability Model');
    xlabel('Measured Permeability');ylabel('Estimated Permeability');grid
on;refline(1,0);
    %axis([0.0001 9000 0.01 9000]);
    %-----
    %-----
    subplot(2,2,2); plot(k-k_mod_th2,'ro','MarkerFaceColor','r')
    xlabel('Number of data sample');ylabel('Errors');grid on;refline(0,0);
    axis([0 207 -100 100]);
    %-----
    %-----
    subplot(2,2,4);histfit(k-k_mod_th2)
    hr = findobj(gca,'Type','patch');set(hr,'FaceColor','g','EdgeColor','b');
    title ('Histogram of Errors');xlabel('Residuals or Percent Relative
Errors');ylabel('Frequency')
    %=====

%% Huet-Blasingame Permeability Model
% Correlation calculation
int = ones(size(k));
A1 = [int.*phi_inj pd1 Lumda1];
A2 = [int.*phi_inj pd2 Lumda2];
b = [1538.710489 2.6088 -0.91696 -2.0602];
% options = statset('MaxIter',2000,'TolFun',1e-8);
bn1 = nlinfit(A1,k,@k_function_HB,b,options);
bn2 = nlinfit(A2,k,@k_function_HB,b,options);
k_mod_HB1 = k_function_HB(bn1,A1);
k_mod_HB2 = k_function_HB(bn2,A2);
Er_HB1 = Error(k,k_mod_HB1);
Er_HB2 = Error(k,k_mod_HB2);
% .....
% .....
% plots - Huet-Blasingame Permeability Model
    figure(4) % Crossplot
    subplot(2,2,[1 3]) ; loglog(k_mod_HB1,k,'ko','MarkerFaceColor','y');
    title ('Huet-Blasingame Permeability Model');
    xlabel('Measured Permeability');ylabel('Estimated Permeability');grid
on;refline(1,0);
    %axis([0.0001 9000 0.01 9000]);
    %-----
    %-----
    subplot(2,2,2); plot(k-k_mod_HB1,'ro','MarkerFaceColor','r')
    xlabel('Number of data sample');ylabel('Errors');grid on;refline(0,0);
    axis([0 207 -100 100]);
    %-----

```

```

%-----
subplot(2,2,4);histfit(k-k_mod_HB1)
hr = findobj(gca,'Type','patch');set(hr,'FaceColor','g','EdgeColor','b');
title ('Histogram of Errors');xlabel('Residuals or Percent Relative
Errors');ylabel('Frequency')

figure(5) % Crossplot
subplot(2,2,[1 3]) ; loglog(k_mod_HB2,k,'ko','MarkerFaceColor','y');
title ('Huet-Blasingame Permeability Model');
xlabel('Measured Permeability');ylabel('Estimated Permeability');grid
on;refline(1,0);
%axis([0.0001 9000 0.01 9000]);
%-----
%-----
subplot(2,2,2); plot(k-k_mod_HB2,'ro','MarkerFaceColor','r')
xlabel('Number of data sample');ylabel('Errors');grid on;refline(0,0);
axis([0 207 -100 100]);
%-----
%-----
subplot(2,2,4);histfit(k-k_mod_HB2)
hr = findobj(gca,'Type','patch');set(hr,'FaceColor','g','EdgeColor','b');
title ('Histogram of Errors');xlabel('Residuals or Percent Relative
Errors');ylabel('Frequency')
%=====

%% Swanson Permeability Model
% Correlation calculation
A = 100.*apex_swan;
% A = rwgm;
b = [259.589101 1.3703];
% options = statset('MaxIter',2000,'TolFun',1e-8);
bn = nlinfit(A,k,@k_function_swan,b,options);
k_mod_swan = k_function_swan(bn,A);
Er_swan = Error(k,k_mod_swan);
% .....
% .....
% plots - Swanson Permeability Model
figure(6) % Crossplot
subplot(2,2,[1 3]) ; loglog(k_mod_swan,k,'ko','MarkerFaceColor','y');
title ('Swanson Permeability Model');
xlabel('Measured Permeability');ylabel('Estimated
Permeability');refline(1,0);
%axis([0.0001 9000 0.01 9000]);
%-----
%-----
subplot(2,2,2); plot(k-k_mod_swan,'ro','MarkerFaceColor','r')
xlabel('Number of data sample');ylabel('Errors');grid on;refline(0,0);
axis([0 207 -100 100]);
%-----
%-----
subplot(2,2,4);histfit(k-k_mod_swan)
hr = findobj(gca,'Type','patch');set(hr,'FaceColor','g','EdgeColor','b');
title ('Histogram of Errors');xlabel('Residuals or Percent Relative
Errors');ylabel('Frequency')
%=====

%% Winland Permeability Model
% Correlation calculation

Aw = [phi_inj r35] ;
Ap = [phi_inj r_apex] ;

```

```

b                = [156.2098038  1.2467  1.8324];

% options        = statset('MaxIter',2000,'TolFun',1e-8);
bw              = nlinfit(Aw,k,@k_function_win,b,options);
bp              = nlinfit(Ap,k,@k_function_win,b,options);
k_mod_win       = k_function_win(bw,Aw);
k_mod_pit       = k_function_win(bp,Ap);
Er_win          = Error(k,k_mod_win);
Er_pit          = Error(k,k_mod_pit);
% .....
% .....
% plots - Winland Permeability Model
figure(7) % Crossplot
subplot(2,2,[1 3]) ; loglog(k_mod_win,k,'ko','MarkerFaceColor','y');
title ('Winland Permeability Model');
xlabel('Measured Permeability');ylabel('Estimated
Permeability');refline(1,0);
%axis([0.0001 9000 0.01 9000]);
%-----
%-----
subplot(2,2,2); plot(k-k_mod_win,'ro','MarkerFaceColor','r')
xlabel('Number of data sample');ylabel('Errors');grid on;refline(0,0);
axis([0 207 -100 100]);
%-----
%-----
subplot(2,2,4);histfit(k-k_mod_win)
hr = findobj(gca,'Type','patch');set(hr,'FaceColor','g','EdgeColor','b');
title ('Histogram of Errors');xlabel('Residuals or Percent Relative
Errors');ylabel('Frequency')
%=====

%% OU Permeability Model
% Correlation calculation

A                = [phi_inj rwgm] ;
b                = [107132.4  3.06  1.64];
% options        = statset('MaxIter',2000,'TolFun',1e-8);
bn              = nlinfit(A,k,@k_function_ou,b,options);
k_mod_ou        = k_function_ou(bn,A);
Er_ou           = Error(k,k_mod_ou);
% .....
% .....
% plots - Winland Permeability Model
figure(8) % Crossplot
subplot(2,2,[1 3]) ; loglog(k_mod_ou,k,'ko','MarkerFaceColor','y');
title ('OU Permeability Model');
xlabel('Measured Permeability');ylabel('Estimated
Permeability');refline(1,0);
%axis([0.0001 9000 0.01 9000]);
%-----
%-----
subplot(2,2,2); plot(k-k_mod_ou,'ro','MarkerFaceColor','r')
xlabel('Number of data sample');ylabel('Errors');grid on;refline(0,0);
axis([0 207 -100 100]);
%-----
%-----
subplot(2,2,4);histfit(k-k_mod_ou)
hr = findobj(gca,'Type','patch');set(hr,'FaceColor','g','EdgeColor','b');
title ('Histogram of Errors');xlabel('Residuals or Percent Relative
Errors');ylabel('Frequency')
%=====

%% Buiting and Clerke Permeability Model

```

```

% Correlation calculation
int = ones(size(k));
A1 = [int.*phi_inj pd1 Fg1];
A2 = [int.*phi_inj pd2 Fg2];
b = [281531.6067 1.6923 -1.3766 -4.9101];
% options = statset('MaxIter',2000,'TolFun',1e-8);
bn1 = nlinfit(A1,k,@k_function_bc,b,options);
bn2 = nlinfit(A2,k,@k_function_bc,b,options);
k_mod_bc1 = k_function_bc(bn1,A1);
k_mod_bc2 = k_function_bc(bn2,A2);
Er_bc1 = Error(k,k_mod_bc1);
Er_bc2 = Error(k,k_mod_bc2);
% .....
% .....
% plots - Buiting and Clerke Permeability Model
figure(9) % Crossplot
subplot(2,2,[1 3]) ; loglog(k_mod_bc1,k,'ko','MarkerFaceColor','y');
title ('Buiting and Clerke Permeability Model');
xlabel('Measured Permeability');ylabel('Estimated Permeability');grid
on;refline(1,0);
%axis([0.0001 9000 0.01 9000]);
%-----
%-----
subplot(2,2,2); plot(k-k_mod_bc1,'ro','MarkerFaceColor','r')
xlabel('Number of data sample');ylabel('Errors');grid on;refline(0,0);
axis([0 207 -100 100]);
%-----
%-----
subplot(2,2,4);histfit(k-k_mod_bc1)
hr = findobj(gca,'Type','patch');set(hr,'FaceColor','g','EdgeColor','b');
title ('Histogram of Errors');xlabel('Residuals or Percent Relative
Errors');ylabel('Frequency')

figure(10) % Crossplot
subplot(2,2,[1 3]) ; loglog(k_mod_bc2,k,'ko','MarkerFaceColor','y');
title ('Buiting and Clerke Permeability Model');
xlabel('Measured Permeability');ylabel('Estimated Permeability');grid
on;refline(1,0);
%axis([0.0001 9000 0.01 9000]);
%-----
%-----
subplot(2,2,2); plot(k-k_mod_bc2,'ro','MarkerFaceColor','r')
xlabel('Number of data sample');ylabel('Errors');grid on;refline(0,0);
axis([0 207 -100 100]);
%-----
%-----
subplot(2,2,4);histfit(k-k_mod_bc2)
hr = findobj(gca,'Type','patch');set(hr,'FaceColor','g','EdgeColor','b');
title ('Histogram of Errors');xlabel('Residuals or Percent Relative
Errors');ylabel('Frequency')
%=====

%% Hasan Permeability Model
% Correlation calculation
int = ones(size(k));
A1 = [int.*phi_inj pc_apex s_apex];
A2 = [int.*phi_inj kDt apex_swan ];
b = [0 0 0 0];
% options = statset('MaxIter',2000,'TolFun',1e-8);
bn1 = nlinfit(A1,k,@k_function_ha,b,options);
bn2 = nlinfit(A2,k,@k_function_ha,b,options);
k_mod_ha1 = k_function_ha(bn1,A1);
k_mod_ha2 = k_function_ha(bn2,A2);

```

```

Er_hal      = Error(k,k_mod_hal)
Er_ha2      = Error(k,k_mod_ha2);
% .....
% .....
% plots - Hasan Permeability Model
figure(11) % Crossplot
subplot(2,2,[1 3]) ; loglog(k_mod_hal,k,'ko','MarkerFaceColor','y');
title ('Hasan Permeability Model');
xlabel('Measured Permeability');ylabel('Estimated Permeability');grid
on;refline(1,0);
%axis([0.0001 9000 0.01 9000]);
%-----
%-----
subplot(2,2,2); plot(k-k_mod_hal,'ro','MarkerFaceColor','r')
xlabel('Number of data sample');ylabel('Errors');grid on;refline(0,0);
axis([0 207 -100 100]);
%-----
%-----
subplot(2,2,4);histfit(k-k_mod_hal)
hr = findobj(gca,'Type','patch');set(hr,'FaceColor','g','EdgeColor','b');
title ('Histogram of Errors');xlabel('Residuals or Percent Relative
Errors');ylabel('Frequency')

figure(12) % Crossplot
subplot(2,2,[1 3]) ; loglog(k_mod_ha2,k,'ko','MarkerFaceColor','y');
title ('Hasan Permeability Model');
xlabel('Measured Permeability');ylabel('Estimated Permeability');grid
on;refline(1,0);
%axis([0.0001 9000 0.01 9000]);
%-----
%-----
subplot(2,2,2); plot(k-k_mod_ha2,'ro','MarkerFaceColor','r')
xlabel('Number of data sample');ylabel('Errors');grid on;refline(0,0);
axis([0 207 -100 100]);
%-----
%-----
subplot(2,2,4);histfit(k-k_mod_ha2)
hr = findobj(gca,'Type','patch');set(hr,'FaceColor','g','EdgeColor','b');
title ('Histogram of Errors');xlabel('Residuals or Percent Relative
Errors');ylabel('Frequency')
%=====

```

```

%% Purcell Perm Model Function
function kc = k_function_pur(b,A)
phi      = A(:,1);
purcell  = A(:,2);

kc       = b(1).*phi.^b(2).*purcell.^b(3);

%% Thomeer Perm Model Function
function kc = k_function_th(b,A)
phi      = A(:,1);
pd       = A(:,2);
Fg       = A(:,3);

kc       = b(1)*Fg.^b(2).*(phi.*100).^b(3).*(pd).^b(4);

%% Huet-Blasingame Perm Model Function

```

```

function kc = k_function_HB(b,A)
phi      = A(:,1);
pd       = A(:,2);
lu       = A(:,3);

kc       = b(1).*(pd).^b(3).*(lu./(lu+2)).^b(4).*phi.^b(2);

%% Swanson Perm Model Function
function kc = k_function_swan(b,A)
apex     = A(:,1);

kc       = b(1).*apex.^b(2);

%% Winland Perm Model Function
function kc = k_function_win(b,A)
phi      = A(:,1);
r35     = A(:,2);
kc       = b(1).*r35.^b(2).*phi.^b(3);

%% OU Perm Model Function
function kc = k_function_ou(b,A)
phi      = A(:,1);
wgm     = A(:,2);
kc       = b(1).*wgm.^b(3).*phi.^b(2);

%% Buiting and Clerke Perm Model Function
function kc = k_function_bc(b,A)
phi      = A(:,1);
pd       = A(:,2);
Fg       = A(:,3);

kc       = b(1).*phi.^b(2).*pd.^b(3).*exp(b(4).*(Fg).^0.5);

%% Hasan Perm Model Function
function kc = k_function_ha(b,A)
para     = A(:,1);
pd       = A(:,2);
Fg       = A(:,3);

kc       = b(1).*para.^b(2).*pd.^b(3).*Fg.^b(4);

%% Error Function
function [Error_model] = Error(perm,perm_model)
Er       = ((perm-perm_model)./perm)*100;
MaxEr    = max(abs(Er));
MinEr    = min(abs(Er));
ARE      = mean(Er);
AARE     = mean(abs(Er));
Std      = std(perm-perm_model);
R = corrcoef(perm,perm_model);
Mse= mse(perm-perm_model);
Rms = Mse.^0.5;
Error_model= [ MaxEr  ARE  AARE  R(2,1) Std Rms];

```


Matlab code used for permeability models with published constants

```

function perm_models(varargin)
clear all;           % removes all variables, globals and functions
close all;          % closes all the open figure windows
clc;                % clear command window
format short g;      % Set output format
%% Reading Input Data
data = xlsread('Model_Parameter_Output_Finalv2.xls','matlab_output');
%
%

k      = data(:,1);
phi_plug = data(:,2);
phi_inj = data(:,3);
Vb      = data(:,4);
Vp      = data(:,5);
purcell = data(:,6);
pd1     = data(:,7);
pd2     = data(:,8);
Fg1     = data(:,9);
Fg2     = data(:,10);
r35     = data(:,11);
apex_swan = data(:,12);
rwgm    = data(:,13);
Lumda1  = data(:,14);
Lumda2  = data(:,15);
r36     = data(:,16);
fzi     = data(:,18);
ct      = data(:,19);
kDt     = data(:,20);
rqi     = data(:,21);
s_apex  = data(:,23);
pc_apex = data(:,24);
r_apex  = data(:,25);
kbc_lap = data(:,28);

% .....
%% Purcell Permeability Model
% Correlation calculation
int      = ones(size(phi_inj));
A        = [int log(phi_inj.*int) log(purcell)];
b        = regress(log(k),A);
k_mod_pur = 10.66.*(480*cos(2.443460953)).^2.*0.216.*phi_inj.*purcell;
% k_mod_pur = 6600/0.068046^2*0.216.*phi_inj.*purcell;
k_mod_pur_con = phi_inj.*purcell.*14254*21.6; %check this number
Er_pur      = Error(k,(k_mod_pur))
% Er_pur_con = Error(k,k_mod_pur_con) %published constant

% .....
% .....
% plots - Purcell Permeability Model
figure(1) % Crossplot
subplot(2,2,[1 3]) ; loglog(k_mod_pur,k,'ko','MarkerFaceColor','y');
title('Purcell Permeability Model');
xlabel('Measured Permeability');ylabel('Estimated
Permeability');refline(1,0);
axis([0.01 10000 0.01 10000]);
%-----
%-----
subplot(2,2,2); plot(k-k_mod_pur,'ro','MarkerFaceColor','r')

```

```

xlabel('Number of data sample');ylabel('Errors');grid on;refline(0,0);
axis([0 207 -100 100]);
%-----
%-----
subplot(2,2,4);histfit(k-k_mod_pur)
hr = findobj(gca,'Type','patch');set(hr,'FaceColor','g','EdgeColor','b');
title ('Histogram of Errors');xlabel('Residuals or Percent Relative
Errors');ylabel('Frequency')
axis([-1000 1000 0 200]);
%-----
%--

%      %=====

%% Thomeer Permeability Model
% Correlation calculation
int      = ones(size(k));
A1       = [int log(Fg1) log(phi_inj.*100./pd1)];
% A2     = [int log(Fg2) log(phi_inj./pd2)];
b1       = regress(log(k),A1);
% b2     = regress(log(k),A2);
k_mod_th1 = 3.8068.*Fg1.^(-1.3334).*((100.*phi_inj)./pd1).^2;
% k_mod_th2 = 3806.8.*Fg1.^(-1.3334).*(phi_inj./pd1).^2;
Er_th1   = Error(k,k_mod_th1)
% Er_th2   = Error(k,k_mod_th2)
% .....
% .....
% plots - Thomeer Permeability Model
figure(2) % Crossplot
subplot(2,2,[1 3]) ; loglog(k_mod_th1,k,'ko','MarkerFaceColor','y');
title ('Thomeer Permeability Model');
xlabel('Measured Permeability');ylabel('Estimated
Permeability');refline(1,0);
axis([0.01 10000 0.01 10000]);
%-----
%-----
subplot(2,2,2); plot(k-k_mod_th1,'ro','MarkerFaceColor','r')
xlabel('Number of data sample');ylabel('Errors');grid on;refline(0,0);
axis([0 207 -100 100]);
%-----
%-----
subplot(2,2,4);histfit(k-k_mod_th1)
hr = findobj(gca,'Type','patch');set(hr,'FaceColor','g','EdgeColor','b');
title ('Histogram of Errors');xlabel('Residuals or Percent Relative
Errors');ylabel('Frequency')
axis([-1000 1000 0 200]);
%-----
%-----

%      %=====

%% Huet-Blasingame Permeability Model
% Correlation calculation
int      = ones(size(k));
A1       = [int log(int.*phi_inj) log(pd1) log(Lumda1./(2+Lumda1))];
% A2     = [int log(int.*phi_inj) log(pd2) log(Lumda2./(2+Lumda2))];
b1       = regress(log(k),A1);
% b2     = regress(log(k),A2);
k_mod_HB1 = 1017003.2395.*pd1.^(-
1.7846).*(Lumda1./(2+Lumda1)).^1.6575.*phi_inj.^1.6498;
% k_mod_HB2 = exp(A2*b2);
Er_HB1    = Error(k,k_mod_HB1)
% Er_HB2    = Error(k,k_mod_HB2)

```

```

% .....
% .....
% plots - Huet-Blasingame Permeability Model
figure(3) % Crossplot
subplot(2,2,[1 3]) ; loglog(k_mod_HB1,k,'ko','MarkerFaceColor','y');
title ('Huet-Blasingame Permeability Model');
xlabel('Measured Permeability');ylabel('Estimated
Permeability');refline(1,0);
axis([0.01 10000 0.01 10000]);
%-----
%-----
subplot(2,2,2); plot(k-k_mod_HB1,'ro','MarkerFaceColor','r')
xlabel('Number of data sample');ylabel('Errors');grid on;refline(0,0);
axis([0 207 -100 100]);
%-----
%-----
subplot(2,2,4);histfit(k-k_mod_HB1)
hr = findobj(gca,'Type','patch');set(hr,'FaceColor','g','EdgeColor','b');
title ('Histogram of Errors');xlabel('Residuals or Percent Relative
Errors');ylabel('Frequency')
axis([-1000 1000 0 200]);

% =====
%

%% Swanson Permeability Model
% Correlation calculation
A = [int log(apex_swan)];
b = regress(log(k),A);
k_mod_swan = 399.*(100.*apex_swan).^1.691;
Er_swan = Error(k,k_mod_swan)
% .....
% .....
% plots - Swanson Permeability Model
figure(4) % Crossplot
subplot(2,2,[1 3]) ; loglog(k_mod_swan,k,'ko','MarkerFaceColor','y');
title ('Swanson Permeability Model');
xlabel('Measured Permeability');ylabel('Estimated
Permeability');refline(1,0);
axis([0.01 10000 0.01 10000]);
%-----
%-----
subplot(2,2,2); plot(k-k_mod_swan,'ro','MarkerFaceColor','r')
xlabel('Number of data sample');ylabel('Errors');grid on;refline(0,0);
axis([0 207 -100 100]);
%-----
%-----
subplot(2,2,4);histfit(k-k_mod_swan)
hr = findobj(gca,'Type','patch');set(hr,'FaceColor','g','EdgeColor','b');
title ('Histogram of Errors');xlabel('Residuals or Percent Relative
Errors');ylabel('Frequency')
axis([-1000 1000 0 200]);
% =====
%

%% Winland Permeability Model
% Correlation calculation

A = [int log(int.*phi_inj) log(r35)] ;
b = regress(log(k),A);
k_mod_win = 49.45.*r35.^1.7.*(phi_inj).^1.47;
k_mod_pitt = 4.6*r_apex.^2.105.*(phi_inj).^0.208 ; % Pittman model
Er_win = Error(k,k_mod_win)

```

```

Er_pitt          = Error(k,k_mod_pitt)
% .....
% .....
% plots - Winland Permeability Model
figure(5) % Crossplot
subplot(2,2,[1 3]) ; loglog(k_mod_win,k,'ko','MarkerFaceColor','y');
title ('Winland Permeability Model');
xlabel('Measured Permeability');ylabel('Estimated
Permeability');refline(1,0);
axis([0.01 10000 0.01 10000]);
%-----
%-----
subplot(2,2,2); plot(k-k_mod_win,'ro','MarkerFaceColor','r')
xlabel('Number of data sample');ylabel('Errors');grid on;refline(0,0);
axis([0 207 -100 100]);
%-----
%-----
subplot(2,2,4);histfit(k-k_mod_win)
hr = findobj(gca,'Type','patch');set(hr,'FaceColor','g','EdgeColor','b');
title ('Histogram of Errors');xlabel('Residuals or Percent Relative
Errors');ylabel('Frequency')
axis([-1000 1000 0 200]);
% =====
%
%% Dastidar Permeability Model
% Correlation calculation
A          = [int log(int.*phi_inj) log(rwgm)] ;
b          = regress(log(k),A);
% k_mod_ou = exp.^(-2.51).*(phi_inj.*100).^ (3.06).*(rwgm).^1.64;
k_mod_ou   = 107132.4.*(phi_inj).^ (3.06).*(rwgm).^1.64;

[k_mod_ou k];
Er_ou       = Error(k,k_mod_ou)
% .....
% .....
% plots - Permeability Model
figure(6) % Crossplot
subplot(2,2,[1 3]) ; loglog(k_mod_ou,k,'ko','MarkerFaceColor','y');
title ('Dastidar Permeability Model');
xlabel('Measured Permeability');ylabel('Estimated
Permeability');refline(1,0);
axis([0.01 10000 0.01 10000]);
%-----
%-----
subplot(2,2,2); plot(k-k_mod_ou,'ro','MarkerFaceColor','r')
xlabel('Number of data sample');ylabel('Errors');grid on;refline(0,0);
axis([0 207 -100 100]);
%-----
%-----
subplot(2,2,4);histfit(k-k_mod_ou)
hr = findobj(gca,'Type','patch');set(hr,'FaceColor','g','EdgeColor','b');
title ('Histogram of Errors');xlabel('Residuals or Percent Relative
Errors');ylabel('Frequency')
axis([-1000 1000 0 200]);
% =====
%% Butting and Clerke Permeability Model
% Correlation calculation
int        = ones(size(k));
A1         = [int log(int.*phi_inj./pd1.^2) Fg1.^0.5];
A1         = [int log(int.*phi_inj) log(pd1) Fg1.^0.5];

```

```

% A2 = [int log(int.*phi_inj) log(pd2) Fg2.^0.5];
% A2 = [int log(phi_inj./pd1.^2) Fg1.^0.5];
b1 = regress(log(k),A1);
% b2 = regress(log(k),A2);
% k_mod_bc1 = 406000.*phi_inj.*exp(-2.92.*(Fg1).^0.5)./pd1.^2;
k_mod_bc2 = 506000.*phi_inj.*exp(-4.43.*(Fg1).^0.5)./pd1.^2;
k_mod_bc1 = kbc_lap;
% k_mod_bc2 = exp(A2*b2);
Er_bc1 = Error((k),(k_mod_bc1));
Er_bc2 = Error((k),(k_mod_bc2))

% Er_bc2 = Error((k),(k_mod_bc2))
.....
.....
% plots - Buiting and Clerke Permeability Model
figure(7) % Crossplot
subplot(2,2,[1 3]) ; loglog(k_mod_bc1,k,'ko','MarkerFaceColor','y');
title ('Buiting and Clerke Permeability Model');
xlabel('Measured Permeability');ylabel('Estimated
Permeability');refline(1,0);
axis([0.01 10000 0.01 10000]);
%-----
%-----
subplot(2,2,2); plot(k-k_mod_bc1,'ro','MarkerFaceColor','r')
xlabel('Number of data sample');ylabel('Errors');grid on;refline(0,0);
axis([0 207 -100 100]);
%-----
%-----
subplot(2,2,4);histfit(k-k_mod_bc1)
hr = findobj(gca,'Type','patch');set(hr,'FaceColor','g','EdgeColor','b');
title ('Histogram of Errors');xlabel('Residuals or Percent Relative
Errors');ylabel('Frequency')
axis([-1000 1000 0 200]);

%=====

%% Hasan Permeability Model
% Correlation calculation
int = ones(size(k));
A1 = [int log(int.*phi_inj.*s_apex) log(pc_apex) ];
% A2 = [int (kDt) log(phi_inj.*s_apex./pc_apex)];
% A2 = [ int (kDt).^0.5 2.*log(phi_inj) log(r35)];
A2 = [int (phi_inj.*kDt) log(apex_swan)];
% A2 = [int (phi_inj.*kDt) log(int.*phi_inj.*s_apex)
log(pc_apex)];
% A2 = [int (phi_inj.*kDt) log(int.*phi_inj.*s_apex)
log(pc_apex)];

% b1 = regress(log(k),A1);
b1 = regress(log(k),A1);
b2 = regress(log(k),A2);
k_mod_ha1 = exp(A1*b1);
k_mod_ha2 = exp(A2*b2);
[k exp(A2*b2) abs(k-exp(A2*b2))];
Er_ha1 = Error((k),(k_mod_ha1));
Er_ha2 = Error((k),(k_mod_ha2));
% .....
% .....
% plots - Hasan Permeability Model
figure(8) % Crossplot
subplot(2,2,[1 3]) ; loglog(k_mod_ha1,k,'ko','MarkerFaceColor','y');
title ('Hasan Permeability Model');

```

```

xlabel('Measured Permeability');ylabel('Estimated
Permeability');refline(1,0);
axis([0.01 10000 0.01 10000]);
%-----
%-----
subplot(2,2,2); plot(k-k_mod_ha1,'ro','MarkerFaceColor','r')
xlabel('Number of data sample');ylabel('Errors');grid on;refline(0,0);
axis([0 207 -100 100]);
%-----
%-----
subplot(2,2,4);histfit(k-k_mod_ha1)
hr = findobj(gca,'Type','patch');set(hr,'FaceColor','g','EdgeColor','b');
title ('Histogram of Errors');xlabel('Residuals or Percent Relative
Errors');ylabel('Frequency')
xlim([-1000 1000]);

figure(9) % Crossplot
subplot(2,2,[1 3]) ; loglog(k_mod_ha2,k,'ko','MarkerFaceColor','y');
title ('Hasan Permeability Model');
xlabel('Measured Permeability');ylabel('Estimated
Permeability');refline(1,0);
axis([0.01 10000 0.01 10000]);
%-----
%-----
subplot(2,2,2); plot(k-k_mod_ha2,'ro','MarkerFaceColor','r')
xlabel('Number of data sample');ylabel('Errors');grid on;refline(0,0);
axis([0 207 -100 100]);
%-----
%-----
subplot(2,2,4);histfit(k-k_mod_ha2)
hr = findobj(gca,'Type','patch');set(hr,'FaceColor','g','EdgeColor','b');
title ('Histogram of Errors');xlabel('Residuals or Percent Relative
Errors');ylabel('Frequency')
xlim([-1000 1000]);
%=====

%% Error Function
function [Error_model] = Error(perm,perm_model)
Er = ((perm-perm_model)./perm)*100;
MaxEr = max(abs(Er));
MinEr = min(abs(Er));
ARE = mean(Er);
AARE = mean(abs(Er));
Std = std(perm-perm_model);
R = corrcoef(perm,perm_model);
Mse= mse(perm-perm_model);
Rms = Mse.^0.5;
Error_model= [ MaxEr ARE AARE R(2,1) Std Rms];

```

Matlab code used to determine parameters of all permeability models

```
% this program is intended to validate MICP raw data
% injection capillary pressure - Hasan Abdulelah Nooruddin 10/8/1432
%-----
function perm_parameters(output)
%-----
clear all; close all; clc;
% data = xlsread('xxx_19','455');
% [ndata, headertext, rawdata] = xlsread('xxxx_19','455');
%-----
% [type, sheets] = xlsinfo('MICP_test');
[type, sheets] = xlsinfo('xxxx_ALL');
%-----
xx = 0 ; % this count is used to report unvalid samples' name.
x = 0 ;
%-----
% for i=6:6 % for testing
for i=1:length(sheets); % whole data set
%% -----
%small data set for testing
%-----
% data = xlsread('MICP_test',i,'A23:E129'); % pc, sw, r , sm
% data2 = xlsread('MICP_test',i,'K7:K16'); % air permeability , poro
%-----
%all data set
%-----
data = xlsread(xxxx,i,'A23:E129'); % pc, sw, r , sm
data2 = xlsread(xxxx,i,'K7:K16'); % air permeability , poro
%-----
%%
t = 2.5 ; % time in minutes
m_vis = 1.526 ; % mercury viscosity in cp
%-----
k_air = data2(1,1); % air permeability
phi Plug = data2(2,1); % plug porosity
phi_inj = data2(3,1); % injection sample porosity
Vp_inj = data2(4,1); % injection pore volume
Vb_inj = data2(5,1); % injection bulk volume
swan = data2(9,1); % Swanson Parameter
fzi = data2(10,1);
%-----
%-----
pc = data(:,1); % mercury capillary pressure
sm = data(:,2); % mercury saturation
sw = data(:,3); % Equiv water saturation
r = data(:,4); % pore throat radius microns
%-----
%MICP poro & plug air poro
%-----

poro_diff=abs(phi Plug-phi_inj);

if poro_diff>0.01;
    xx =xx+1;
    unvalid_samples(xx) = sheets(i);
    continue
end

%-----
x = x+1;
```

```

%-----
sample(x)=sheets(i);

%      zz_kk(x)      = trapz(s(1:end-1),k_Lc);
%% Sample Parameters

    k(x)              = k_air;
    Vb(x)              = Vb_inj;
    Vp(x)              = Vp_inj;
    poro_inj(x)        = phi_inj;
    poro_plug(x)       = phi_plug;

%% Purcell Parameters

    Y                  = (1./pc).^2;
    IP(x)              = trapz(sm,Y);
%% Thomeer Parameters
    su                 = 0.1;
    Bv                 = phi_inj.*sm;
    Bv1                = Bv(find(Bv>0));
    Bv2                = Bv(find(sm>su));
    pc1                = pc(find(Bv>0));
    pc2                = pc(find(sm>su));

    Pd1(x)             = interp1(Bv1 ,pc1 ,0,'linear','extrap');
    Pd2(x)             = min(pc2);

    intercept1         = ones(size(Bv1));
    intercept2         = ones(size(Bv2));
    A1                  = [intercept1.*phi_inj   pc1   intercept1.*Pd1(x)];
    A2                  = [intercept2.*phi_inj   pc2   intercept2.*Pd2(x)];
    b                   = 0;
    options              = statset('MaxIter',5000,'TolFun',1e-8);
    b1                  = nlinfit(A1,Bv1,@Bv_function,b,options);
    b2                  = nlinfit(A2,Bv2,@Bv_function,b,options);
%      Bv1_model       = Bv_function(b1,A1);
%      Bv2_model       = Bv_function(b2,A2);

% Thomeer Geometrical Factor
Fg1(x)= b1;
Fg2(x)= b2;

Pc_m1 = Pd1(x).*exp(-2.3.*Fg1(x)./log(sm));
Pc_m2 = Pd2(x).*exp(-2.3.*Fg2(x)./log(sm));

%      figure(2)
%      loglog(Bv,Pc_m1,'r');hold on;
%      loglog(Bv,Pc_m2,'b');
%      title ('Validation Plot');xlabel('Bv');ylabel('Pc')
%      loglog(Bv,pc,'k');
%      legend('Pc Thomeer','Pc actual')
%      axis([0.0 0.35 0 50000]);
%% Winland parameter
r35(x)= interp1(sm(find(sm>0)),r(find(sm>0)),0.35,'linear','extrap');

%% Swanson Parameters

```



```

        vvv      = sm.*phi_inj./pc;
    s_apex(x)    = sm(find(vvv==max(vvv)));
    pc_apex(x)   = pc(find(vvv==max(vvv)));
    r_apex(x)    = r(find(vvv==max(vvv)));
    apex_swan(x) = max(vvv);

    swan2(x)     = swan;
    FZI(x)       = fzi;

%% Pittman
r36(x)= interp1(sm(find(sm>0)),r(find(sm>0)),0.36,'linear','extrap');

%% Huet-Blasingame
    sw1          = sw(find(Bv>0));
    sw2          = sw(find(sm>su));

    A1           = [sw1(1:end-1)    intercept1(1:end-1).*Pd1(x)];
    A2           = [sw2(1:end-1)    intercept2(1:end-1).*Pd2(x)];
    b            = [0.5];
    options      = statset('MaxIter',5000,'TolFun',1e-8);
    b1           = nlinfit(A1,pc1(1:end-1),@BC_function,b,options);
    b2           = nlinfit(A2,pc2(1:end-1),@BC_function,b,options);
    BC1_model    = BC_function(b1,A1);
    BC2_model    = BC_function(b2,A2);

    % Thomeer Geometrical Factor
    Lumda1(x)= b1(1);
    Lumda2(x)= b2(1);

%       figure(2)
%       semilogy(sw1(1:end-1) ,BC1_model,'r');hold on;
%       semilogy(sw2(1:end-1),BC2_model,'b');
%       title ('Validation Plot');xlabel('Bv');ylabel('Pc')
%       semilogy(sw,pc,'k');
%       legend('Pc Thomeer','Pc actual')
%       axis([0.0 1 0 50000]);

%% Dastidar Parameter

    RWGM(x)= exp(sum(sm.*log(r))./sum(sm));

%% RQI
rqi(x)=0.0314.*(k_air./phi_inj).^0.5;
#####
#####
end
%% wrighting all data to Excel file
%% Hasan Perm Model
    sa      = sm(1:end-1);

    DSS     = sa+diff(sm)./2;
    DPP     = 1./diff(pc);

    dpp(x)  = trapz(DSS,DPP);

%% Buitting and Clerke Parameters

    Dy      = 1.56;

```

```

Q   = log(pc);
Qd  = log(Pd);
Y   = Bv.*exp(-2.*Dy.*Q);
I   = trapz(Q,Y);
kbc(x) = (1000.*107.^2./16.*Dy.*exp(-2.*(1-Dy).*Qd).*I);

bc_intg(x)=I;

%% Thomeer Parameters
function Bvc = Bv_function(b,A)
    poro     = A(:,1);
    pc       = A(:,2);
    pd       = A(:,3);

    Bvc      = poro.*exp(-b(1)./(log10(pc)-log10(pd)));

%% Brooks and Corey
function BCpc = BC_function(b,A)

    sw       = A(:,1);
    pd       = A(:,2);

%   BCpc     = pd.*((sw-b(2))./(1-b(2))).^(-1./b(1));
BCpc       = pd.*sw.^(-1./b(1));

```

VITAE

Name : Hasan Abdul-Elah Nooruddin

Nationality : Saudi

Date of Birth : 4/30/1984

Email : hasan.a.nooruddin@gmail.com

Present Address : Dhahran

Permanent Address : Duba – Tabuk Province

Academic Background : Petroleum Engineering

Telephone Number : +966555368771